IMPROVING FLUID RECOVERY AND PERMEABILITY TO GAS IN SHALE FORMATIONS

A Dissertation

by

AMENEH ROSTAMI

Submitted to the Office of Graduate and Professional Studies of
Texas A&M University
in partial fulfillment of the requirements for the degree of

DOCTOR OF PHILOSOPHY

Chair of Committee,	Hisham A. Nasr-El-Din
Committee Members,	Jerome J. Schubert
	Mahmoud M. El-Halwagi
	Robert H. Lane
Head of Department,	A. Daniel Hill

May 2015

Major Subject: Petroleum Engineering

ABSTRACT

Despite all advantages of slickwater fracturing such as low cost, high possibility of creating complex fracture networks, and ease of clean-up, large quantities of water are still left within the reservoir after flowback. Invasion of aqueous fracturing fluids can reduce the relative permeability to gas and thereby cause a water blockage.

Compared to conventional surfactants that lose activity after contacting the first few inches of the formation due to adsorption to the rock surface, microemulsions with advantage of having combined effect of microemulsion-forming surfactants and organic solvents, outperform pure organic solvent or pure surfactant when used independently. Microemulsions can provide maximum surface area of contact with the formation due to their structure and can increase penetration and cleaning efficiency.

The research proposed in this study has been designed to assess the performance of microemulsions when it is used as an additive to the fracturing fluid to stimulate the gas bearing formations. Microemulsions formulated with a blend of anionic surfactant, nonionic surfactant, oil and water were used to prepare the microemulsion systems.

The average size of the microemulsion-V droplet (as received) was detected by transmission electron micrographs (TEM). Microemulsions were tested to assess their efficiency in reducing the surface tension and in wettability alteration. Experiments were conducted using cores from an outcrop of Bandera sandstone to measure the effect of microemulsions on the gas permeability enhancements. The increase in gas permeability was quantified by comparing the relative gas permeability before and after treatment. The alteration of wettability after the chemical treatment was evaluated by measuring the

contact angles between the treatment fluid and rock. Thermal stability tests were conducted using hot rolling cells for temperatures up to 400°F, which proved the high stability of microemulsions at high-temperature conditions. Microemulsions caused enhancement in the relative gas permeability, when compared to the mutual solvent, fluoropolymer surfactant, anionic, and non-ionic surfactant solutions. Microemulsions altered the wettability of water-wet rocks to less water-wet.

Aging the shale rock particles in contact with different treatment solutions, showed an increase in the concentration of tested elements including Ca, Mg, Al, and Si in the solutions that can be an explanation of high total dissolved solid (TDS) in the flow back fluid after completion.

DEDICATION

This dissertation is dedicated to

my beloved parents, for their love and effort to make me who I am;

my beloved husband for his support and love during this journey

my dear brother and lovely sister, for their support and help.

ACKNOWLEDGEMENTS

I would like to express my deepest gratitude and appreciation to my advisor and committee chair, Dr. H. A. Nasr-El-Din, for his continuous encouragement, guidance, and support. I would also like to extend my appreciation to Dr. Jerome J. Schubert, Dr. Robert Lane and Dr. Mahmoud M. El-Halwagi for their advice, guidance, and encouragement.

Many thanks are due to all my colleagues who helped me during the course of this research. I would like to acknowledge financial support from the Crisman Institute at Texas A&M University. The facilities and resources provided by the Harold Vance Department of Petroleum Engineering of Texas A&M University are gratefully acknowledged.

I would like to thank Nalco and OilChem for providing the microemulsion samples and Akzonoble for providing the surfactant samples.

NOMENCLATURE

A	Cross-Sectional Area, ft^2
b_k	Klinkenberg slippage factor, psi
EOR	Enhanced Oil Recovery
F	Force acting on the balance, N
k_a	Apparent gas permeability, md
K_{eg}	Effective permeability to gas, md
k_∞	Equivalent liquid (Klinkenberg corrected) permeability, md
k_{rg}	Relative permeability to gas, -
k_{rgcw}	End-point relative permeability to gas at S_{wirr}, -
k_{rw}	Relative permeability to brine, -
k_{rwgc}	End-point relative permeability to brine at S_{gc}, -
L	Total length of the linear system, ft
n_g	Corey exponent for non-wetting phase, -
n_w	Corey exponent for wetting phase, -
P_1	Inlet pressure, psi
P_2	Outlet pressure, psi
P_{av}	Average pressure, psi
P_c	Capillary pressure, psi
Q_{sc}	Gas flow rate at standard conditions, scf/day
R	Radius of pore throat, µm
S_w	Brine saturation, %

S_{wirr}	Irreducible brine saturation, %
t	Time, min
T	Temperature, °R
Z	Gas compressibility factor, -
β	Constant coefficient, psi
φ	porosity, -
Φ	Volumetric fraction of oil/water
θ	Contact angle, degree
μ_g	Gas viscosity, cp
σ	Surface or interfacial tension, mN/m

TABLE OF CONTENTS

Page

LIST OF TABLES

Page

LIST OF FIGURES

Page

INTRODUCTION*

Introduction and Literature Review

Phase trapping refers to temporary or permanent trapping of oil or water-based fluids introduced into the porous media during drilling and completion operations and results in a reduction in the effective permeability to the producing fluid. It is a common mechanism of formation damage in a variety of oil, gas, or water bearing formations. In gas producing formations, water-based trapping is the most common phase trapping. Sub-irreducible saturation is the initial basis for establishment of an aqueous phase trap, where the initial water saturation in the reservoir is less than what would be typically quantified as the irreducible water saturation in the porous media. Bennion et al. (2000c) recognized a combination of factors like dehydration, desiccation, compaction, and digenetic effects which occur over the life of certain reservoirs as causes for establishment of the sub-irreducible saturation.

Phase trapping has been found to be related to some phenomena such as capillary pressure and relative permeability, both of which are direct functions of pore geometry, interfacial tension between the invaded fluid and the produced reservoir fluid, wettability, and fluid saturation levels.

Phase trapping is also a function of depth of invasion, fluid penetration, and reservoir temperature, pressure, and drawdown potentials (Bennion et al. 2006). When the reservoir is undersaturated, the equilibrium saturations achieve by imbibing the water to the formation, which reduces the relative gas permeability. When the well starts to produce, the gas must overcome the capillary pressure and reach the fracture face. The gas breaks through the fluid leaving a large volume of trapped water in the formation and therefore reducing the effective flow area at the fracture face (Penny et al. 2005).

One of the main methods that has been tried to restore gas permeability is reducing the interfacial tension. This includes use of light alcohols such as methanol in dry gas wells, heavier alcohols such as propanol and butanol in gas reservoirs containing both water and liquid hydrocarbons, dense carbon dioxide, mutual solvent, and surfactant treatments (Bennion et al. 1994).

Light alcohols can create sludge and emulsion when oil or condensate liquids are present in the formation (Bennion et al. 2006). Carbon dioxide can cause low gas-brine interfacial tension, and it has high solubility in both water and hydrocarbon phases. However, effective contact and incompatibility between CO_2 and some hydrocarbons are the main challenges for this method (Bennion et al. 2006). Mutual solvents have been used as a method to reduce interfacial tension and increase the volatility of trapped fluid often combined with CO_2 (Al-Anazi et al. 2005). Effective contact and potential compatibility issues are the main limitations of this method (Bennion et al. 2006). Various authors discussed application of different surfactants as a method to remove both hydrocarbons and water phase traps (Li and Firoozabadi 2000; Vijapurapu and Rao 2003; Ahmadi et al.

2011). Pursley et al. (2004) explained the problem of using surfactant treatment solutions as quick adsorption and activity loss after first few inches in the formation.

Recently, microemulsions were of great interest due to their desirable properties for enhanced recovery applications. According to Santanna et al. (2012), "microemulsions are thermodynamically stable, isotropic, and macroscopically homogeneous dispersions of two immiscible fluids, generally oil and water, stabilized with surfactant molecules, either alone or mixed with a co-surfactant." Having low interfacial tension between the microemulsion and the excess oil and/or water phases, enables them to overcome the capillary pressures that trap oil or water in a porous medium. A microemulsion system was tested by Willhite et al. (1980) to investigate the effect of phase behavior on displacement efficiency of miceller flooding in Berea cores containing brine and residual nonane. The results showed 48 to 70 % oil recovery and low interfacial tension between microemulsion and nonane. Delshad et al. (1985) conducted experiments using a microemulsion system containing brine/oil/surfactant/alcohol mixture in both Berea sandstone and sandpack to measure the steady state relative permeabilities. The dispersion was measured with radioactive and chemical tracers. The results showed that the microemulsion was the wetting phase when flowing with either excess-oil or excess-brine phases. Pursley et al. (2004) developed a microemulsion additive to the conventional gelled fluid and performed fracture proppant cleanup tests. The results showed that the pressure to initiate cleanup was lowered by 50% and regained permeability to gas was doubled when microemulsion was used in conventional gelled fluids. Penny et al. (2005) used a microemulsion system to cleanup of injected fluid in tight gas cores. The

microemulsion caused a pressure decrease needed to displace injected fluids from low permeability core samples and enhanced relative permeability to gas. Several field examples were presented for unconventional coals and shales treatments. Water recovery and producibility were increased by 50% (Penny et al. 2005). Paktinat et al. (2005) presented the laboratory experiments of using microemulsion which showed 80% permeability enhancement in sandstone cores. Babadagli (2005) studied the injection of several pore volumes of microemulsion into the sandstone plugs, which contained 35% of residual oil, observing a linear relationship between the values of injected pore volume and the oil recovery. Low interfacial tensions between aqueous and oily phases as well as improved solubilization for both polar and non-polar compounds were explained as the most desirable properties of microemulsion for enhance recovery applications. Yang et al. (2009) tested a microemulsion based demulsifier (ME-DeM) on a range of crude oils. The results showed effectiveness of the microemulsion-demulsifier, ME-DeM, compared with commercially available non-microemulsion based demulsifiers. Liu et al. (2010) discussed the benefits of applying the microemulsion together with a polymer in hydraulic fracturing. Ali et al. (2011) studied microemulsions in wettability alteration of the rock and resulted that the amount of water imbibed into the formation was reduced after using microemulsion. Nguyen (2013) developed a microemulsion as a flowback aid added to stimulation fluid that showed enhanced relative oil and gas permeabilities.

Several field examples of microemulsion additive treatments were presented for different oil and gas basins, including the D.J. of Colorado, San Juan of New Mexico and Colorado, Uintah of Utah, Raton of Colorado, Green River, Pinedale, and Gig Horn of

Wyoming, Forth worth of Texas and Williston of North Dakota (Pursley et al. 2004; Penny et al. 2005). In the majority of the wells, productivity enhancement was obtained. Water recovery and producibility were increased more than 50% in some of the wells. Lower lifting costs have been reported for some of the wells that were treated by microemulsions (Pursley et al. 2004; Penny et al. 2005).

Although many studies have been conducted to investigate microemulsions in recovery enhancement, many aspects of the microemulsion interactions with the rock are still poorly understood. Most of the studies described above were conducted on oil-water-rock systems instead of gas-water-rock systems. Some of these studies explained the increased production by wettability alteration, but they did not demonstrate that the wettability had been altered.

This work describes the formulation and use of microemulsions instead of conventional surfactant systems in order to reduce the capillary pressure and capillary end effects by reducing both the interfacial tension between the injected fluid and the gas and the interfacial tension between the injected fluid and the reservoir rock. Microemulsions can be dispersed in the treating fluid, whether water or oil based. It can overcome the capillary forces that "trap" condensate or water in a porous medium by having a low interfacial tension between the microemulsion phase and the excess oil and/or water phases. A newly developed microemulsion (Nguyen 2013) formulated with a blend of anionic, nonionic surfactants, short chain alcohol, oil and water was tested and showed a significant reduction in the surface tension between water and nitrogen gas, when compared with mutual solvent and fluoropolymer surfactant solutions

Objectives

The research in this study was designed to answer the questions regarding the effects of microemulsions in changing rock wettability. This study will investigate improving gas permeability and reduction in capillary pressure in gas bearing formations.

Microemulsion was first characterized by measuring droplet size of the microemulsion-V. Surface tension of the microemulsions was measured and compared with conventional surfactant solutions. Then thermal stability of these chemicals was investigated for temperatures up to 400°F after 24 hours. The compatibility of the microemulsions were tested for three types of microemulsions with 2 wt% brine solutions and condensate. The rock was characterized by running X-ray diffraction (XRD) on the rock samples to determine bulk and clay mineralogy. The fluid-rock interactions were studied by measuring the electrical charges at fluid/rock interfaces using zeta potential technique.

The contact angle technique was used to study the effect of microemulsions in reducing interfacial tension and capillary pressure and changing wetting characteristics of the surface.

Coreflood tests on Bandera sandstone cores with permeability greater than 10 md were performed to investigate the potential of microemulsions to improve gas permeability and fluid recovery in gas bearing formations.

In addition, the effect of salinity and aging were investigated to determine the factors that are important in the performance of the microemulsions.

By completing this research, we developed an investigation for a chemical treatment that improves the unconventional resource recovery. We developed an experimental procedure through a focused research program that helps technically recoverable unconventional gas resource to economically recoverable gas that can be harvested in an environmentally sound manner.

Dissertation Outline

First part after introduction explains the phase trapping phenomena and the methods to prevent and remove the trapped fluid.

Next part presents the chemistry of microemulsions and their applications in oil/gas industry.

Then the procedures of the conducted experiments and the apparatus used in this study is presented. The properties of the fluids and rocks that were used in the experiments are presented.

The results are presented next, including the fluid characteristics such as droplet size measurement, surface tension, and thermal stability studies of microemulsions in comparison to the conventional surfactant solutions. The rock was characterized by bulk and clay analysis for out crop and reservoir shale rock samples. The fluid-rock interactions were investigated. Tests including coreflood experiments that were run to investigate the potential of microemulsions in improving gas recovery and effective gas permeability in gas bearing formations with permeabilities greater than 10 md. Contact angle technique was used to study the effect of microemulsions on reducing interfacial tension and

capillary pressure. Furthermore, the electrical charges at fluid/rock interfaces were measured using zeta potential technique.

The effect of salinity and aging on microemulsion performance and fluid-rock interactions is presented then.

And finally, last chapter summarizes the dissertation with conclusions and recommendations.

Phase Trapping

One of the common formation damages in oil, gas or water bearing formations is phase trapping which can cause significant productivity reduction. The phase trapping could be temporary or permanent after introducing a fluid into the porous media during drilling and completion operations. In wet gas reservoirs, condensate trapping is a result of reservoir depletion when pressure drops below the dew point pressure and causes permeability reduction and impairs well productivity.

In gas producing formation aqueous phase trapping is caused by water-based fluid injection during drilling, completion or kills fluid.

Capillary pressure and relative permeability are the main factors in creation of phase trapping. These two factors are functions of pore geometry, interfacial tension between the invading trapped fluid and the produced reservoir fluid, wettability, and fluid saturation levels. Phase trapping also depends on depth of fluid penetration, reservoir pressure, temperature, and drawdown potentials (Bennion et al. 2006). Capillary pressure can be expressed with Eq. 1.

$$Pc = \frac{2\sigma cos\theta}{Rp} \quad \text{(1)}$$

Where

P_c = capillary pressure

R_p = pore throat radius

σ= interfacial tension

θ= contact angle, degrees

Two general approaches can be considered for phase trapping issues in the reservoirs that have the potential to be damaged. The preferred approach is to design a drilling, completion, and production operation that prevent or minimize the phase trapping. The other approach, which is more common in the industry, is to use conventional drilling, completion and production practices and then try to remove the damage created by phase trapping.

Prevention of Phase Trapping

Original reservoir conditions of fluid saturation, pore geometry, and wettability are factors that should be understood to avoid phase trapping. When designing a drilling or completion operation following recommendations will help to minimize phase trapping:

Using fluids mutually miscible with producing reservoir fluids

Using of hydrocarbon based fluids in water wet sandstone or carbonate oil reservoirs with low initial water saturation, will result in no external water being introduced into the formation and the fluid saturations and wettability remaining unchanged and eliminating the potential for phase trapping (Bennion et al. 2006). Using air/foamed based drilling in tight gas reservoirs at low water saturation conditions (Bennion et al. 1994; Nasr-El-Din et al. 2002; Davis and Wood 2004), water based fluids for water injection and disposal wells (Zhang et al. 1993; Lingen et al. 1996), as well as nitrogen, air, or carbon dioxide in some gas reservoir applications are examples of these situations.

Using non-polar hydrocarbon based fluids in tight gas reservoirs

Not having the wetting/spreading affinity for the naturally water wet surface of the reservoir, combined with the significantly lower interfacial tension (IFT) between natural gases and light refined oils vs. water, non-polar oils have are great candidates to prevent water blockage. Less total fluid being retained in contrast to water based system in the same circumstances (Bennion et al. 1996; Bennion et al. 2000a; Bennion et al. 2000b).

Reducing Invasion Depth

Using of low density drilling and completion fluids or underbalanced drilling/completion operations, combined with improving fluid rheology and filter cake building ability to reduce fluid loss potential, causes invasion depth during drilling and conventional completion operations to be reduced. In fracturing job, the volume of injected fluid required to propagate the hydraulic frac generally exceeds the volume of the closed fracture by about 20 times. This results in invasion depth being greater in these applications than would normally be associated with a conventional overbalanced drilling and completion operation (Bennion et al. 2006).

Increasing Reservoir Drive Energy

Capillary drawdown gradient is also directly impacted by available reservoir pressure. Larger drawdown gradients will be applied in high pressure formations. Low pressure or depleted formations have little drive energy to unload and recover trapped fluids. Invasion depth is increased in low pressure reservoirs due to the fact that higher overbalance pressures are present resulting in the potential for increased fluid loss and invasion in conventional overbalanced drilling and completion operations in contrast to

normally pressured or over pressured formations. Energized fluid systems, where either nitrogen or dense phase carbon dioxide are entrained in the injected water or oil based fluid, can combat this effect in low pressure situations when fracturing operations are considered. The capillary gradient will be increased and the recovery of the introduced fluid to the formation will be improved, since presence of these gases acts to both reduce the total volume of oil or water phase entering the reservoir as a potentially trapping fluid and provides an area of localized assisted high pressure for flowback.

In high pressure environments where bottomhole drawdown pressures will still remain high enough on the flowback phase, nitrogen is used. In these situations, carbon dioxide would remain as a relatively incompressible dense fluid and provide limited expansion to assist in the recovery of the trapped filtrate. The highly compressible nature of nitrogen allows it to retain the ability to provide compressible drive energy under pressure reduction conditions at even very high pressures. Carbon dioxide has greater water carrying capacity, higher solubility in oil and water and lower interfacial tension, compared to the nitrogen gas.

Significant drive energy can be obtained if low enough flowback pressures in the area of the fracture face exist, and the volumetric transition from dense phase to gas phase for carbon dioxide happens. To prevent the entrained, low viscosity gas from dispersing from the area surrounding the fracture face into the bulk formation, rapid flowback after the fracture treatment is essential for both gases (Bennion et al. 1996; Bennion et al. 2006).

Reducing Interfacial Tension

Phase trapping is mainly created by capillary pressure which is a function of interfacial tension and contact angle. At a given level of reservoir pressure/drawdown, reducing the interfacial tension between the trapped fluid and the producing/injected reservoir fluid reduces the capillary pressure and makes the recovery of the trapped fluid much easier. Using proper blend of surfactants can create a low interfacial tension. Effective contact, adsorption and emulsion issues are the main limitations of using these chemicals.

Interfacial reducing agents include light alcohols for dry gas situations, heavier alcohols such as propanol, butanol for reservoir applications containing both gas, water and liquid hydrocarbons, various glycol solutions, liquid phase carbon dioxide, and various surface tension reducers (water based) to reduce water-gas surface tension for gas reservoir applications (Bennion et al. 2006).

Transient Wettability Modifiers

By changing the preferential wettability of the rock surface in the reservoir, the capillary pressure can be reduced. Strong capillary pressure effects are created in strongly water wet and oil wet porous media which have contact angles of near zero or 180 degrees respectively. There is less spreading tendency for either water or oil on the surface of the formation, when the wettability moves to a more neutral condition and the cosine of the contact angle approaches zero and capillary pressure decreases (Vijapurapu and Rao 2003).

Transient wettability modifiers, temporarily alter the surface chemistry of the water wet surface of the solid to a more neutral wet condition which facilitates the sheeting/filming of the water off the surface. Their use as a low concentration, low cost, environmentally friendly alternative to some of the materials make these chemicals a potential candidate to be applied in industry (Bennion et al. 2006).

Removal of Existing Phase Traps

Remediation methods are more challenging compare to the prevention methods due to limitations such as obtaining effective contact with trapped filtrates. Therefore prevention is generally far more effective in the long term from an economic perspective than remediation. If the volume of trapped fluid is relatively small and localized to the immediate vicinity of the wellbore/frac face area, there are techniques that can be considered (Nasr-El-Din et al. 2002). Potential options include high drawdown pressures for water and hydrocarbon phase traps, static repressurization for hydrocarbon phase traps, extended flow for water based phase traps, static shut in/imbibition which is primarily applicable for water based phase traps, dry gas injection for water based phase traps, formation heat treatment for water based phase traps, lean gas injection for hydrocarbon based phase traps, rich gas injection for hydrocarbon phase traps, in-situ combustion for hydrocarbon phase traps, water displacement for hydrocarbon phase traps, carbon dioxide injection for water and hydrocarbon phase traps, mutual solvent injection for water and hydrocarbon phase traps, surface tension agent reducer injection for water and hydrocarbon phase traps, acid injection for water and hydrocarbon based phase traps,

wettability modification for water based phase traps (Hamberlin et al. 1990; Bennion et al. 2006).

High drawdown pressure

By increasing capillary pressure gradient, more trapped fluid is recovered and less trapped fluid saturation is created. One cause of increasing capillary pressure gradient is increased drawdown pressure. In tight gas reservoir which are sub normally saturated, capillary pressure becomes very high at relatively high water saturations, and this method is not effective. Usually the drawdown in not enough to fully mobilize the water saturation value back to the original subnormal value.

In retrograde gases, condensate phase traps cannot be removed by this method. By increasing the drawdown pressure in these reservoirs, the volume of the liquid retrograding from the gas phase is increasing in the near wellbore region and severe the condensates phase trapping (Bennion et al. 2006; Noh and Firoozabadi 2008).

Static Pressure Buildup

This method is used for condensate traps in rich gas wells when drawdown pressures are high. After temporary shutting the well, the pressure starts to buildup in the reservoir to a value above the original dew point pressure of the gas and subsequent revaporization of the condensate. But this method is not very successful, since condensate is separated out from a large volume of flowing gas phase and now is in static contact with only a very limited gas volume (Bennion et al. 2006).

Extended Reservoir Flow

Long term evaporative effect will cause removing of trapped water and the permeability will improve due to the fact that water carrying capacity of natural gases increases with decreasing in pressure. Several lab studies investigate this method in a controlled lab environment by injecting very large volume of the gas to the core samples. In real filed applications, this method is not very effective since only a small volume of liquid would be removed unless gas flow rates are extremely high. Only high permeability porous media in which phase trapping problems are not significant can have such a high gas flow rate (Penny et al. 1983; Bennion et al. 2006).

Static Shut in

Imbibition of the trapped phase which has the same wetting characteristics as that exists in the reservoir will disperse the fluid deeper into the formation and the saturation in the near wellbore area is decreasing. The formation permeability and wettability characteristics are the most important factors in determining the speed of this process. Matrix permeability in the range of 0.5 to 2 md showed the most effective permeabilities for this method. In this range of permeability, the cleanup of phase trapping might take weeks to months instead rather than years. The formation has enough low permeability that trap the fluid, but high enough to allow imbibition to proceed at reasonable rates. Static shut in showed the best results for theses reservoirs compare to the flowing wells where drawdown slows the rate of imbibition of the trapped fluid back into the formation (Bennion et al. 2006; Noh and Firoozabadi 2008).

Dry Gas Injection

In this method, the mobile water is displaced and trapped water is dehydrated by injecting dehydrated methane or nitrogen gas to the wellbore. Only small volume of the water can be displaced since the natural gases has low evaporation capacity. This technique is not suitable for highly saline trapped water (over 100,000 ppm), since it might cause precipitations of the salts and plugging the pores during evaporation process (Branagan et al. 1981; Bennion et al. 2006).

Formation Heat Treatment

The evaporation rate could be increased by increasing the temperature applied by electrically powered downhole heating tools (Jamaluddin et al 1996). This method is not successful due to the limited radius of effective treatment (Bennion et al. 2006).

Lean Gas Injection

When a good source of lean methane gas is available, trapped condensate or light hydrocarbon liquids can be removed from the fracture face or near wellbore area by miscible vaporizing/displacing of the trapped fluid using gas cycling operations. Nitrogen is usually used to increase the pressure since this method needs high contact pressure (35-40 MPa) to be successful (Luo et al. 2001; Bennion et al. 2006).

Rich Gas Injection

At moderate low pressures, miscible displacement and extraction of light to mid-gravity hydrocarbon/condensate phase traps can be achieved by CO_2, ethane, propane, and butane injection (Gupta and Leshchyshyn 2005). Incompatibility of the injected solvent

with the trapped hydrocarbon liquid might cause deasphalting and plug the pore throat (Bennion et al. 2006).

In-Situ Combustion

Another method is auto-ignition of trapped light hydrocarbon/condensate saturations by injecting air or enriched air in the near wellbore region. The application of this method is limited due to potential downhole explosions on return flow (Bennion et al. 2006; Oskouei et al. 2010).

Water Displacement

This method is water injection followed by dry gas injection. Nitrogen gas is usually used in high permeability formations (1000 md plus) to displace condensate traps from near wellbore regions. Low permeability reservoirs are less successful because of potential water based fluid trapping due to relative permeability and capillary pressure issues (Bennion et al. 2006).

Dense Phase CO_2 Injection

One of the effective methods to remove both water and hydrocarbon based phase traps is use of carbon dioxide which has high solubility in both water and hydrocarbons and can generate low gas-brine interfacial tension and zero or near zero gas-oil interfacial tension. Effective contact and incompatibility between CO_2 and some hydrocarbon liquids from the asphaltene precipitation are the most limiting factors in using this method (Gupta and Leshchyshyn 2005; Bennion et al. 2006).

Mutual Solvent Displacement

Another method that can reduce interfacial tension and increase volatility of trapped water and hydrocarbon phases is use of mutual solvents such as light and heavy alcohols, glycols. The major challenges for this method would be effective contact and potential compatibility issues between light alcohols, such as methanol, and many liquid hydrocarbons (Hamberlin et al. 1990; Bennion et al. 2006).

Surfactant Treatments

To remove both hydrocarbon and water based phase traps, surface active agents or surfactants have been used and discussed in many papers (Vijapurapu and Rao 2003). These chemicals reduce the interfacial tension/surface tension between injected and producing fluid and as a result enhance the removal of water trapping by decreasing the capillary pressure in low permeability reservoirs (Bennion et al. 2006).

Acid Treatments

In an acid soluble formation like carbonate, acid treatment can reduce capillary pressure by dissolution of the matrix which increase the pore throat radius (Sayed and Nasr-El-Din 2013).

Trapping of spent acid phase, potential sludge, emulsion creation, and precipitations between the in-situ fluids and spent acid are the most limiting factors to be considered for this method. Proper design and acid selection can help reducing or eliminating these issues (Bennion et al. 2006).

Wettability Modification

To temporary change the wettability characteristics of the rock surface, chemicals called transient wettability modifiers can be used. More neutral wet condition is achieved by use of these chemicals to reduce capillary pressure and increase the ability of the formation release trapped water based fluids. Again, the main issue to be considered for this method is effective contact in the trapped zone (Noh and Firouzabadi 2008; Vijapurapu and Rao 2003).

In all these methods presented above, the effective contact of the phase trapped zone is very important factor. Designing appropriate drilling, completion and production practices as a preventing method can result in better net present value in almost any situation where the potential for phase trapping induced formation damage exists (Bennion et al. 2006).

MICROEMULSION CHEMISTRY, PROPERTIES AND APPLICATIONS

Microemulsion Chemistry

According to Santanna et al. (2012), "Microemulsions are thermodynamically stable, isotropic, and macroscopically homogenous dispersion of two immiscible fluids, generally oil and water, stabilized with surfactant molecules, either alone or mixed with a co-surfactant." Cosurfactant is a non-ionic molecule such as a short chain of alcohols or an amine that has the function of stabilizing a microemulsified system by decreasing the repulsion forces between the hydrophilic parts of the surfactant.

It is important to consider the differences between emulsions and microemulsions to optimize the design of their applications. Microemulsions are a particular type of colloidal system and the typical dimensions of the local structure explains why microemulsions are transparent. The relative oil and water domains that form in microemulsion systems are usually so small in an order of 10-20 nm in diameter, and they do not scatter light. For the sake of comparison, in emulsion systems, the structures are large enough to scatter light and as such they appear as cloudy colloidal solutions. **Table 1** shows the main differences between emulsion and microemulsion.

Table 1—Main differences between emulsions and microemulsions (Santanna et al. 2012).

Emulsion	Microemulsion
Unstable, with eventual phase separation	Thermodynamically stable
Relatively large-sized droplets (1-10 μm)	Small aggregates (around a few tens of nanometers)
Relatively static systems	Highly dynamic systems
Moderately large interfacial area	Very high interfacial area
Small amount of surfactant required for stabilization	Large amount of surfactant required for stabilization
Low curvature of the water-oil interface	Interfacial film may be highly curved

Friberg and Bothorel (1987) classified microemulsion equilibrium to four types of systems: WINSOR I (WI), where the microemulsion phase is in equilibrium with an organic phase in excess; WINSOR II (WII), where the microemulsion phase is in equilibrium with an aqueous phase in excess; WINSOR III (WIII), where the microemulsion phase is in equilibrium with both aqueous and organic phases (three-phase system); and WINSOR IV (WIV), which is a one-phase system in a macroscopic scale as can be seen in **Fig. 1**.

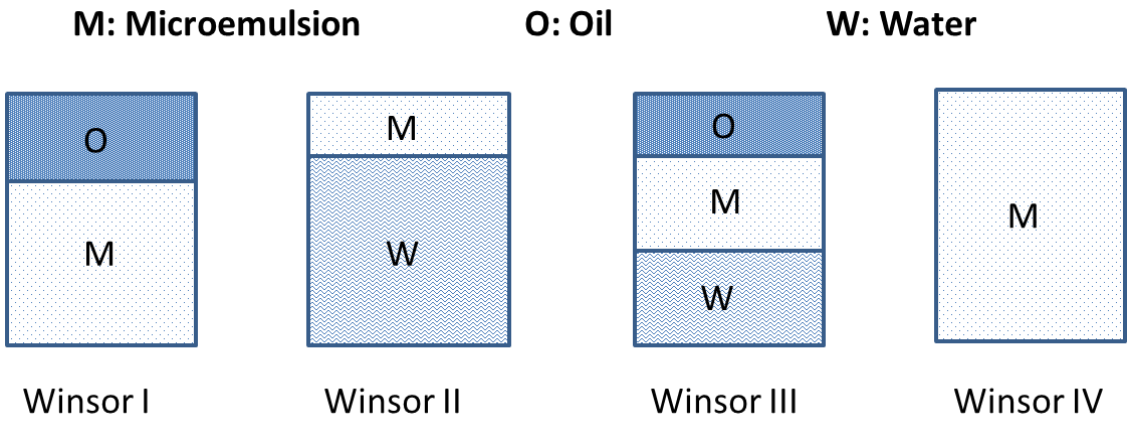

Fig. 1—Schematic showing Winsor's classification (Friberg and Bothorel 1987).

Water, oil, surfactant, and cosurfactant are the main four constituents of microemulsions that can be represented by a pseudo ternary diagram as shown in **Fig. 2**. Each corner of the phase diagram represents a pure compound. Each side represents the different compositions of a blend of two components, and a point inside the diagram represents the composition of a blend of the three components. Near the oil corner, where the water content of microemulsion is low, the local structure consists of swollen inverse

micelles. Surfactant and co-surfactant molecules are disposed on the interface between water and oil (AMETECH 2012).

The shape and the volume of the hydrophilic core of the inverse micelle expands, as the water content increases. At a given water content, there exist a continuous water path; the water phase becomes continuous. The water and the oil phase make an interpenetrated bi-continuous network. The microemulsion looks like a direct miceller solution, near the water corner, where the oil content is low.

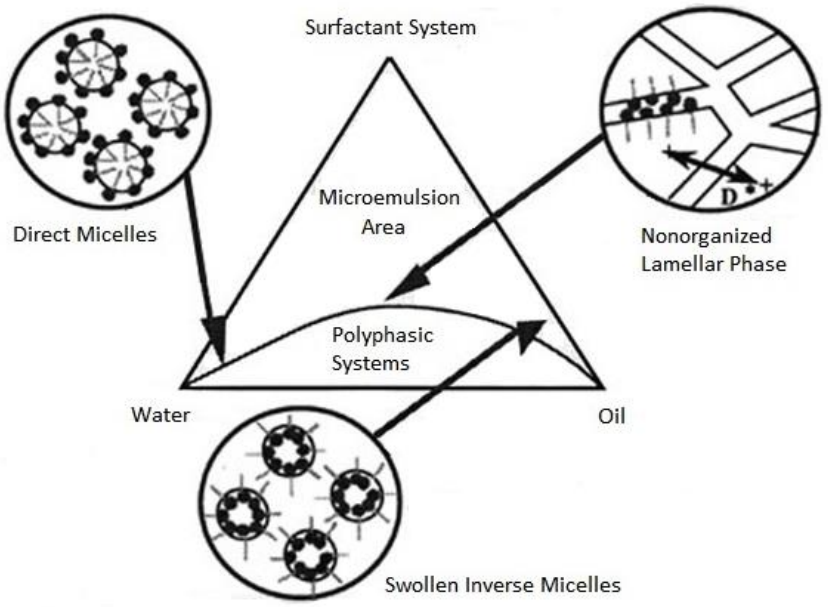

Fig. 2—Constituents of microemulsions that can be represented by pseudo ternary diagram (AMETECH 2012).

Solvents can be added to the microemulsion system to enhance the performance. High flash point, non-toxicity, and high solubilizing properties of the active ingredient (to avoid crystallization during storage) are some of the criteria for the choice of a solvent.

Surfactants are basic components in microemulsions. To obtain a stable formulation over a large temperature range, appropriate surfactants and co-surfactants should be found. Microemulsions require quite high concentrations of surfactants (typically 2 to 30%). This high amount is due to the small size of the oil and water domains and so to the large area of the interface. By optimizing the choice of surfactant and co-surfactant, this amount can be reduced. A blend of non-ionic and anionic surfactants is recommended to achieve the physical stability vs. temperature. This effect is illustrated in **Fig**. **3**. It represents the affinity of a surfactant (non-ionic or anionic) with oil or water at different temperatures. A non-ionic surfactant has a better affinity with oil (area b) at high temperature and at a lower temperature it has a better affinity with water (area a). For anionic surfactant, it is the contrary.

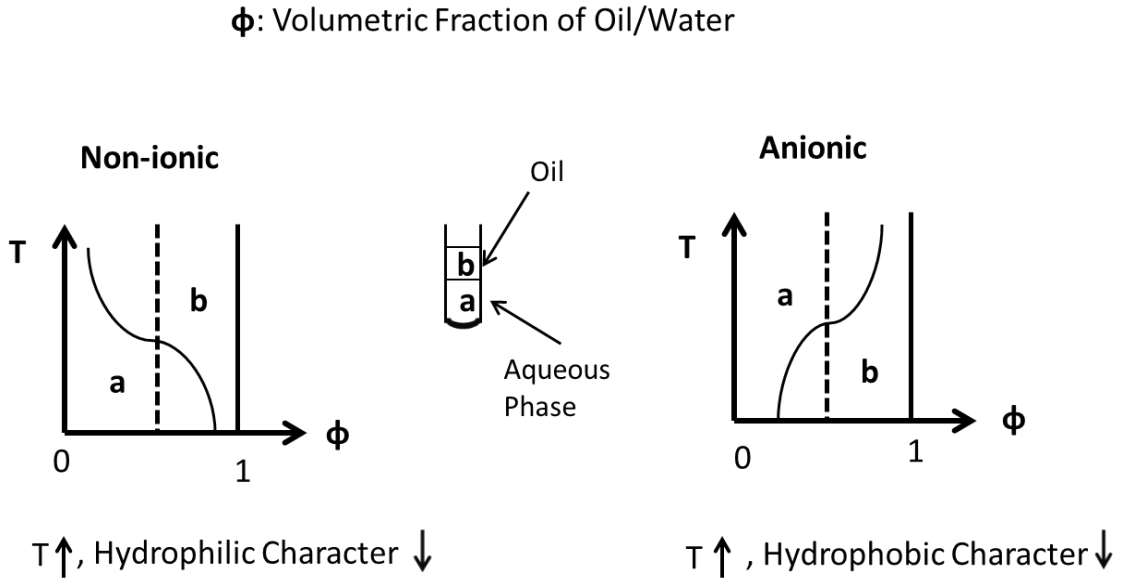

Fig. 3—Microemulsion blend physical stability vs. temperature. (a) is the aqueous phase and (b) is oil (AMETECH 2012).

It is possible to combine these effects and obtain a microemulsion that remains stable over a large range of temperature by blending non-ionic and anionic surfactant. To obtain the best thermal stability, the ratio between these emulsifiers must be optimized (AMETECH 2012). Co-surfactant is often added to the mixture to increase the solubilizing power of the surfactant system. Small molecules which have a great affinity for oil/water interface are the best co-surfactants. They have to be chosen according to the nature of the surfactants and to the nature of the oil to be microemulsified.

Application of Microemulsions in Oil and Gas Industry

Hydraulic Fracturing

Samuel et al. (1999) developed a surfactant based polymer-free fluid. The surfactant was a quaternary ammonium salt, derived from a long-chain fatty acid. The results of the viscosity measurement showed that in brine, the fluid viscosity occurs due to the formation of elongated worm-like micelles. When the fluid is exposed to hydrocarbons or diluted with formation water breaking occurs. Then, no conventional breaker is needed and the produced oil or gas can act as breaker for this fluid system.

A surfactant-based gel was developed by Castro Dantas et al. (2003). The fluid composition was 18 wt % soap, 9 wt% isoamyl alcohol, 14 wt% pine oil, and 59 wt% water. The results of the tests on the solution showed that the capacity of the surfactant-based solution to sustain the ceramic 16/20 mesh in function of time was great. The authors concluded that the surfactant based solutions had compatible characteristics when compared with the hydroxypropylguar.

Liu et al. (2010) discussed the benefits of applying the microemulsion together with a polymer in hydraulic fracturing. This fluid was a combination of a single phase microemulsion and a gelled polymer system. A series of comparative experiments were performed with new fluid and conventional gel without microemulsion. In the solutions that contained microemulsion, micelles assembled in a group, forming microscopic spheres, rods, and plates that can create a deformable barrier, reducing leak off protection on the surface of the fractured rock. From different measurements obtained, it was observed that properties of the microemulsified solution were more predominant than conventional fluids. This solutions was a great candidate for reducing formation damage and lowering the initial cleanup pressure.

Break Down Emulsions

Rock pore clogging is a formation damage which is caused by injection of drilling and completion fluid. To restore the permeability of the rock acid solutions are added which can promote the formation of highly viscous emulsions and dregs. The formation of emulsions and dregs during the well stimulation process is a serious problem and can result in large losses of oil (Castro Dantas et al., 2001a). Application of microemulsions is a proposed alternatives to break down emulsions which suggested by many studies.

Castro Dantas et al. (2001a) used a microemulsion system for breaking down the petroleum emulsions. The microemulsion systems studied were composed of HCl 5.2% solution; toluene; and isopropyl alcohol (C)/surfactants (S), with a ratio C/S of 9.0.

A direct contact method between the microemulsions and crude (W/O) emulsions was used to evaluate the microemulsion efficiency to break down oil emulsion. All

systems were achieved to a good percentage of emulsions breakdown. The results indicated that the breakdown efficiency is directly dependent on the microemulsion composition and the physicochemical properties of the oil.

The authors concluded that some commercial surfactants used for the formation of microemulsion systems were able to completely break down oil emulsions formed during production operations of Brazilian petroleum fluids.

Corrosion Inhibitor

Saline media is the best one for corrosion in petroleum industry. Localized pitting corrosion is a common type of corrosion that acts in the inner walls of oil pipelines. Surfactant molecules can act as corrosion inhibitors in order to minimize and control corrosion. Surfactant molecules form films on metallic surfaces that protect them from corrosion by impairing the action of electrolytes. The adsorption of surfactants on metal surfaces depends on the structure and concentration of surfactant molecules in the contacting medium determining the final adsorption layout with the formation of monolayers or multilayers of surfactant molecules (Reyes et al. 2005).

The microemulsions also have the characteristic of adsorbing onto interfaces. When microemulsions are used, an oil film is adsorbed onto the surface with the surfactants tails oriented towards it, in view of the usually positive character of the surface.

The anticorrosion capacity can be tested by electrochemical cells. A reference electrode, a counter electrode, and a work electrode are used in such assays. These electrodes are immersed in the corrosive medium, which can be a saline or acidic solution, with or without an inhibitor. The reference electrode is involved directly in the corrosion

potential measurements, from which anodic and cathodic polarizations are affected. The counter electrode is used as an auxiliary to complete the cell and balance charges.

Moura et al. (2009) studied the anticorrosion ability of three novel surfactant molecules in solution and microemulsion media. Adsorption phenomenon was studied electrochemically and the Frumkin isotherm model indicated that the surfactant solutions tested can inhibit corrosion with levels as high as 95%. The authors verified that the chemical groups attached to the hydrocarbon chains enable adsorption phenomena with different levels of intensity at the surface. When in solution, surfactants behave as better inhibitors, if compared to microemulsion systems. This comparison provides clear evidence that the adsorption promoted by miceller solutions is stronger than microemulsion systems. Microemulsion systems also interact with the metallic surface, although via a less intense physical mechanism. On the other hand, the microemulsion systems, although featuring relatively lower performance, are advantageous considering that they are able to dissolve more active matter.

Enhanced Oil Recovery

Thermal methods, miscible methods, and chemical methods are the main classifications of the enhanced oil recovery applications. Microemulsion flooding is included into chemical methods classification.

High viscosity and having a low interfacial tension, and increasing oil extraction efficiency are the main and unique properties of the microemulsion systems that help enhance oil recovery (Santanna et al. 2009).

Very low interfacial tension that have been attained between the contacting oil and water micro phases that are constituent of the microemulsion systems make these chemicals a great candidate in enhanced oil recovery Gurgel et al. (2008). This results in flowing microemulsions more easily through the porous medium, which enhance oil extraction performance rates.

According to Babadagli (2005), surfactant solution is the most common chemical injection technique that have been used in several oil fields as a tertiary oil recovery method. The advantages of using surfactant is its relatively lower cost when compared to miceller or microemulsion injection.

To optimize the technique of chemical injection, operation costs and/or reduce the amount of treated material, are the factors that should be considered. Babadagli (2005) studied the injection of several pore volumes of microemulsion into the sandstone plugs, which contained 35% of residual oil, observing a linear relationship between the values of injected pore volumes and the oil recovery. Very low interfacial tension between aqueous and oily phases as well as improved solubilization for both polar and non-polar compounds are the most desirable properties of microemulsion for enhance recovery applications. Microemulsion systems were used in gas reservoirs in order to reduce the capillary pressure by both reducing the surface tension between the injected fluid and gas and also the interfacial tension between the injected fluid and the reservoir rock (Pursely et al. 2004; Penney et al. 2005).

Alternative Fuel

Possibility of using microemulsified systems as alternative fuels was introduced by several authors (Castro Dantas et al. 2001b; Ochoterena et al. 2010; Lif et al. 2010; Dantas Neto et al. 2011).

Castro Dantas et al. (2001b) studied a microemulsified systems containing diesel and different percentage of vegetable oils (soy, palm and castor), surfactant, and cosurfactant. The mass ratio of cosurfactant/surfactant and composition of oil phase are the main parameters that affect formation of microemulsions. Among all studied systems, microemulsions containing diesel and soy oil could be formed over the widest composition range, indicating the possibility to apply them as alternative fuels. Engine performance and emissions with the use of this new fuel were assessed. Their results for specific fuel consumption showed that the presence of water in microemulsions improves diesel fuel combustion. Carbon dioxide emissions were higher for the diesel/surfactant blend as well as all microemulsion fuels. Nevertheless, this difference decreased with increasing engine power when compared with neat diesel. The values of NOx emissions increased with increasing engine power, and decreased with increasing water content in the microemulsion fuels. They also observed a reduction in black smoke emissions for all microemulsion fuels tested, as compared with neat diesel. This was attributed to a better combustion reaction effected in the presence of water and surfactant, thereby reducing the formation of black smoke.

This projects aims to show the applications of microemulsions in enhancing the gas productivity of gas bearing formations by decreasing the interfacial tension and

enhancing the relative permeability to gas. This study compares the microemulsion system with conventional anionic, non-ionic, and cationic surfactants and identifies the effectiveness of microemulsions in enhancing permeability to gas and mitigating aqueous phase trapping by conducting coreflood experiments.

EXPERIMENTAL APPARATUS AND PROCEDURE*

Materials

Brine (2 wt% KCl) and nitrogen were used as aqueous and gaseous phases, respectively, in the coreflood experiments. The density and viscosity of the brine were 1.02 g/cm^3 and 0.97 cp, respectively at 70°F. The surface tension between the nitrogen gas and the brine was 73 Nm/m at ambient conditions. The synthetic condensate was the oleic phase in some of the coreflood experiments. It is a mixture of short chain hydrocarbons (C_6-C_{12}). The specific gravity of synthetic condensate was 0.82 at 70°F. It had a density of 0.816 g/cm^3 and a viscosity of 1.54 cp at 70°F. Coreflood experimental conditions were 165°F and there was a back pressure of 700 psi at the outlet. This resulted in the supercritical state of the nitrogen at the inlet which was above the nitrogen critical temperature (-232.6°F) and critical pressure (493 psi). Based on the national institute of standards and technology (NIST) data, the density and viscosity of nitrogen gas were 0.001160 g/ml and 0.01763 cp, respectively at room temperature and pressure. At the supercritical state of the core inlet, the values of density and viscosity of nitrogen were 0.04643 g/ml and 0.02069 cp, respectively (NIST 2012).

Three microemulsions (ME-V, ME-N, and ME-E) were used in the compatibility tests to assess the potential microemulsions for the coreflood experiments.

---

*Part of this chapter is reprinted with permission from *Improving Gas Relative Permeability in Tight Gas Formations by Using Microemulsions* by A. Rostami, D.T. Nguyen, H.A. Nasr El Din, 2014, Paper IPTC 17675, Copyright [2014] by International Petroleum Technology Conference. And *Microemulsion vs. Surfactant Assisted Gas Recovery in Low Permeability Formations with Water Blockage* by A. Rostami and H.A. Nasr El Din, 2014, Paper SPE 169582, Copyright [2014] by Society of Petroleum Engineers.

Two of them, ME-V and ME-E, were used to alter the wettability of the core plugs to preferentially gas-wetting. Microemulsions were a blend of anionic surfactant, nonionic surfactant, short-chain alcohol, and water. Different surfactants and solvents were used in the structure of these three microemulsions. The chemistry of the microemulsions ME-E and ME-N, was not disclosed by the company that provided the samples. Microemulsion ME-V had 6 wt% sulfated alcohol (C12) as anionic surfactant, 15 wt% ethoxylated alcohol (C13) as nonionic surfactant, 15 wt% isopropyl alcohol (IPA), 5 wt% oil, and 55 wt% water. The microemulsion with pH of around 7 was prepared at room temperature, and tested for stability at higher temperatures up to 400°F. Microemulsion ME-V had 21 wt% active ingredient (sulfated alcohol (C12) and ethoxylated alcohol (C13)) and was prepared at concentration of 0.2 wt% of chemicals in 2 wt% KCl as the treatment fluid for the tests. The role of alcohol was to tune or adjust the phase behavior of the brine-surfactant-oil system. The addition of a short-chain alcohol as a co-surfactant can increase the total interfacial area at low alcohol concentrations, thus increasing solubilization of surfactant.

A fluoropolymer surfactant and a mutual solvent solution were used in the coreflood experiments with the same concentration and at the same experimental conditions as microemulsions for comparison purposes. Both mutual solvent and fluoropolymer surfactant had been used in controlling the wettability and surface characteristics in the literature (Hamberlin et al. 1990; Noh and Firoozabadi 2008). These chemicals provide water and oil repelling characteristics and change the surface properties of the rock to neutral-wetting.

Bang et al. (2010) used a similar product which was nonionic polymeric fluorinated surfactant in a mixture with an organic solvent as the treatment solution to reduce water and condensate blockage in gas-condensate wells. The selection of appropriate solvents was the most important part of developing a successful chemical treatment in their tests. The fluoropolymer surfactant that was used in this paper was obtained from 3M and DuPont. It had 19-26 wt% fluorinated acrylic copolymer, 74-81 wt% water, and 0.003-0.01 wt% tetramethylsuccinonitrile. Mutual solvent was 30-60 wt% isopropanol, 1-5 wt% ethoxylated alcohol, and 30-60 wt% ethoxylated branched C7-9, C8-rich alcohols. The properties of these chemicals at 165°F are given in **Table 2**. The viscosity was measured using a capillary viscometer and density was measured using an Anton Paar densitometer model DMA 4100/4500/5000 M.

Table 2—Properties of the chemicals used in the coreflood tests at a concentration of 0.2 wt% of chemical in 2 wt% KCl.

Chemical	Density (g/cm^3)	Viscosity (cp)
Fluoropolymer Surfactant at 165°F	0.974	0.97
Microemulsion-V at 165°F	0.973	0.95
Microemulsion-E at 165°F	0.972	0.94
Mutual Solvent at 165°F	0.971	0.96
Brine (2 wt% KCl) at 165°F	0.974	0.96
Condensate (not diluted) at 165°F	0.747	1.43

To compare the efficiency of the microemulsions with surfactants, three types of surfactants were used in the tests which included a cationic surfactant, an anionic surfactant, and a non-ionic surfactant. The cationic surfactant (Surf-C) had 45-55% by weight quaternary ammonium compounds, coco alkyl tri-methyl, chlorides, 30-35%

isopropanol, and 10-20% water. The anionic surfactant (Surf-A) was composed of 40 wt% sulfonic acids, C_{14-16}-alkane hydroxyl and C_{14-16}-alkene, sodium salts, 58 wt% water, 1 wt% sodium chloride, and 1 wt% sodium sulfate and trace amounts of formaldehyde. The non-ionic surfactant (Surf-N) consisted of ethoxylated caster oil and trace amounts of ethylene oxide.

Rock Samples

Bandera sandstone cores were used in the coreflood experiments. The mineralogy of Bandera sandstone is given in **Table 3**, while the dimensions and properties of the cores are given in **Table 4**.

Table 3—Mineral composition of Bandera sandstone cores.

Mineral	Concentration (wt%)
Quartz	59
Dolomite	15
Illite	10
Kaolinite	3
Chlorite	1
Albite	12

Table 4—Dimensions and properties of Bandera sandstone cores.

	Core F	Core C	Core D	Core E
Diameter (in.)	1.5	1.5	1.5	1.5
Length (in.)	20	20	20	20
Dry Weight (g)	1221.2	1216.8	1240.2	1213.3
Saturated Weight (g)	1310.2	1295.9	1307.3	1301.5
Pore Volume (cm^3)	89.0	79.1	67.1	88.2
Porosity (vol%)	15.3	13.6	11.5	15.2
Permeability (md)	20.2	21.8	18.1	22.7

Three different shale rocks including outcrop of Barnett shale, Marcellus shale, and reservoir rock of the New Albany shale from Illinois basin were used to investigate fluid-rock interactions. Barnett shale was used for the contact angle measurements.

Bulk and clay mineralogy analysis was performed on these shale rocks using X-ray diffraction (XRD) and results are shown in **Table 5**.

Table 5—Clay and bulk mineralogy results for shale rocks.

		Barnett	Marcellus	New Albany
Clays	Chlorite (ClO^{2-})	0	0	3
	Kaolinite ($Al_2Si_2O_5(OH)_4$)	5	0	0
	Illite/Mica*	31	18	27
	Mx IS (Mixed Layer Illite and Smectite)	16	8	11
Carbonates	Calcite ($CaCO_3$)	1	18	1
	Dolomite ($CaMg(CO_3)_2$)	0	4	1
Other Minerals	Quartz (SiO_2)	33	42	40
	K-Feldspar ($KAlSi_3O8$)	3	0	8
	Plagioclase $(Na,Ca)(Si,Al)_4O_8$	1	4	5
	Pyrite (FeS_2)	4	5	3
	Barite ($BaSO_4$)	0	0	1
	Fluoroapatite $Ca_5(PO_4)_3F$	5	1	Tr
	Anatase (TiO_2)	1	Tr	0

(*) Illite Chemical Formula: $(K,H_3O)(Al,Mg,Fe)_2(Si,Al)_4O_{10}[(OH)_2,(H_2O)]$

Core Preparation

Bandera sandstone cores with dimensions of 1.5 in. diameter by 20 in. length were placed in the oven for 4 hours at 220°F. The weight of the dry core was measured. Then, the core was saturated in 2 wt% KCl under a vacuum for 5 hours and then weighted again.

The pore volume and porosity were calculated using dry and saturated weights as shown in Table 4. The flow was downward through a vertical core.

The brine was injected at a flow rate of 5 cm^3/min and the system started to heat up until it reached 165°F. A solution of 2 wt% KCl was injected until the differential pressure stabilized and the absolute permeability of the core was calculated. The Bandera sandstone cores had absolute liquid permeabilities from 17 to 22 md.

Surface Tension Test

A fully automated tensiometer (Kruss model K-20), which featured a Wilhelmy-type wetting force measurement technique, was used to measure the surface tension of the chemicals at different concentrations at 75°F. Chemicals were diluted in deionized (DI) water. The platinum plate was rinsed with acetone followed by deionized water before starting the measurements. The plate was then flamed to remove any possible organic contaminations. The tensiometer was tested to measure the surface tension of the deionized water before each set of experiments. The reproducibility of the measurements was within $\pm$ 0.2 mN/m. Each test was repeated three times, and the average was reported as the final result for each data point.

When the vertically suspended plate touches the liquid surface, a force (F), which correlates with the surface tension σ acts on the plate. Platinum was chosen since it is chemically inert and easy to clean. Also, platinum can be optimally wetted on account of its very high surface free energy and therefore generally forms a contact θ of 0° ($\cos \theta$ =

1) with liquids. The required variable σ can be calculated directly from the measured force. The tension is calculated using the following equation:

$$\sigma = \frac{F}{L.cos\theta} \quad \text{..... (2)}$$

σ is surface or interfacial tension, N/m

F is force acting on the balance, N

L is wetted length, m

θ contact angle

The surface and interfacial tension measuring range is 1 to 999 mN/m with a resolution of 0.1 mN/m. The temperature range is from -10 to 100°C with a sensor resolution of 0.1°C. Surface tension was measured for different concentrations of microemulsions and surfactant solutions prepared in deionized water and brine solutions at room temperature and atmospheric pressure.

Thermal Stability Test

Aging cells were used to identify the thermal stability of microemulsions after 24 hours in the oven at different temperatures up to 400°F. The aging cells were a pressure vessel constructed of grade 303 or 316 stainless steel and were used for high temperatures up to 400°F. The aging cell walls were protected by the teflon liners shown in **Fig. 4**. A calibrated rupture disk was installed in the inner cap to release pressure at a predetermined set point. The cells were used at 165, 250, and 400°F temperatures in a roller oven with 24 hours of aging time.

Fig. 4—Teflon liner and aging cell for thermal stability tests.

Compatibility Test

Two series of compatibility tests were done to assess the potential microemulsions for the coreflood experiments. The first one was the brine compatibility test, in which the microemulsions were mixed with 2 wt% KCl at a concentration of 0.2 wt% of the microemulsions in 2 wt% KCl. In the second test, the compatibility of the prepared microemulsion treatment fluids with condensate were tested. The microemulsion treatment fluids were mixed with condensate at a ratio of 1:1. A 5 ml sample of the microemulsion treatment fluid was mixed with 5 ml of the condensate, and the mixture was left for 1 hour at ambient conditions. The compatibility tests were investigated visually at room temperature for any color changes, phase separation, or precipitation in the fluids.

Zeta Potential Measurements

The zeta potential analyzer (ZetaPALS, Brookhaven Instrument Corporation) was used to measure the zeta potential. Zeta potential measurement can help with

understanding and controlling the suspension of colloids in the solution. To neutralize a charged colloid, a double layer is formed on the colloid, causing an electro-kinetic potential between the surfaces of the colloid at any point in the mass of the suspending liquid. This voltage difference is in the order of millivolts and is referred to as the surface potential. Zeta potential could be an indication of degree of repulsion between adjacent, similarly charged particles in dispersion. The magnitude of the surface potential is related to the surface charge and thickness of the electrical double layer as shown in **Fig. 5**. A high zeta potential will confer stability for small particles (i.e., the solution or dispersion will resist aggregation). Low potential means that attraction exceeds repulsion and the dispersion will break and flocculate. So, colloids with high zeta potential (negative or positive) are electrically stabilized while colloids with low zeta potentials tend to coagulate or flocculate.

The instrument electrodes were coated with palladium, and He/Ne laser was used as a light source. This determined the electrophoretic mobility of charged, colloid suspensions. Electrophoresis was used for estimating the zeta potential of particulates. In practice, the zeta potential of dispersion is measured by applying an electric field across the dispersion. Particles within the dispersion with a zeta potential migrates toward the electrode of opposite charge with a velocity proportional to the magnitude of the zeta potential. The zeta potential was measured for three types of shale rocks including the outcrop of Barnett, Marcellus, and the reservoir rock of New Albany shale. Shale rocks were grinded and sieved using standard sieves. The rock samples were agitated for 15 minutes in a sieve shaker and separated to 20, 40, 70, and 140 mesh sizes, which corresponded to 841, 400,

210, and 105 μm, respectively. The rock particles with an average size of 105 μm were mixed with the fluid and left for 24 hours before running the test. The fluids were 0.5 wt% of three microemulsions and three types of surfactants in deionized water. Samples were shaken and transferred to a standard four-sided, 1 cm^3 cuvette. A polystyrene cuvette was used to hold 1.2-1.5 cm^3 of the solution samples. A parallel-plate electrode was then inserted into the cuvette and the zeta potential was calculated from the measured electrophoretic mobility. The mobility range for this instrument was 10^{-11} to 10^{-7} $m^2/V.s$.

Fig. 5—The zeta potential indicates the degree of repulsion between adjacent, similarly charged particles in a dispersion

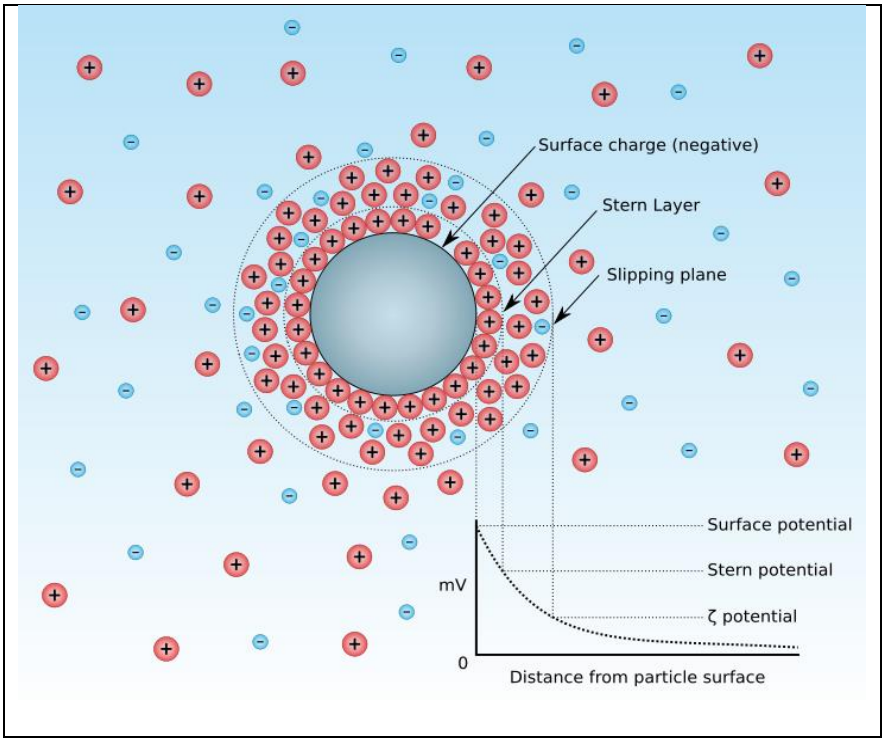

Fig. 5—Continued

Contact Angle Measurements

The high-pressure/high-temperature (HP/HT) drop shape analysis (KRUSS model DSA100) was used to determine contact angle from the shape of sessile drops. It can measure contact angles from 1-180° and surface tensions between 0.01 and 1000 mN/m. The measurement resolution for contact angle was 0.1° and interfacial tension was 0.01 mN/m. A digital camera acquired the image of the droplet. A digital temperature controller was used to increase the temperature gradually to up to 400°F. For each test three drops were evaluated and the average was reported as the final result for each data point. **Fig. 6** shows the instrument used for contact angle measurements. The Barnett shale was cut to

the cubes of size 1.57 cm by 1.83 cm by 0.64 cm. The rocks were put in the oven for 4 hours. The surface of the rock was smoothed by using 600-mesh and then 300-mesh size sand papers to minimize the effect of surface roughness on contact angle measurements. The apparatus was cleaned using acetone and deionized water and the system was tested for leakage before running the experiments. According to Wang and Gupta (1995), contact angle is not sensitive to pressure and only temperature has significant effect on wettability characteristics. Tests were run at atmospheric pressure and 165°F. A stainless steel capillary tube (ID = 0.007 in) was inserted inside the chamber to make a droplet for contact angle measurements.

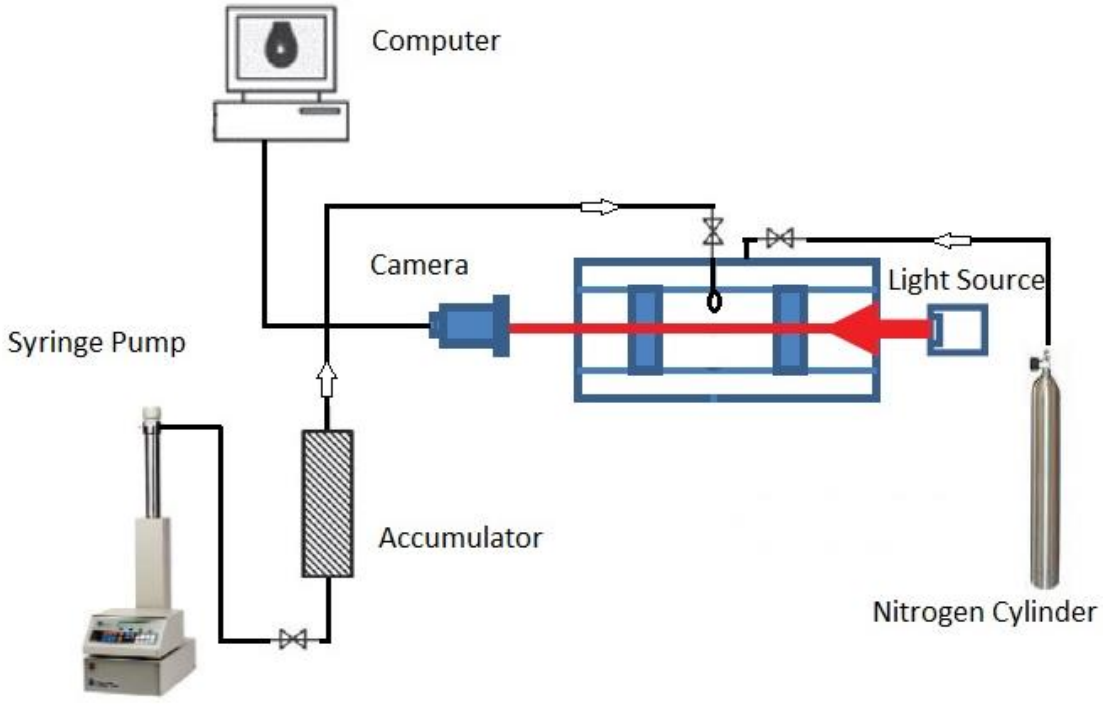

Fig. 6—High temperature/ high pressure drop shape analysis instrument.

Coreflood Experiment

The coreflood setup consisted of a core holder, four accumulators, a syringe pump, and a hydraulic pump, as shown in **Fig. 7**. The core samples were placed in the core holder with a heating jacket around it to simulate reservoir temperature. An ISCO syringe pump was used to inject the fluids that were stored in stainless-steel accumulators at room temperature, into the core at a constant rate. The overburden pressure on the core was applied using a hydraulic pump by injection of hydraulic oil in an oil tank between the internal surface of the core holder and the rubber sleeve that cased the core. The flow was controlled by using two backpressure regulators to avoid any undesirable high pressure after heating the system. One of these was used to regulate the core outlet flow at a pressure of 700 psi and the other to keep the overburden pressure at 1800 psi. A differential pressure transducer was used to measure the pressure drop between the core inlet and outlet. The effluent samples were collected in a compact fraction collector.

Effective gas permeability was measured using the linear flow equation for compressible fluids (Ahmed and McKinney 2005).

$$Q_{sc} = \frac{0.111924\ A\ K\ (P_1^2 - P_2^2)}{TLZ\mu_g} \quad \text{..........} \quad (3)$$

Where

A = cross-sectional area, ft^2

K_{eg} = effective gas permeability, md

L = total length of the core, ft

P_1 = inlet pressure, psi

P_2 = outlet pressure, psi

Q_{sc} = gas flow rate at standard conditions, scf/day

T = temperature, °R

Z = gas compressibility factor, -

μ_g = gas viscosity, cp

Equation (2) is valid for applications when the inlet and outlet pressures are less than 2000 psi. Both inlet and outlet pressures were less than 2000 psi in the coreflood tests. Outlet pressure kept constant at 700 psi and inlet pressure was varied until differential pressure stabilized for each test. The gas viscosity and gas compressibility must be evaluated at 165°F and the average pressure P_{av} as defined in Eq. 4.

$$P_{av} = \sqrt{\frac{P_1^2 - P_2^2}{2}} \quad \text{.....} \quad (4)$$

The Z-factor was determined from Standing-Katz chart, and the viscosity of the gas at 165°F and P_{av} was obtained from the national institute of standards and technology database (NIST 2012).

Bandera sandstone cores with dimensions of 1.5 in. diameter by 20 in. length were placed in the oven for 4 hours at 220°F. The weight of the dry core was measured. Then, the core was saturated in 2 wt% KCl under a vacuum for 5 hours and then weighted again. The pore volume and porosity were calculated using dry and saturated weights.

The flow was downward through a vertical core. The brine was injected at a flow rate of 5 cm^3/min and the system started to heat up until it reached 165°F. A solution of 2 wt% KCl was injected until the differential pressure stabilized and the absolute permeability of the core was calculated. The Bandera sandstone cores had absolute liquid permeabilities from 17 to 22 md. A differential pressure transducer was used to measure

the pressure drop between the core inlet and outlet. The effective gas permeability was compared before and after the treatment.

The effectiveness of the chemical treatments was quantified by calculating the change in the effective gas permeability values before and after treatment by defining the improvement factor (IF) as the ratio of effective gas permeability after treatment to that of before treatment.

$$\text{Improvement Factor} = \frac{k_{gf}}{k_{gi}} \quad \text{...} (5)$$

Where

kgf = final effective permeability to gas, md

kgi = initial effective permeability to gas, md

An inductively coupled plasma optical emission spectroscopy (ICP-OES) model Optima 7000DV, Perkin Elmer, was used to determine the sulfur concentration in the core effluent samples in wash-off test. Sulfated alcohol (C12) and ethoxylated alcohol (C13) were active components of the microemulsion ME-V and used sulfur concentration as an indication of microemulsion adsoption to the core samples.

Corey correlation were used to calculate the gas relative permeabilities using end point relative permeabilities in second set of coreflood tests (Lake 1989).

$$K_{rw} = K_{rwgc}[\frac{S_w - S_{wirr}}{1 - S_{wirr}}]^{nw}, \text{...} (6)$$

$$K_{rg} = K_{rgcw}[\frac{S_g - S_{gc}}{1 - S_{gc} - S_{wirr}}]^{n_g}, \text{...} (7)$$

Where S_w is the brine saturation, S_{wirr} is the irreducible brine saturation, k_{rw} is relative permeability to brine, k_{rwgc} is the end-point relative permeability to brine at S_{gc}, k_{rg} is the

relative permeability to gas, and k_{rgcw} is the end-point relative permeability to gas at S_{wirr} and n_g and n_w are saturation exponents, which were 2.5 and 3.5, respectively.

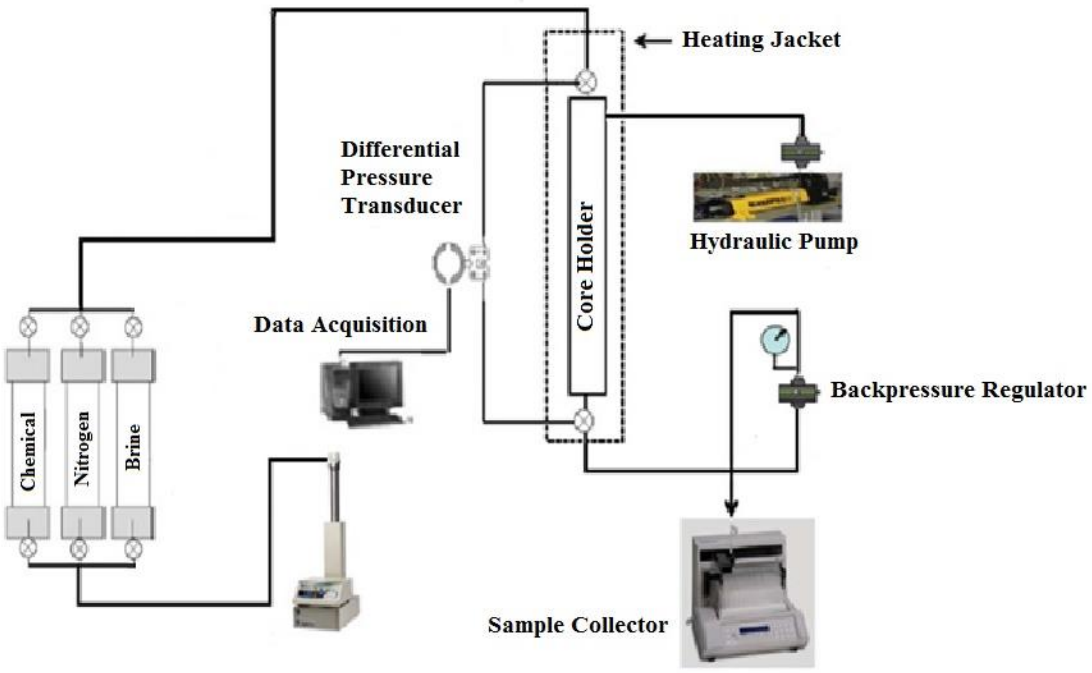

Fig. 7—Coreflood setup used for fluid recovery tests.

Klinkenberg effect corrections were made using linear relationship between the measured gas permeability (k_a) and the reciprocal mean pressure ($\frac{1}{P}$), which is given as:

$$k_a = k_\infty[1 + \frac{b_k}{P}], \quad \ldots\ldots (8)$$

Where b_k is the "gas slippage factor" and k_∞ is the "equivalent liquid permeability" also called Klinkenberg-corrected permeability (Ziarani and Aguilera 2012). Taking the Klinkenberg equation as fact, gas slippage factor was determined using a correlation of the form:

$$b_k = \beta[\frac{k_\infty}{\emptyset}]^{-0.5}, \quad (9)$$

The "β –term" in Eq. 7 is a parameter that depends on the type of gas used in the core flow experiment. For nitrogen this value has been reported as 43.345 psi (Florence et al. 2007; Ziarani and Aguilera 2012). Using measured porosity and mean pressure values, equivalent liquid permeability (k_∞) can be calculated in Eq. 9 for each chemical tested in the coreflood test.

RESULTS AND DISCUSSIONS*

Fluid Characterization

Interfacial Tension Measurements

Fig. 8 shows the surface tension of the microemulsions (dashed lines) prepared at concentrations of 0.05, 0.1, 0.2, 0.5, 1, and 2 wt% in deionized water. The surface tension decreased as the concentration of the microemulsions was increased. Decreasing the surface tension value beyond a 0.5 wt% concentration was not significant. This trend was noted for all microemulsions. Surface tension results for all microemulsions were less compared to the surface tensions of surfactant solutions at all different concentrations. Fanun (2008) explained the advantages of microemulsions over surfactant solutions as providing longer interfacial contact and higher surfactant solubility capacity. This could explain lower surface tension value of the microemulsions compared to the surfactant solutions at the same concentration. This is especially important in low permeability reservoirs where capillary forces are high and fluid invasion is one of the main sources of fluid trapping inside the formation.

---

*Part of this chapter is reprinted with permission from *Improving Gas Relative Permeability in Tight Gas Formations by Using Microemulsions* by A. Rostami, D.T. Nguyen, H.A. Nasr El Din, 2014, Paper IPTC 17675, Copyright [2014] by International Petroleum Technology Conference. And *Microemulsion vs. Surfactant Assisted Gas Recovery in Low Permeability Formations with Water Blockage* by A. Rostami and H.A. Nasr El Din, 2014, Paper SPE 169582, Copyright [2014] by Society of Petroleum Engineers.

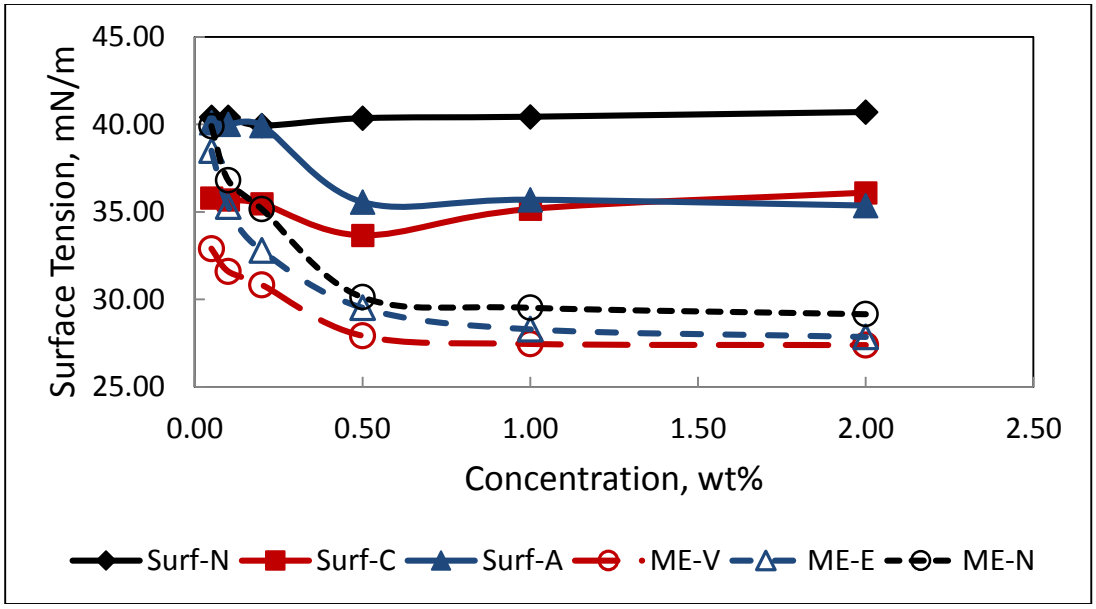

Fig. 8—Surface tension of microemulsions and surfactant solutions.

Thermal Stability Tests

Thermal stability of the microemulsions was evaluated by comparing the surface tension values of the fluids after being aged in the oven for 24 hours at 150, 250, and 400°F. The samples were 100 ml of 0.5 wt% microemulsions in DI water. Surface tension measurements were conducted at 70°F after the samples were reached room temperature. **Fig. 9** shows the results of the experiments for microemulsions ME-E, ME-V, and ME-N. The surface tension values for ME-E changed from 29.5 mN/m at 70°F to 31.3, 32.9, and 33 mN/m at 150, 250, and 400°F respectively. For ME-N, surface tension was changed from 30.1 mN/m to 31.3, 32.1, and 34.6 mN/m at 70, 150, 250, and 400°F respectively after 24 hours aging time. The surface tension values for ME-V showed the lowest values at all different temperatures when compared to other microemulsions and changed from 27.9 mN/m at 70°F to 28, 28.9, and 29.5 mN/m after 24 hours in the oven at 150, 250, and

400°F respectively. Insignificant change in the surface tension values after 24 hours aging time at temperatures up to 400°F showed high thermal stability of the microemulsions.

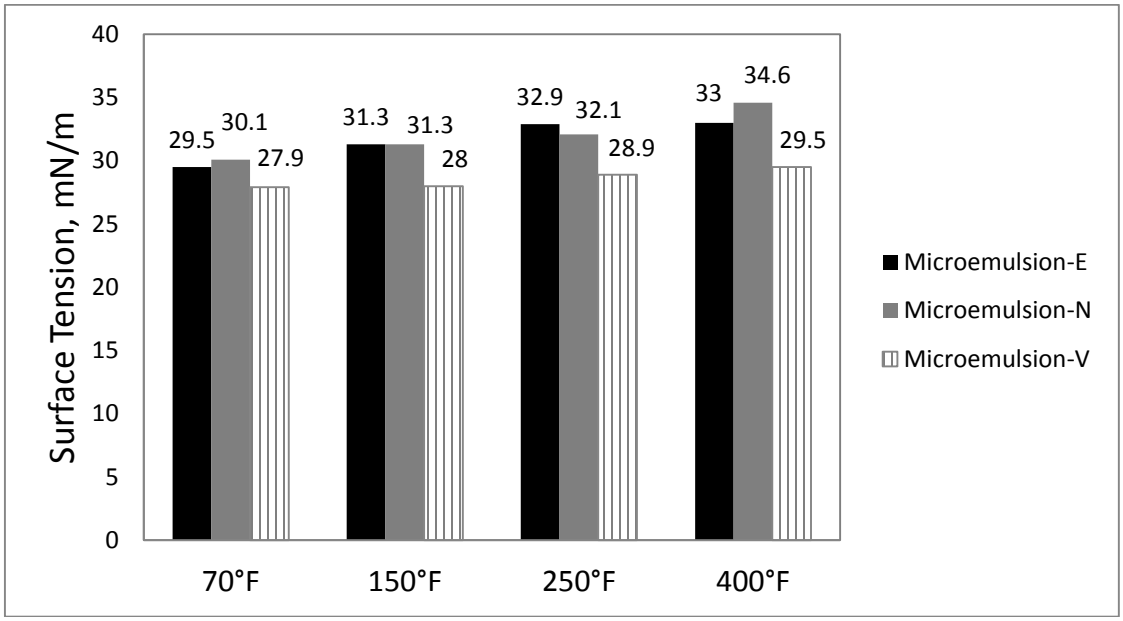

Fig. 9—Surface tension values of microemulsions after being at different temperatures for 24 hours didn't changed significantly, which was representative of high thermal stability of microemulsions.

Droplet Size Measurements

Transmission electron micrograph (TEM) was used to measure the size of the microemulsion-V droplet. Three µl of sample was applied on a glow-discharged C-flat holey carbon grid CF-22-2C (2 µm holes, 2 µm spacing) and vitrified by plunging in liquid ethane using a FEI Vitrobot Mark III apparatus with settings as follows: a blot offset of -2, a blotting time of three seconds, and a humidity 100%. Grids with vitrified samples were stored in liquid nitrogen until Cryo-TEM imaging. TEM micrographs were taken by an FEI TECNAI G2 20F. It was operated at a 200 kV accelerating voltage, equipped with a ZrO2/W Schottky field emission gun and a Gatan imaging filter slow-scan CCD camera.

The average size of the microemulsion (as received) detected was in the range of 30-60 nm. **Fig. 10** shows the TEM micrograph of the ME-V.

The droplet size of the treatment fluid, 0.2 wt% ME-V in 2 wt% KCl, couldn't be detected by TEM. Zelenev et al. (2011) explained that dilution of the microemulsion would result in an increase in the distance between the droplets.

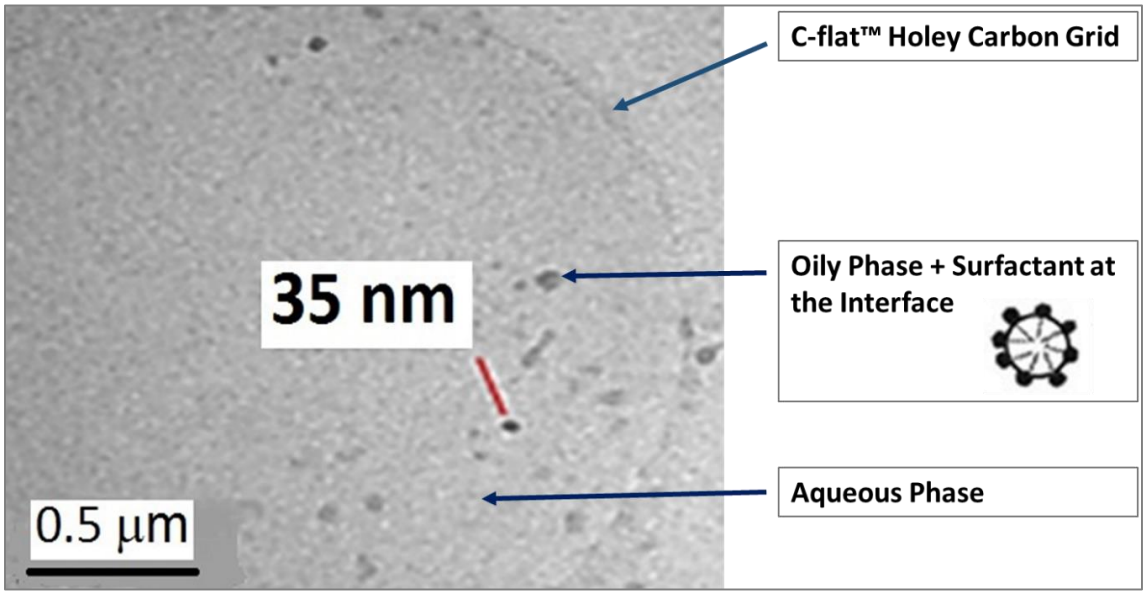

Fig. 10—Transmission electron micrograph (TEM) of ME-V as received.

Compatibility Test

Three types of microemulsions (ME-V, ME-N, and ME-E) were tested to determine the compatibility of the microemulsions with brine and condensate to screen the potential microemulsions for coreflood experiments. First, the microemulsions were mixed with 2 wt% KCl at a concentration of 0.2 wt% of the microemulsions in 2 wt% KCl. No color changing or precipitation was observed for ME-V or ME-E, and a clear solution was obtained for these two microemulsions in the brine solution. ME-N had

precipitations after mixing with brine. **Fig. 11** shows the results of the brine compatibility tests. Then, the compatibility of the prepared microemulsion treatment fluids with condensate were tested. The microemulsion treatment fluids were mixed with condensate at a ratio of 1:1. A sample of 5 ml of the microemulsion treatment fluid was mixed with 5 ml of the condensate, and the mixture was left for 1 hour at room temperature. The results showed an incompatibility of the ME-N with the condensate, and presence of emulsions in the condensate phase that did not separate out after 8 hours. ME-V and ME-E did show compatibility with the condensate, as shown in **Fig. 12**.

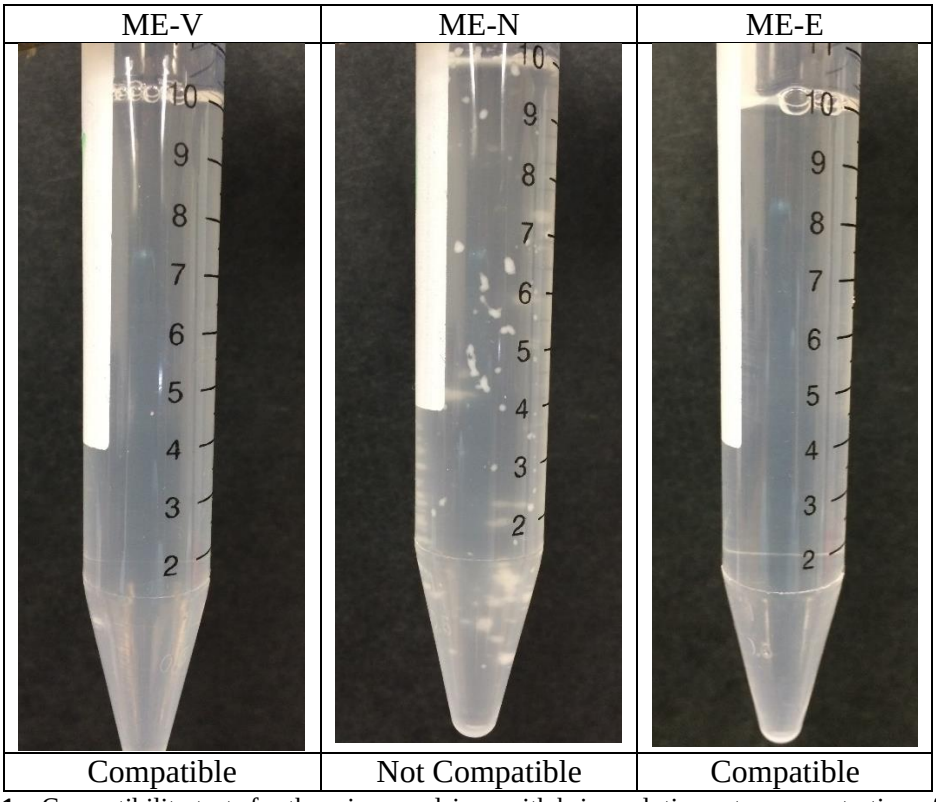

Fig. 11—Compatibility tests for the microemulsions with brine solutions at a concentration of 0.2 wt% of the microemulsions in 2 wt% KCl showed the incompatibility of ME-N with the brine solution.

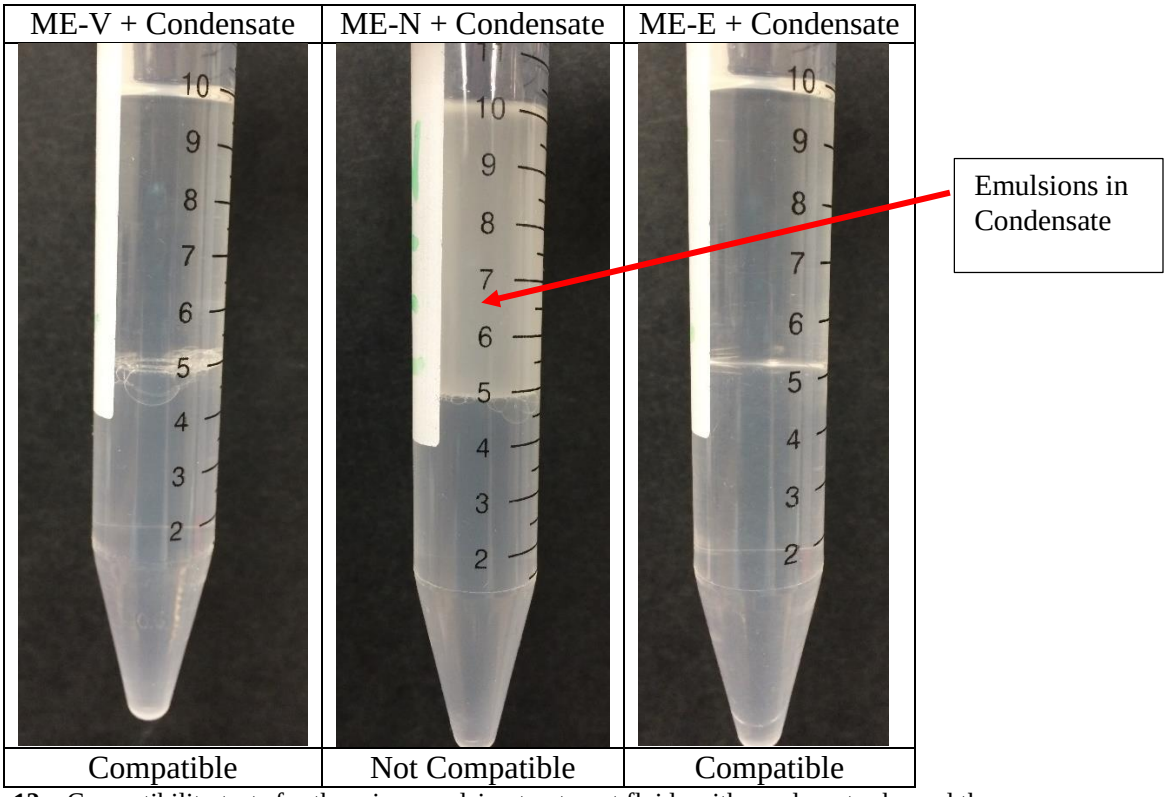

Fig. 12—Compatibility tests for the microemulsion treatment fluids with condensate showed the incompatibility of ME-N with the condensate (microemulsion treatment fluids were 0.2 wt% of the microemulsions in 2 wt% KCl).

Rock Characterization

Three different shale rocks including outcrop of Barnett shale, Marcellus shale, and reservoir rock of the New Albany shale were used to study the fluid-rock interactions. Knowing the rock characteristics including clay and bulk mineralogy before running any experiments, will help us to better understand the interactions between the treatment fluids and the formation rock. X-ray diffraction (XRD) was done on these four rocks to determine the bulk analysis and clay mineralogy (as was shown in Table 5**)**. Clay minerals play an important role in interpreting the results of formation damages. Non-swelling clays such as kaolinite and illite tend to detach from the rock surface and migrate along with the

flow stream (Mohan et al. 1993). Detached and migrated particles can trap and plug the pore throat and reduce the permeability. **Fig. 13** shows different mechanisms of formation damages for some clays.

Pore Bridging	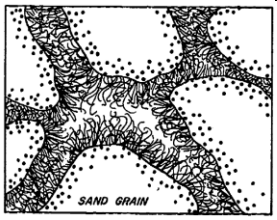	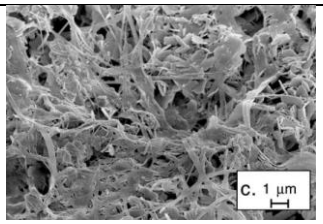	Illite
Pore Lining	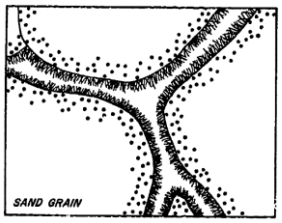		Chlorite
Discrete Particles	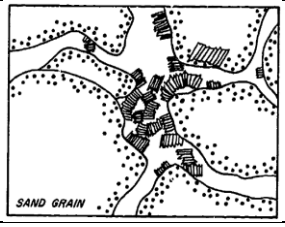	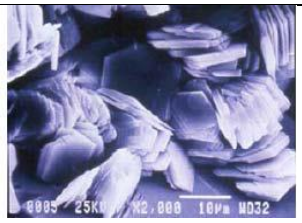	Kaolinite

Fig. 13—Formation damages caused by different types of clays (Neasham 1977; Passey et al. 2010).

XRD results for the shale rocks indicated highest amount of kaolinite/illite/mica in Barnett and New Albany shale. If by applying hydraulic forces during a fracturing job, rock particles detach from the rock surfaces, there is a great chance that they don't stay dispersed in the solution and coagulate with other particles and settle down somewhere in the flow path which might be a pore throat and could cause formation damage. Results of the zeta potential test determined the highest value of surface charges for these two types of rock and confirmed the results of the XRD as will be discussed in the following section.

Fluid-Rock Interactions

Zeta Potential Measurements

Surface charges and thickness of the electrical double layer are important factors in determining the stability of the water film on the rock surface (Dubey and Doe 1993). Buckly et al. (1996) and Hirasaki (1991) explained that the stability of the water film on the rock surface can determine the rock wettability. An electro-kinetic potential creates between the surface of the colloid and the liquid, to neutralize the surface charges by forming a double layer which maintains a thick water film around the particle and make a water-wet rock surface. Hussain et al. (1996) studied the surface charges of the kaolinite, illite, and chlorite by zeta potential measurements. They found that clays were negatively charged over a pH range from 2.5 to 11 and kaolinite was the most negative clay. Alotaibi et al. (2011) concluded that surface charges of sandstone and clay particles were significantly affected by ionic strength of water. Ramez et al. (2013) explained that change of the electrical charge on the rock-brine interface was the primary reason for wettability alteration on mica surfaces. They also concluded that when the electric charges become more negative at the rock/brine surface, the electrical double layer expand and cause stabilization of the water film surrounding the rock. No work was done before to the best of author's knowledge in studying the microemulsions and shale rock interactions using zeta potential test. **Table 6** shows zeta potential and mobility results for New Albany shale in 0.5 wt% ME-V at 75°F as an example of instrument reproducibility of five runs.

Table 6—Zeta potential and mobility results for New Albany shale in 0.5 wt% ME-V at 25°C.

Run	Mobility	Zeta Potential(mV)	Rel. Residual
1	-3.36	-42.97	0.0204
2	-3.34	-43.89	0.0107
3	-3.35	-42.88	0.0130
4	-3.34	-43.85	0.0163
5	-3.29	-42.07	0.0253
Mean	-3.37	-43.13	0.0171
Standard Error	0.03	0.34	0.0026
Combined	-3.37	-43.13	0.0138

Zeta potential and surface charges are affected by the pH. The pH for all different rocks in different fluids were measured to be around 7 as shown in **Table 7.**

Table 7—pH of treatment fluids at 25°C.

Treatment Fluids/Shale Rocks	Barnett	Mancos	Marcellus	New Albany
ME-V	7.48	7.36	7.39	7.43
ME-N	7.37	7.43	7.43	7.40
ME-E	7.47	7.47	7.49	7.37
Surf-A	7.45	7.37	7.39	7.48
Surf-N	7.46	7.36	7.42	7.44
Surf-C	7.36	7.35	7.46	7.48

Fig. 14 shows a summary of the zeta potential results. It can be observed from the figure that the zeta potential values for all microemulsions were negative, due to the repulsion forces between negatively charged shale particles suspended in the microemulsion fluids. Presence of anionic and nonionic surfactants in the structure of microemulsions causes a negatively charged fluid around the particles. The strength of the microemulsion fluids to carry more or less negative charges depends on the structure of the non-ionic and anionic surfactants that were used in the microemulsions. When microemulsions were surrounding the shale particles, a negative value of zeta potential

was resulted. As discussed by Ramez et al. (2013), higher negative value of zeta potential will cause expansion of electrical double layer and stabilization of water film surrounding the rock. The results of the zeta potential tests for microemulsions showed that the ME-V has the lowest negative value of zeta potential compared to the other microemulsions for all different rock types, which resulted in least water-wettability characteristics when compared to the other microemulsions.

The values of zeta potential for Barnett and New Albany shale were higher compared to the Marcellus. This can be due to the high amount of clays including kaolinite, illite, and mica in Barnett and New Albany shale as determined by XRD. Surfactant solutions showed different behaviors depending on the structure of the surfactant. The presence of cationic surfactant solution around the negatively charged shale rock particles neutralized some of the surface charges, but a high positive net charge caused repulsion and dispersion of the particles in the solution.

Results for nonionic surfactant solution showed low zeta potential values. The solution did not change the surface charge properties of the rock particles significantly. The anionic surfactant caused strong repulsion forces between the rock particles in the solution. It can be observed from the figure that the value of zeta potential was strongly negative for the anionic surfactant for all types of rocks. The results indicated that the value of zeta potential depends on the ionic strength of the solutions and depends on the resultant charges on the rock particles.

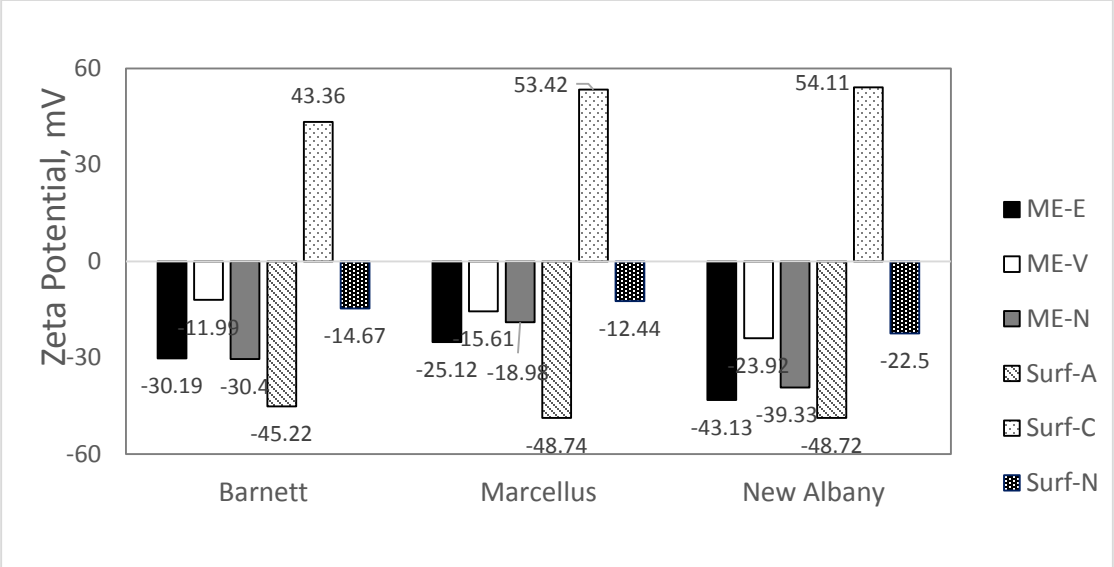

Fig. 14—Zeta potential for shale rocks in 0.5 wt% of three microemulsion fluids and three surfactant solutions in DI at 75°F.

Contact Angle Measurements

By changing the preferential wettability of the rock surface in the reservoir, the capillary pressure can be reduced. Strong capillary pressure effects are created in strongly water wet and oil wet porous media which have contact angles of near zero or 180 degrees respectively. There is less spreading tendency for either water or oil on the surface of the formation, when the wettability moves to a more neutral condition and the cosine of the contact angle approaches zero and capillary pressure decreases.

The wetting characteristics of solid surfaces were evaluated by contact-angle methods. The smoothed surface of the rock was in contact with two immiscible fluids. The apparatus was cleaned using acetone and DI water and the system was tested for leakage before running the experiments. The temperature was controlled manually to the set point at the desired temperatures. A capillary tube with outside diameter of 0.079 cm was inserted inside the chamber to make a droplet for interfacial tension measurements.

Two microemulsions, ME-V and ME-E, and three surfactant solutions, Surf-N, Surf-A, and Surf-C, were prepared at 0.2 wt% of the chemical in 2 wt% KCl. The Barnett shale was cut to the cubes of size 1.57cm*1.83 cm* 0.64 cm. The rocks were put in the oven for 4 hours. The rock was placed in the chamber and the droplet of treatment fluid was put on the rock surface at 165°F and atmospheric pressure. Changes in contact angle were recorded every 10 seconds for 10 min. **Fig. 15** shows the contact angle changes of 0.2 wt% ME-E prepared in 2 wt% KCl at 165°F and atmospheric pressure on Barnett shale rock after 10 min. Right and left angles were read for each droplet and an average was taken. Repeatability of the measurements was up to 3 degrees for all measurements. The average contact angle value changed from 51.4 ± 0.12 at the beginning of contact time to the value of 36.5 ± 0.26 after 10 minutes for microemulsion ME-E. The right angles and left angles reached stabilization after 10 minutes of contact time. Right and left angles decreased and remained stable around 36° after 10 minutes. Images of ME-E on Barnett shale rock at 165°F and atmospheric pressure is presented at time zero and after 10 minutes of contact time in **Fig. 16**.

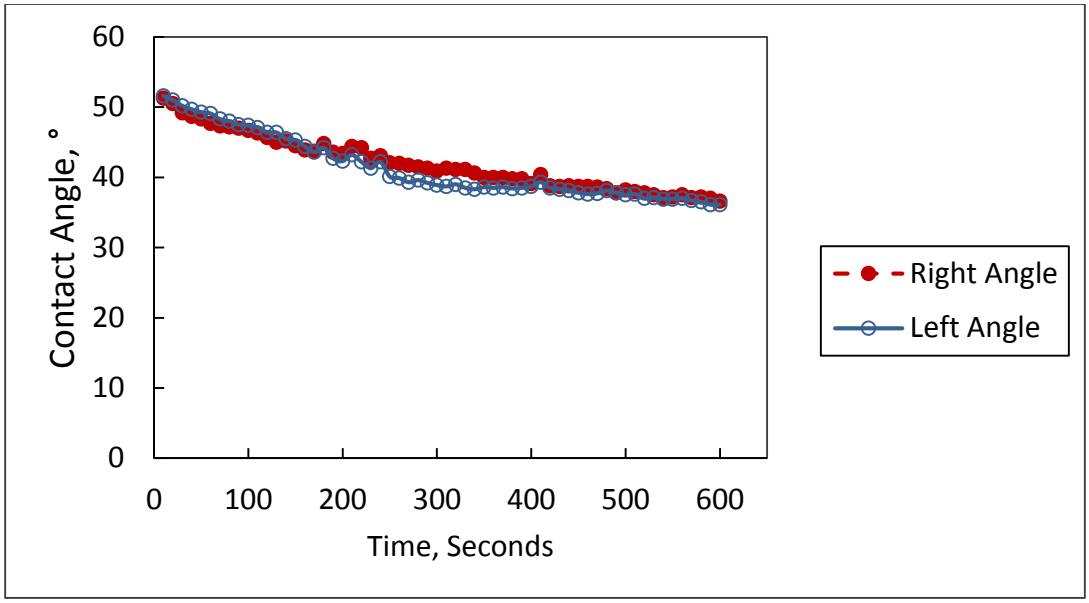

Fig. 15—Contact angles of microemulsion-E, ME-E, as a function of contact time on Barnett shale rock at 165°F and atmospheric pressure.

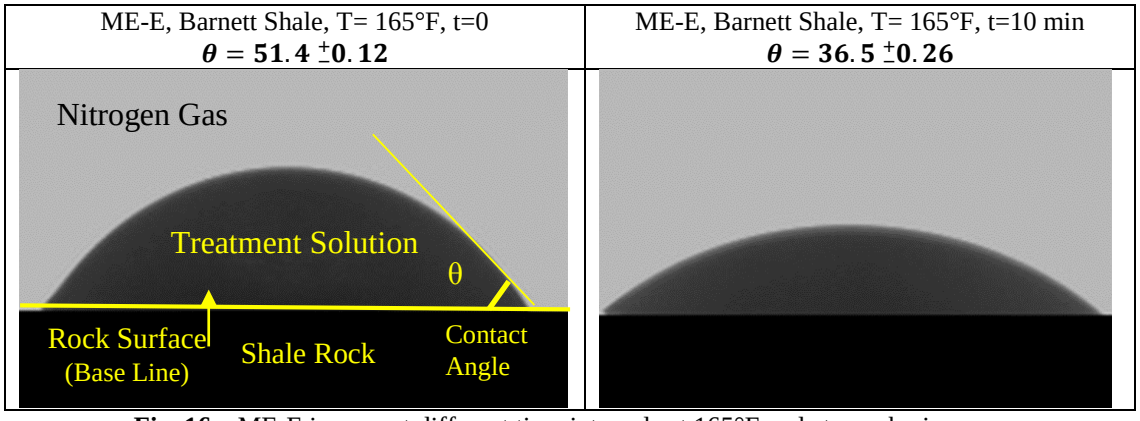

Fig. 16—ME-E images at different time intervals at 165°F and atmospheric pressure.

Fig. 17 shows the contact angle of 0.2 wt% ME-V in 2wt% KCl at 165°F and atmospheric pressure on Barnett shale rock. The average contact angle value changed from 61.6 ± 0.16 at the beginning of contact time to the value of 49.5 ± 0.05 after 10 minutes. The right angles and left angles reached stabilization after 10 minutes. Right and left angles decreased and remained stable at 47° and 51°, respectively after 10 minutes. Images

of ME-V on Barnett shale rock at 165°F and atmospheric pressure is presented at time zero and after 10 minutes of contact time in **Fig. 18**.

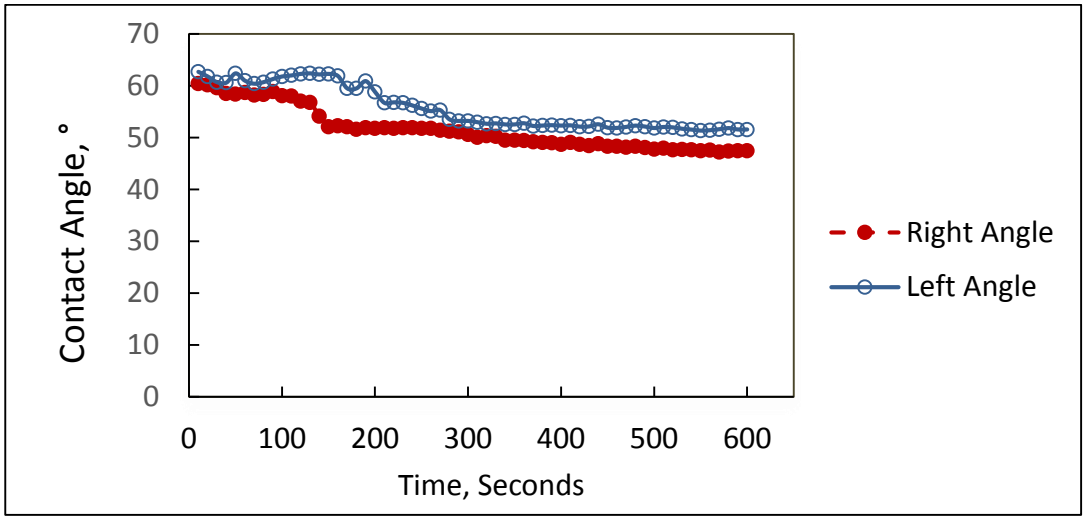

Fig. 17—Contact angles of microemulsion-V, ME-V, as a function of contact time on Barnett shale rock at room temperature and atmospheric pressure.

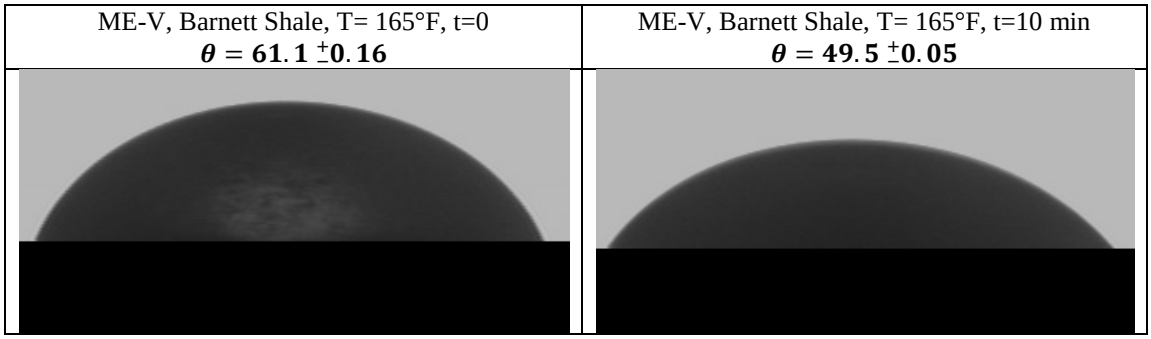

Fig. 18—ME-V images at different time intervals at 165°F and atmospheric pressure.

The non-ionic surfactant (Surf-N), showed a change in contact angle from 40.5 ±0.54 at the beginning of contact time to the value of 33.1±0.99 after 10 minutes. The right and left angles stabilized after 10 min at 35° and 31°, respectively after 10 minutes as shown in **Fig. 19**. Images of Surf-N on Barnett shale rock at 165°F and

atmospheric pressure are presented at time zero and after 10 minutes of contact time in **Fig. 20**.

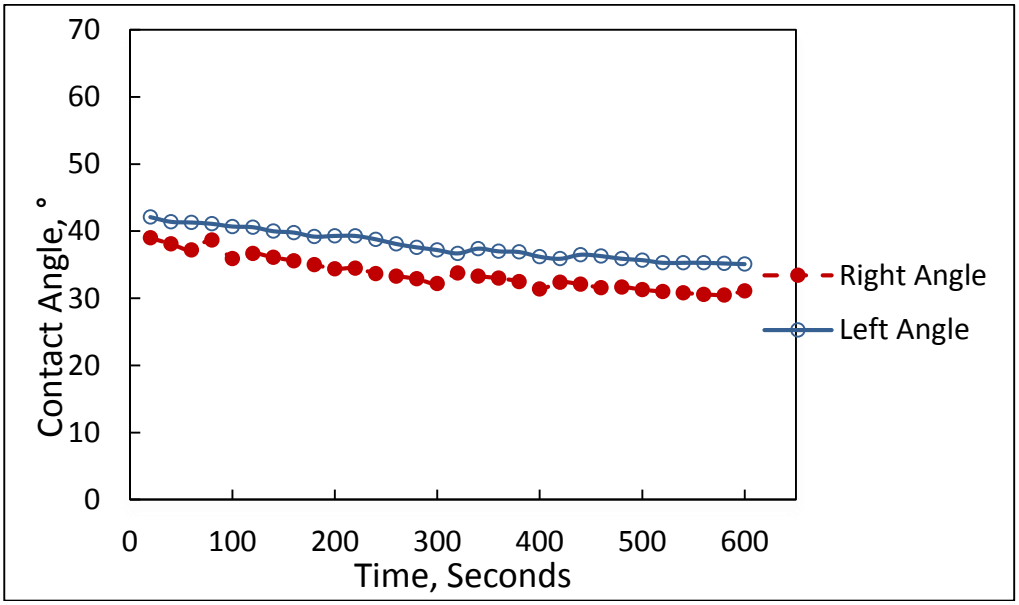

Fig. 19—Contact angles of a non-ionic surfactant, Surf-N, as a function of contact time on Barnett shale rock at 165°F and atmospheric pressure.

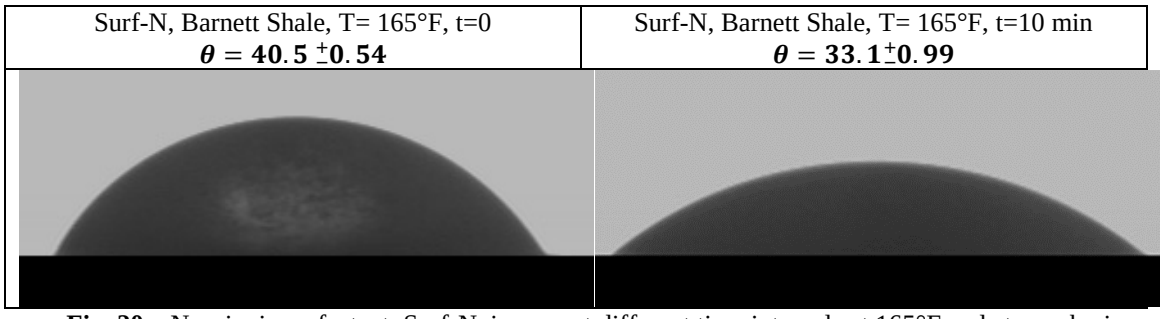

Fig. 20—Non-ionic surfactant, Surf-N, images at different time intervals at 165°F and atmospheric pressure.

Figs. 21 and **22** show the contact angles for the anionic surfactant (Surf-A) at the same condition of temperature and pressure on Barnett shale rock. The average contact angle value changed from 41.2 ± 0.07 at the beginning of contact time to the value of

36.3 ±0.25 after 10 minutes of contact time. Both contact angles on the right and left stabilized around 38 degree after a 10 min time interval.

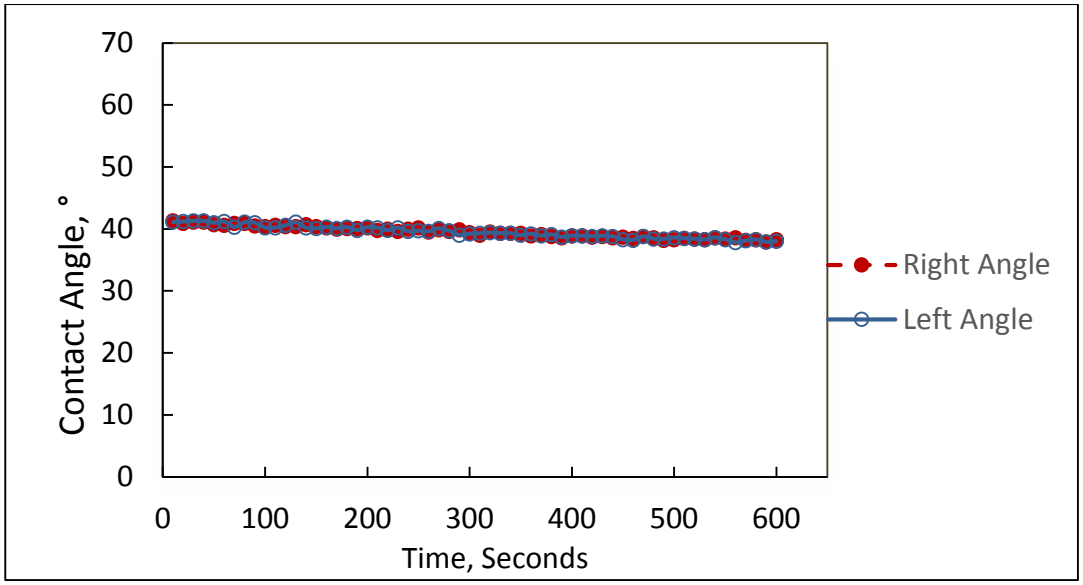

Fig. 21—Contact angles of an anionic surfactant, Surf-A, as a function of contact time on Barnett shale rock at 165°F and atmospheric pressure.

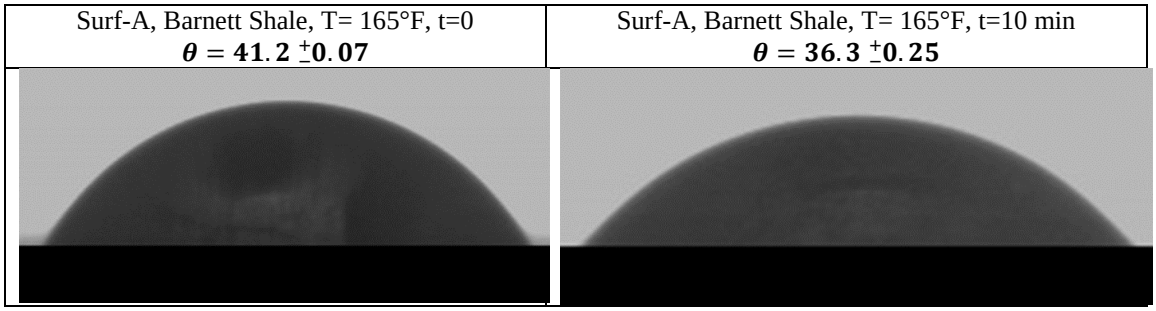

Fig. 22—Anionic surfactant, Surf-A, images at different time intervals at 165°F and atmospheric pressure.

Fig. 23 shows the contact angle of 0.2 wt% cationic surfactant, Surf-C, in 2 wt% KCl at 165°F and atmospheric pressure on Barnett shale rock. The average contact angle value changed from 31.2 ±0.43 at the beginning of contact time to the value of 28.4 ±0.38 after 10 minutes. The right and left angles reached stabilization after 10 minutes of contact

time at around 27 and 30 degree, respectively. Images of Surf-C on Barnett shale rock at 165°F and atmospheric pressure is presented at time zero and after 10 minutes of contact time in **Fig. 24**.

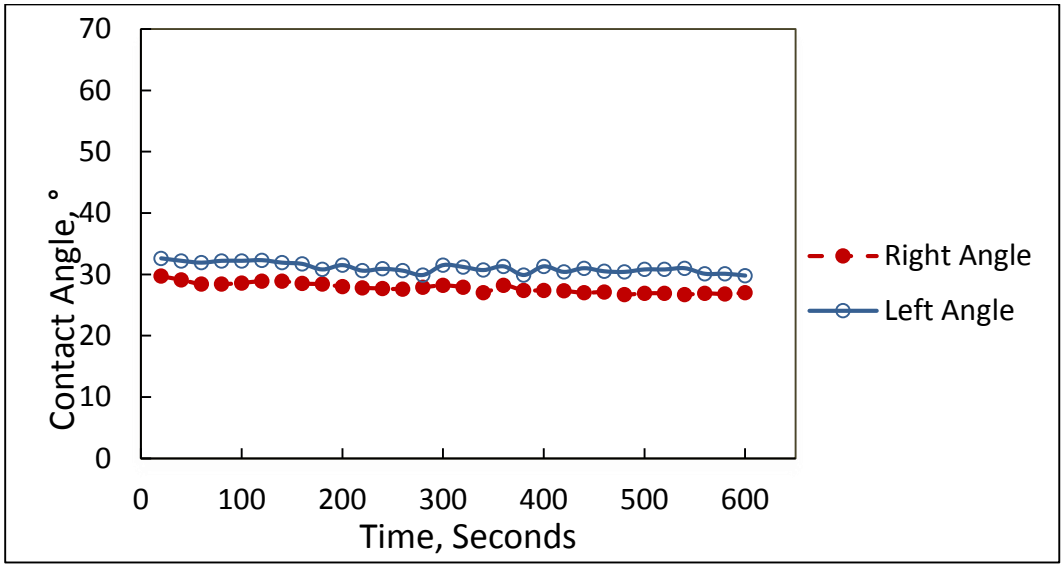

Fig. 23—Contact angles of a cationic surfactant, Surf-C, as a function of contact time on Barnett shale rock at 165°F and atmospheric pressure.

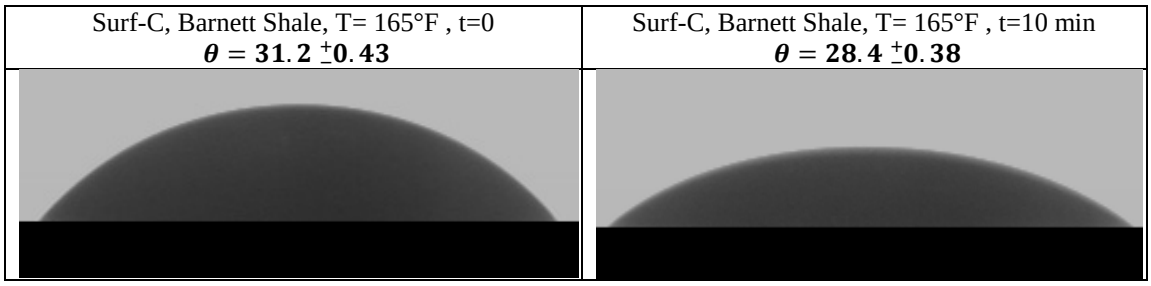

Fig. 24—Cationic surfactant, Surf-C, images at different time intervals at 165°F and atmospheric pressure.

The contact angle was changed from 31.7 ± 0.32 at the beginning of the contact time to the value of 18.9 ± 0.05 after 10 min of contact for 2 wt% KCl as shown in **Figs. 25** and **26**.

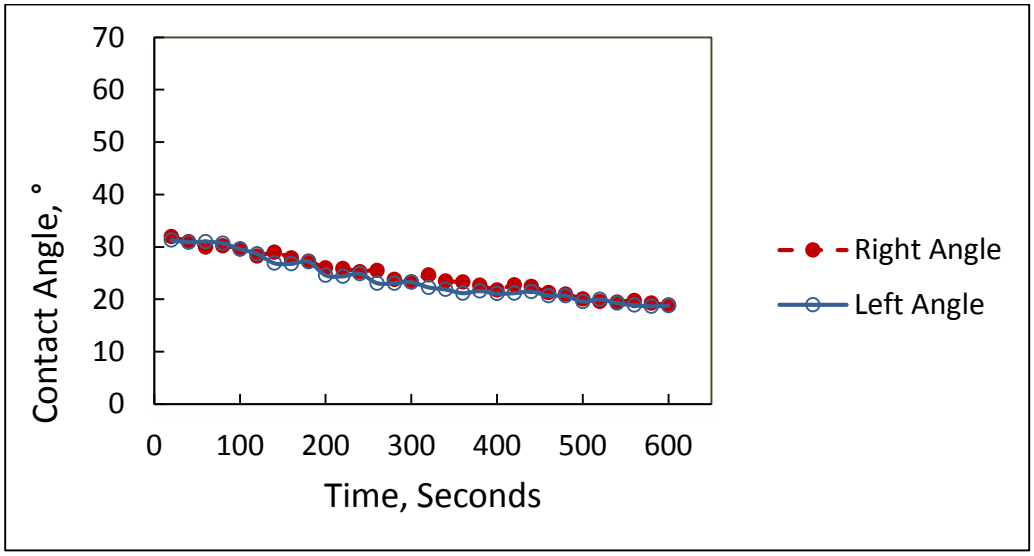

Fig. 25—Contact angles of 2 wt% KCl as a function of contact time on Barnett shale rock at 165°F and atmospheric pressure.

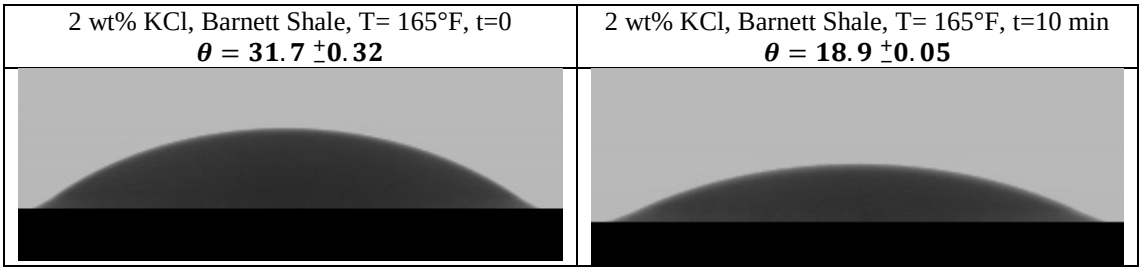

Fig. 26—Brine solution, 2 wt% KCl, images at different time intervals at 165°F and atmospheric pressure.

The solution of 2 wt% KCl showed the most wetting characteristics among the tested chemicals, with the highest change in contact angle during a 10 min time interval. Contact angle changes for tested chemicals after a 10 min time interval at 165°F and atmospheric pressure on Barnett shale rock are summarized in **Table 8.**

Table 8—Contact angle changes for tested chemicals after 10 min time interval at 165°F and atmospheric pressure on Barnett shale rock.

	ME-E	ME-V	Surf-N	Surf-A	Surf-C	2 wt% KCl
θ (M) at t= 0	51.4 ±0.1	61.1 ±0.16	40.5 ±0.54	41.2 ±0.07	31.2 ±0.4	31.7 ±0.32
θ (M) at t=10 min	36.5 ±0.2	49.5 ±0.05	33.1±0.99	36.3 ±0.25	28.4 ±0.3	18.9 ±0.05
Wettability		Least Water -wet				Most water-wet

Improving Gas Recovery by Microemulsion Treatment

Several coreflood experiments were performed in order to investigate and compare the potential of microemulsions to improve the effective gas permeability and fluid recovery in the presence of synthetic condensate and brine. The experiments were performed on Bandera sandstone cores saturated with 2 wt% KCl. The conditions of all experiments were similar: temperature of 165°F, back pressure of 700 psi, overburden pressure of 1800 psi, and flow rate of 5 cm^3/min. Two different microemulsions were tested. Mutual solvent and fluoropolymer surfactant solutions were tested for comparison purposes. The absolute permeability of the all Bandera sandstone cores was measured by injecting 2 wt% KCl into the core until the pressure was stabilized. Then, the condensate was injected until no brine was produced. The results showed that the absolute permeabilities were between 17 to 22 md for these outcrops of Bandera sandstone cores.

Fig. 27 shows the pressure drop across the core vs. the cumulative pore volume of injected fluid for the 0.2 wt% ME-V microemulsion prepared in 2 wt% KCl. After injecting 10 pore volumes of nitrogen gas, the pressure stabilized around 330 psi. The initial effective permeability to nitrogen gas was determined to be 0.33 md at experimental

conditions. Five pore volumes of treatment fluid were injected to make sure that the core was fully saturated with chemical treatment fluid. Nitrogen gas was injected through the core again, until stabilization of pressure around 120 psi, which gave a final effective gas permeability of 0.84 md in the presence of residual brine and condensate in the core. A value of 2.54 improvement factor was observed.

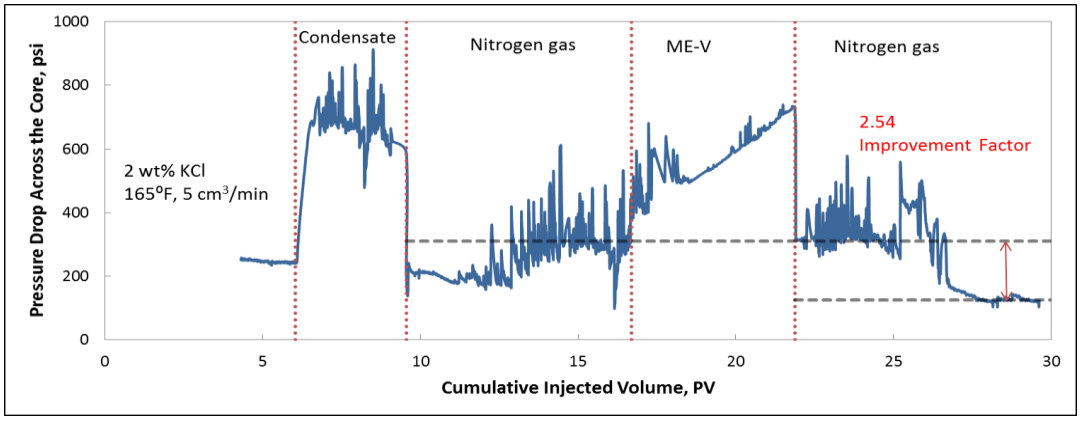

Fig. 27—Pressure drop across the core vs. cumulative injected volume for microemulsion ME-V as a treatment fluid at 165°F.

Fig. 28 shows the core effluent samples that were collected through the experiment. Test tube (a) shows residual condensate and residual brine after N_2 injection. Two separate phases of brine and condensate were observed in test tube (a). Test tube (b) shows the sample after injecting the microemulsion. A clear solution of microemulsion was collected. Test tube (c) shows the effluent sample after flowing nitrogen at the last step, which recovered the treatment fluid and the condensate.

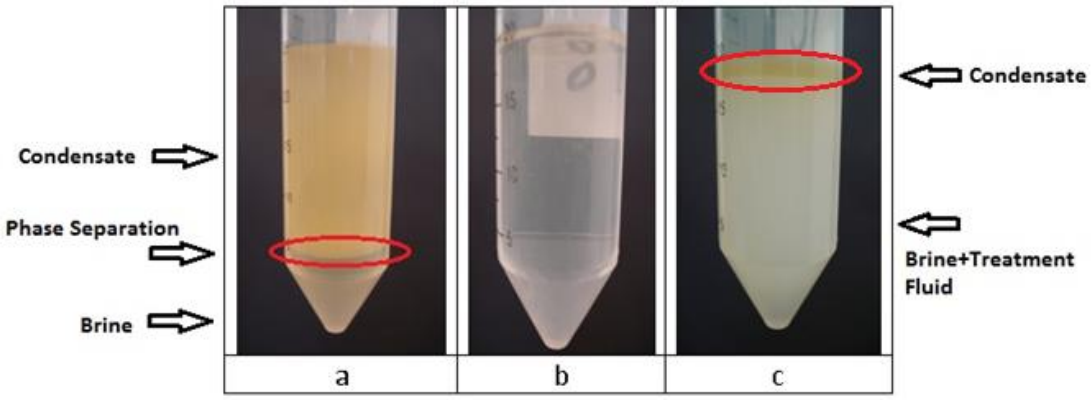

Fig. 28—Core effluent samples that were collected through the experiment for microemulsion ME-V. (a) Residual condensate and residual brine after N_2 injection. (b) After injecting the microemulsion. (c) After injecting nitrogen gas in the last step, in which the microemulsion, brine, and the condensate were recovered.

The coreflood experiment was repeated for the other microemulsion, ME-E, at the same conditions of temperature, back pressure, and overburden pressure. The concentrations of both solutions were chosen to be 0.2 wt% of the treatment chemical in 2 wt% KCl. As shown in **Fig. 29**, the pressure stabilized at 330 psi and an initial effective gas permeability of 0.33 md was measured. After injecting microemulsion ME-E, the effective permeability to gas was enhanced to the 0.39 md and the differential pressure was stabilized at 270 psi. The improvement factor was calculated to be 1.18 for this chemical.

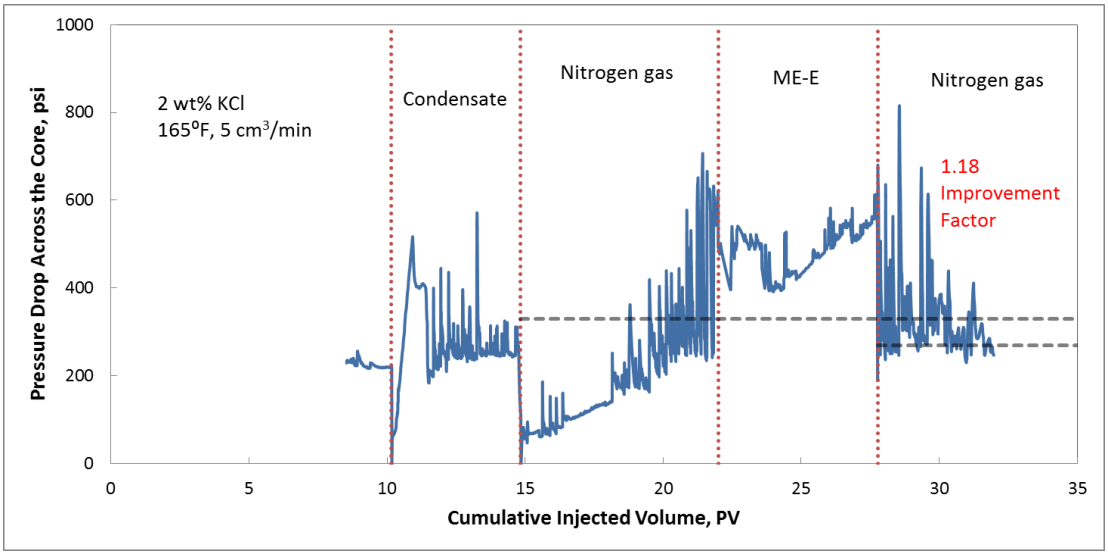

Fig. 29—Pressure drop across the core vs. cumulative injected volume for microemulsion ME-E.

For comparison purposes, the same coreflood experiments were conducted on 20 in. Bandera sandstone cores for a mutual solvent solution and also for the fluoropolymer surfactant at the same concentration of 0.2 wt% chemical in 2 wt% KCl. To keep the tests consistent and comparable, the same concentration was used for all the tests. For mutual solvent the pressure was stabilized around 240 and 650 psi before and after treatment, respectively, as shown in **Fig. 30**. The mutual solvent solution decreased the effective permeability to gas from the initial value of 0.44 to 0.17 md and caused an improvement factor of 0.38.

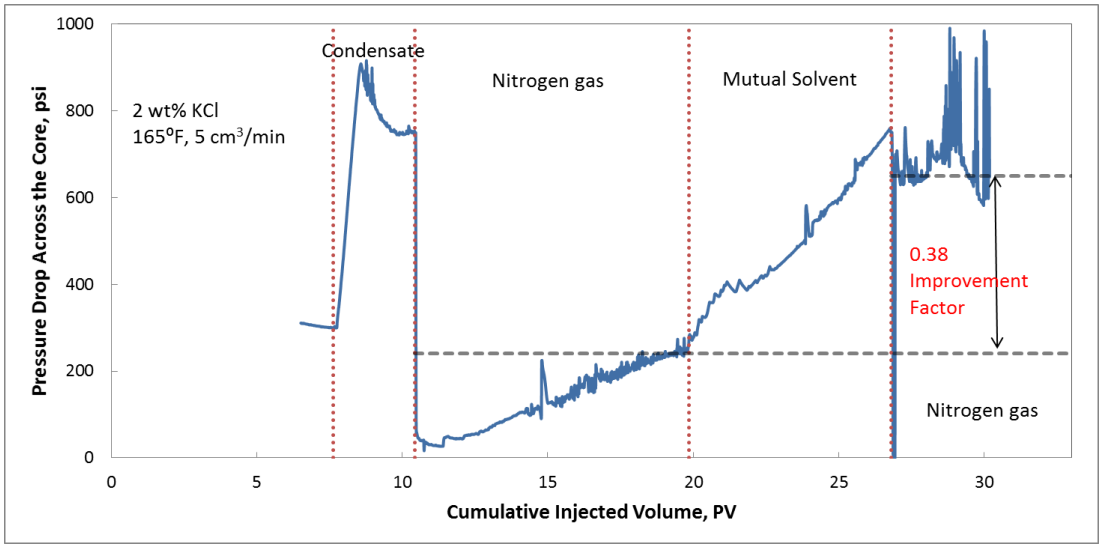

Fig. 30—Pressure drop across the core vs. cumulative injected volume for mutual solvent.

For the fluoropolymer surfactant solution, the pressure was stabilized around 160 and 240 psi before and after treatment, respectively. The large increase in pressure during fluoropolymer surfactant injection might be because of the presence of large polymer molecules in the injected fluid. The fluoropolymer surfactant showed a reduction in the effective gas permeability from the initial value of 0.66 md to a final effective gas permeability of 0.44 md after treatment and caused a 0.66 improvement factor in the 20 in. Bandera sandstone core at the experimental temperature and pressure conditions as shown in **Fig. 31**.

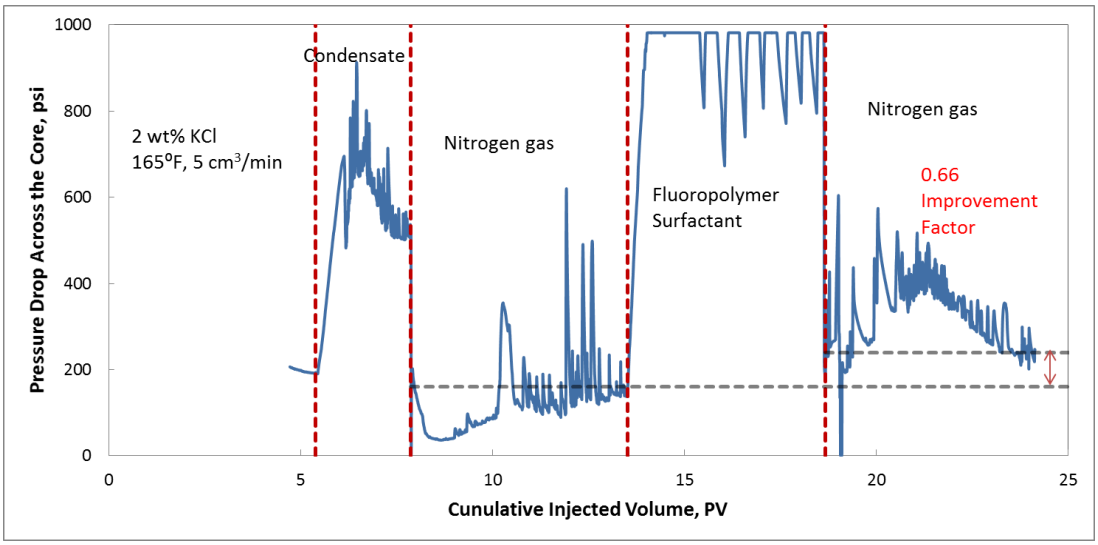

Fig. 31—Pressure drop across the core vs. cumulative injected volume for fluoropolymer surfactant solution.

A comparison of permeability regains for two microemulsions, mutual solvent and fluoropolymer surfactant, were summarized in **Table 9**. When compared to mutual solvent and fluoropolymer surfactant, which caused damage to the cores, both microemulsions improved the effective gas permeability, which agreed with the contact angle and capillary pressure results. The highest permeability regain was achieved by an injection of 0.2 wt% ME-V into the 20 in. Bandera sandstone core, while mutual solvent and fluoropolymer surfactant solutions, caused damage to the core.

Table 9—Summary of coreflood results.

	Core F	Core C	Core D	Core E
Treatment Solutions	ME-V	ME-E	Mutual Solvent	Fluoropolymer Surfactant
Concentration of treatment chemical in 2 wt% KCl	0.2	0.2	0.2	0.2
kgi (md)	0.33	0.33	0.44	0.66
kgf (md)	0.84	0.39	0.17	0.44
Permeability Regain (%)	2.54	1.18	0.38	0.66

Sustainability Against Wash-Off

The coreflood experiment was repeated for the microemulsion ME-V, to confirm the gas permeability enhancement results and also to determine the long term sustainability of the microemulsion against wash-off. The Bandera sandstone core with dimensions of 1.5 in. by 6 in. was placed into the oven for 4 hours at 220°F. The weight of the dry core was determined (W dry= 370.69 g). The core was saturated in 2 wt% KCl and was left in brine solution for a day. The saturated core was vacuumed for 3 hours, and the weight of the saturated core (W_{sat} = 392.41 g) was used to determine the pore volume and porosity of the core. The pore volume was 21.72 cm^3 with a porosity of 13 vol%. The core was placed into the core holder and was set up vertically. Overburden pressure was 1800 psi and the back pressure was 700 psi. The brine was injected at 2 cm^3/min until the pressure stabilized at around 43 psi. The initial permeability of the core was calculated to be 11.91 md. The critical flow rate was determined to be 6 cm^3/min, which was the maximum injection flow rate without creating fines/clay migration. All subsequent fluids were pumped at 6 cm^3/min.

Ten pore volumes of synthetic condensate were injected into the core, and the pressure was stabilized around 340 psi. Nitrogen gas was injected into the core until the pressure was stabilized around 270 psi. The initial effective permeability to gas was determined at residual brine/condensate saturation, and it was calculated to be 0.398 md (K_{gi}). Fifteen pore volumes of treatment fluid, 0.2 wt% of ME-V in 2 wt% KCl, was injected into the core at 6 cm^3/min and effluent samples were captured every 5 pore volumes. Then, nitrogen gas was injected through the core again and the pressure

stabilized around 110 psi. The final effective permeability to nitrogen gas was calculated as 0.966 md (K_{gf}). The improvement factor due to chemical treatment was 2.42, which confirmed the gas permeability enhancement results obtained for microemulsion ME-V (Fig. 27). The pressure drop across the core is shown versus the cumulative injected pore volume for ME-V in **Fig. 32**.

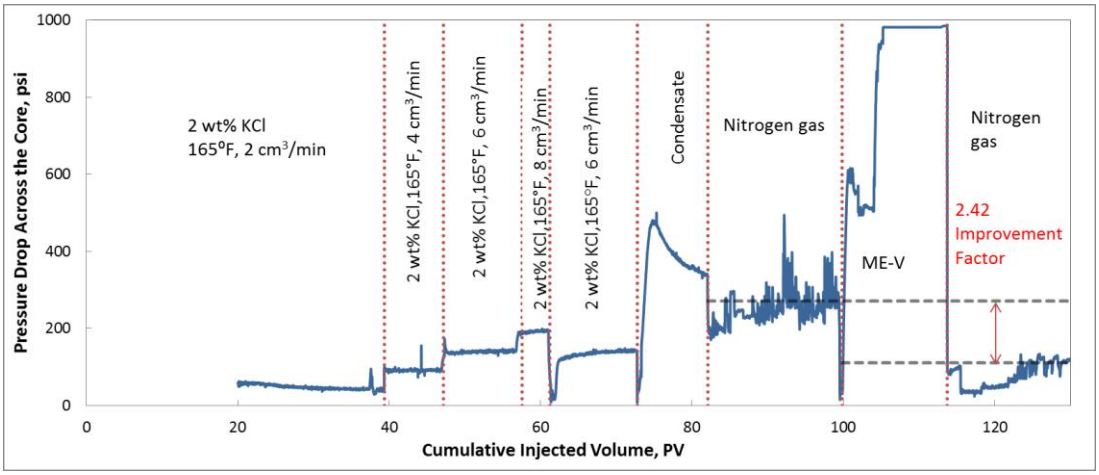

Fig. 32—Pressure drop across the core vs. cumulative injected volume for microemulsion ME-V, confirming the previous results of permeability regain for this microemulsion.

The next step was to determine the long term sustainability against wash-off for this microemulsion by running three cyclic injections of brine and gas into the core after the chemical treatment. This part of the experiment started by injecting 2 wt% KCl into the core at 6 cm3/min and 165°F. Fifteen pore volumes of the brine were injected, and the pressure stabilized around 470 psi. Then, twenty pore volumes of nitrogen were injected, and the pressure stabilized at 115 psi. The effective permeability to gas was determined to be 0.92 md (K_{g1} = 0.92 md). Eighteen pore volumes of 2 wt% KCl injected into the core, and the pressure stabilized at 610 psi. Then, 23 PV of nitrogen gas were injected, and the

pressure stabilized at 150 psi. The effective permeability to gas was determined to be 0.71 md (K_{g2} = 0.71 md). Eighteen pore volumes of 2 wt% KCl were injected into the core and the pressure stabilized at 600 psi. Then, 20 PV of nitrogen were injected and the pressure stabilized at 170 psi. The effective permeability to gas was calculated to be 0.63 md (K_{g3} = 0.63 md), and finally, 15 PV of 2 wt% KCl were injected into the core and the pressure stabilized at 620 psi. This was the end of third cycle after the treatment and the results are shown in **Fig. 33**. **Table 10** and **Fig. 34** summarize the results of the gas effective permeabilities for the wash-off test for three cycles of brine/gas injections and the initial values. As the results of the cyclic injection of brine/nitrogen gas, the effective gas permeability was 0.92, 0.71, and 0.63 md in the first, second, and third cycles, respectively. If these values were compared to the effective gas permeability before the wash-off test (K_{gf} = 0.97), no significant change in the gas permeability values were observed. All of these values after the treatment are still much higher than the initial effective gas permeability before treatment, which was K_{gi} = 0.39 md. These results confirm that the microemulsion ME-V had long term sustainability against wash-off making this chemical an effective additive to fracturing fluids.

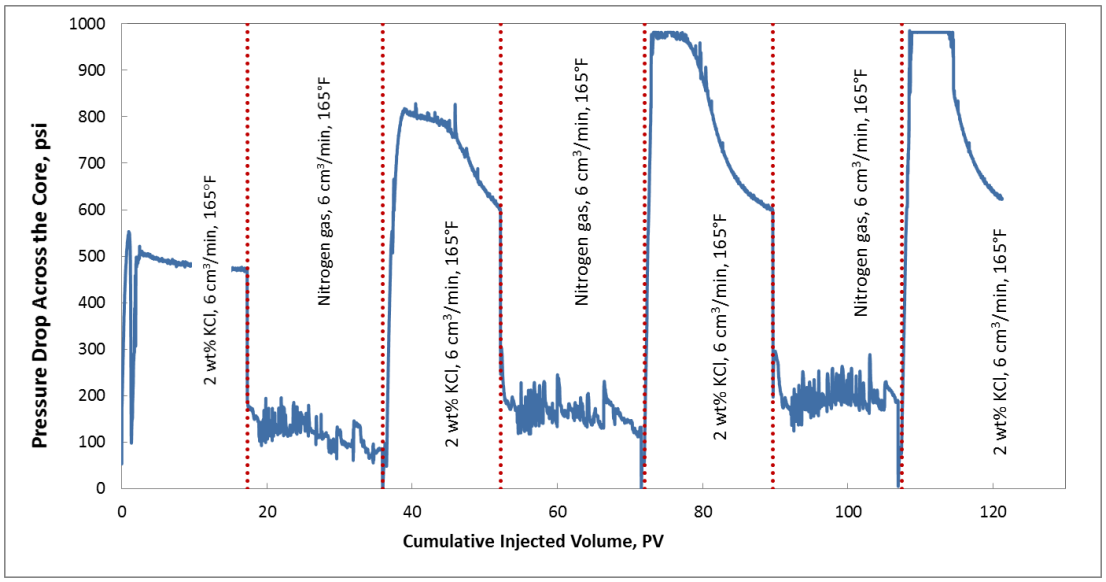

Fig. 33—Pressure drop across the core vs. cumulative volume injected for three cycles of brine/nitrogen gas injection to determine the long term sustainability against wash-off for the microemulsion, ME-V.

Table 10—Summary of gas and liquid permeabilities in the wash-off test after three cycles of brine/gas injection, which showed a great sustainability against wash-off for the microemulsion treatment fluid.

Step	Kgi (md)
Values Before Treatment	K_{gi} = 0.4
Values After Treatment	K_{gf} = 0.97
First Wash-Off Cycle After Treatment	K_{g1} = 0.92
Second Wash-Off Cycle After Treatment	K_{g2} = 0.71
Third Wash-Off Cycle After Treatment	K_{g3} = 0.63

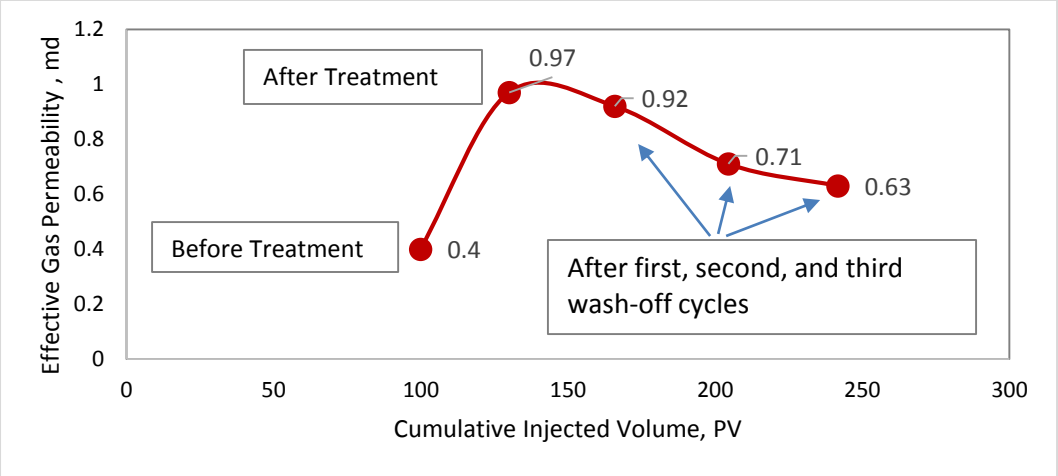

Fig. 34—Summary of gas permeabilities in the wash-off test after three cycles of brine/gas injection.

The adsorption of the microemulsions to the rock surface was investigated. Zelenev et al. (2011) explained that "adsorption of the diluted microemulsion is different from the adsorption from the surfactant solution because of the presence of additional oil-water interface between oil and aqueous phase that influences the net distribution of surfactant in the system. The results suggest that oil adsorb on rock surfaces together with a surfactant and the extent of adsorption of both of these species depends on surfactant (microemulsion) concentration in solution as well as on the O/W ratio. Dilution of microemulsion with constant O/W ratio would result in an increase in the distance between the droplets, and in this case the adsorption process would be governed by the distribution of surfactant between dispersed oil droplets and the solid surface".

To test the adsorption of the microemulison ME-V, the effluent profile of active component vs. pore volume was determined. Sulfated alcohol (C12) and ethoxylated alcohol (C13) were active components of the microemulsion ME-V. Inductive coupled plasma (ICP) technique was used to measure the concentration of sulfur in the effluent

samples. The maximum concentration of the sulfur in the treatment fluid (0.2 wt% ME-V in 2 wt% KCl) before injection to the core was measured to be 6.123 mg/L and used as a controller for the adsorption test. The profile of the measured sulfur concentration is plotted vs. pore volume of the injected fluid as shown in **Figs. 35** and **36** corresponding to the coreflood tests in Figs. 32 and 33. As can be seen from the Fig. 35, the concentration of the sulfur became almost half of the maximum value (3.59 mg/L) in the collected sample which showed medium adsorption of microemulsions to the core. In the wash-off test, the concentration of active ingredient had a small decrease in each cycle showing that even though the microemulsion was slightly washed off from the core in each cycle, but still was present in the core and was effective in reducing gas permeability. The sulfur concentrations had values of 2.12, 2.27, and 2.35 mg/L after first, second, and third cycles after nitrogen injections as shown in Fig. 36.

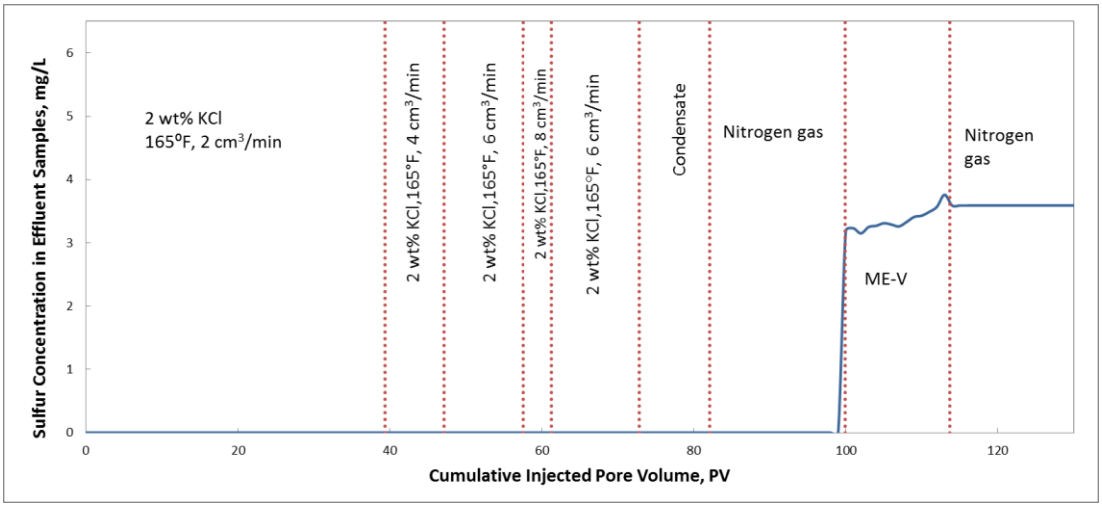

Fig. 35—Concentration of sulfur measured in the core effluent samples.

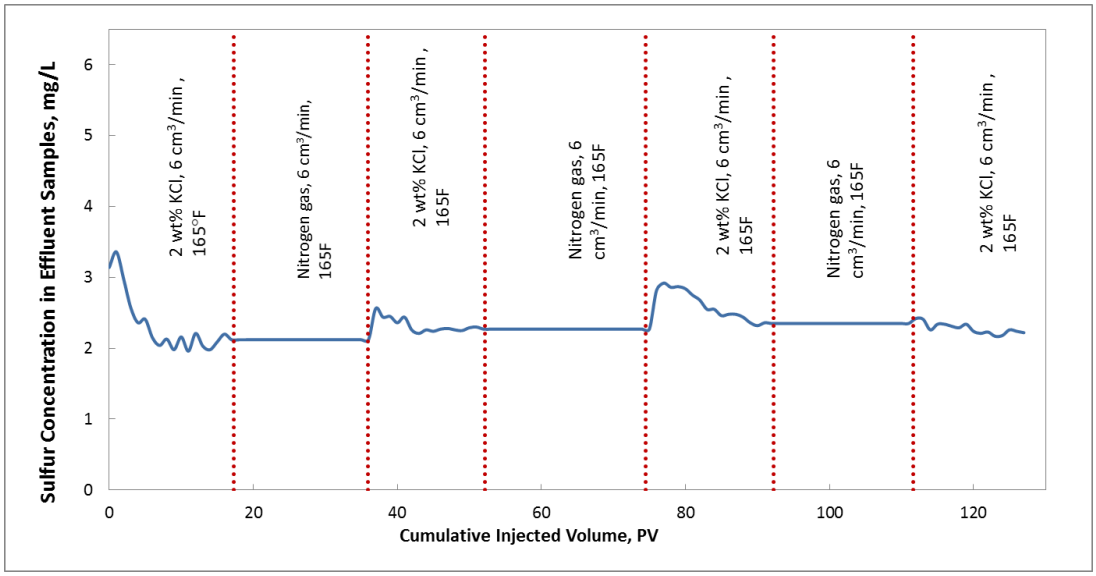

Fig. 36—Concentration of sulfur measured in the core effluent samples in the wash-off test.

Another set of experiments were performed in order to investigate and compare the potential of microemulsions and surfactants to improve the effective permeability to gas in the presence of brine (2 wt% KCl).

The experiments were performed on Bandera sandstone cores saturated with 2 wt% KCl. Temperature of 165°F, back pressure of 700 psi, overburden pressure of 1800 psi, and flow rate of 5 cm^3/min were test conditions. ME-V, which had the lowest surface tension value and showed least water wettability characteristics compared to other microemulsions were tested along with two surfactants including the non-ionic and the anionic surfactants. Since the sandstone cores were negatively charged, the cationic surfactant was not selected for the coreflood experiments.

Before running the coreflood tests, surface tension was measured for ME-V, Surf-N, and Surf-A at 165°F. **Fig. 37** shows the results of surface tension measurements for 0.2 wt% of ME-V, Surf-A, and Surf-N in 2wt% KCl at 165°F. ME-V had the surface tension

of 28 mN/m at 165°F compared to 45.4 and 51.2 mN/m for Surf-N and Surf-A, respectively at 165°F.

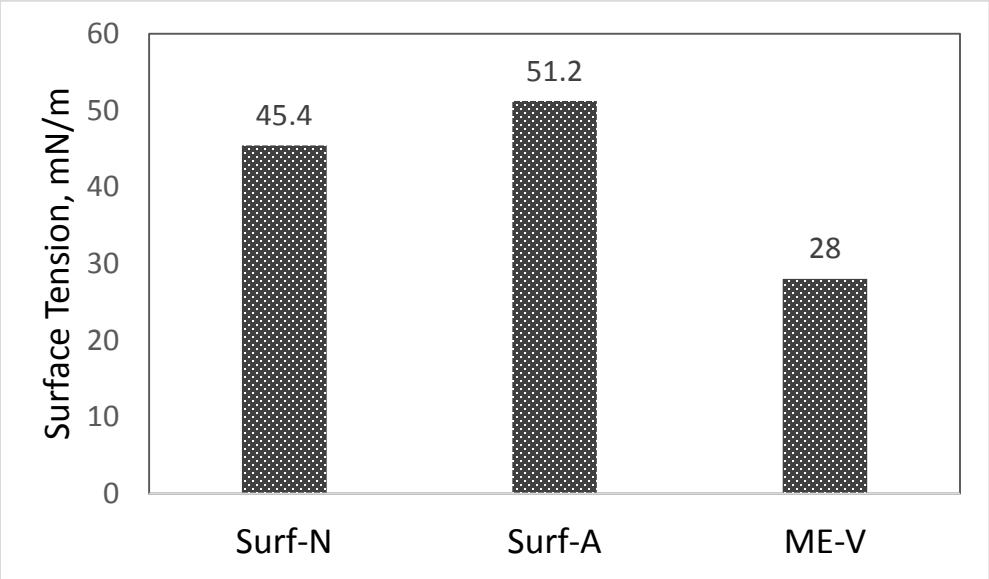

Fig. 37— Surface Tension of 0.2 wt% of chemicals in 2 wt% KCl at 165°F.

The absolute permeability of the all Bandera sandstone cores were measured by injecting 2 wt% KCl into the core until the pressure was stabilized. The results showed that the absolute permeabilities were between 17 to 22 md for these outcrops of Bandera sandstone cores. The effectiveness of the chemical treatment was quantified by calculating the change in the relative gas permeability values before and after treatment by defining the improvement factor (IF) as the ratio of relative gas permeability after treatment to that of before treatment at S_w=58 %. This quantifies the degree of improvement for each test. Klinkenberg effect corrections were made using linear relationship between the measured gas permeability (k_a) and the reciprocal mean pressure ($\frac{1}{P}$), to calculate k_∞ "equivalent liquid permeability" also called Klinkenberg-corrected permeability (Ziarani and Aguilera

2012). Taking the Klinkenberg equation as fact, gas slippage factor was determined using a correlation as mentioned in Eq. 9. Using measured porosity and mean pressure values, equivalent liquid permeability (k_∞) can be calculated in Eq. 8 for each chemical tested in the coreflood test. Values of equivalent liquid permeability and corrected relative gas permeabilities are given in **Table 11**. The Klinkenberg corrected values of gas relative permeabilities are slightly lower than the original values, which showed overestimation of relative permeabilities, if gas slippage be ignored.

Table 11—Summary of coreflood experiments using Bandera sandstone cores.

	Core 1		Core 2		Core 3	
	No Klinkenberg Effect	**Considering Klinkenberg Effect**	**No Klinkenberg Effect**	**Considering Klinkenberg Effect**	**No Klinkenberg Effect**	**Considering Klinkenberg Effect**
Treatment Fluid Injected	Surf-N		Surf-A		ME-V	
Temperature (°F)	165		165		165	
Concentration of Treatment Solution in 2 wt% KCl	0.2		0.2		0.2	
Initial Sw_{irr} (%)	0.506		0.535		0.519	
K_{rgcw} at Initial S_{wirr}	0.022	0.022	0.021	0.021	0.037	0.036
Final S_{wirr} (%)	0.534		0.562		0.478	
K_{rgcw} at Final S_{wirr}	0.016	0.015	0.011	0.011	0.107	0.105
K_{irg} at S_w= 58 %	0.015	0.014	0.016	0.016	0.026	0.025
K_{frg} at S_w= 58 %	0.012	0.011	0.010	0.010	0.062	0.061
Improvement Factor (K_{frg}/ K_{irg})	0.80	0.798	0.63	0.63	2.35	2.37

Corey correlation was used to calculate the gas relative permeabilities at S_w=58 %, using end-points relative permeabilities. The values of irreducible water saturations and endpoint gas relative permeabilities for all tested chemicals are reported in Table 11. The

improvement factor at 58 % water saturation was 2.37 for ME-V solution, where the relative gas permeability was increased from an initial value of 0.025 to a final relative gas permeability of 0.061 after treatment as shown in **Fig. 38**.

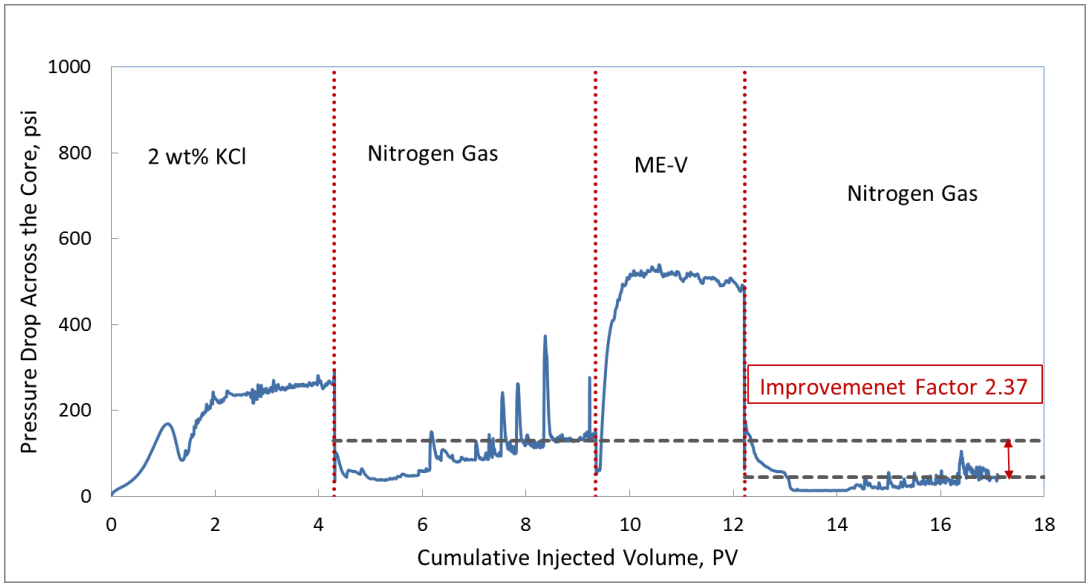

Fig. 38—Pressure drops across the core vs. cumulative injected volume for chemical treatment with microemulsion ME-V at concentration of 0.2 wt% ME-V in 2 wt% KCl at 165°F.

The coreflood experiments were conducted on 20 in. Bandera sandstone cores for the anionic surfactant (Surf-A) and the non-ionic surfactant (Surf-N). The anionic surfactant solution changed the relative permeability to gas from the initial value of 0.016 to 0.010 and caused an improvement factor of 0.63 as shown in **Fig. 39**.

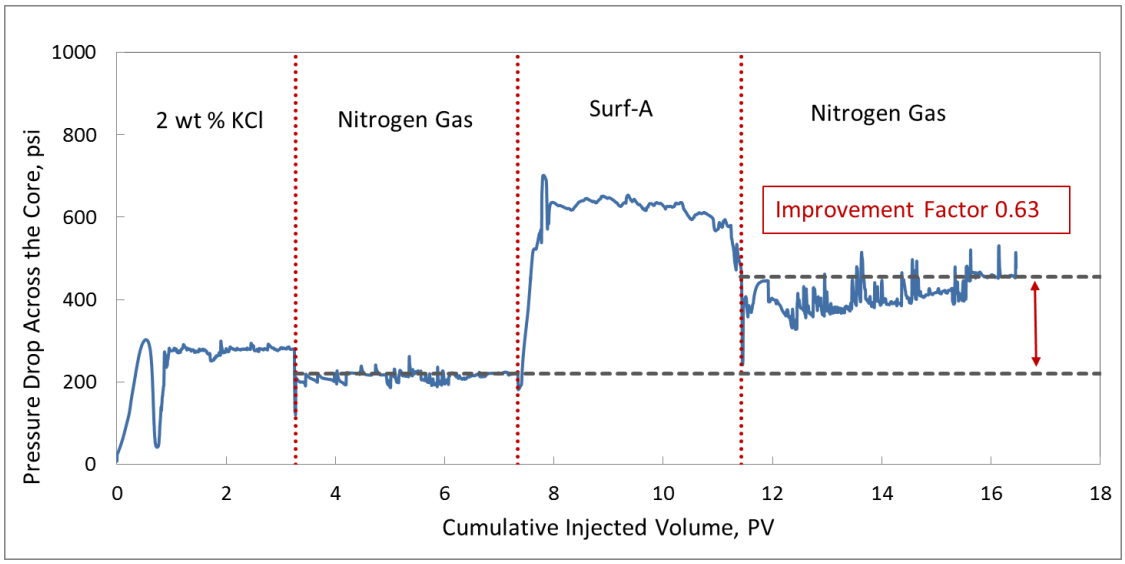

Fig. 39—Pressure drops across the core vs. cumulative injected volume for chemical treatment with anionic surfactant Surf-A at concentration of 0.2 wt% Surf-A in 2 wt% KCl at 165°F.

The non-ionic surfactant (Surf-N) showed a change in the relative gas permeability from an initial value of 0.014 to a final gas relative permeability of 0.011 after treatment and caused 0.80 improvement factor as shown in **Fig. 40**.

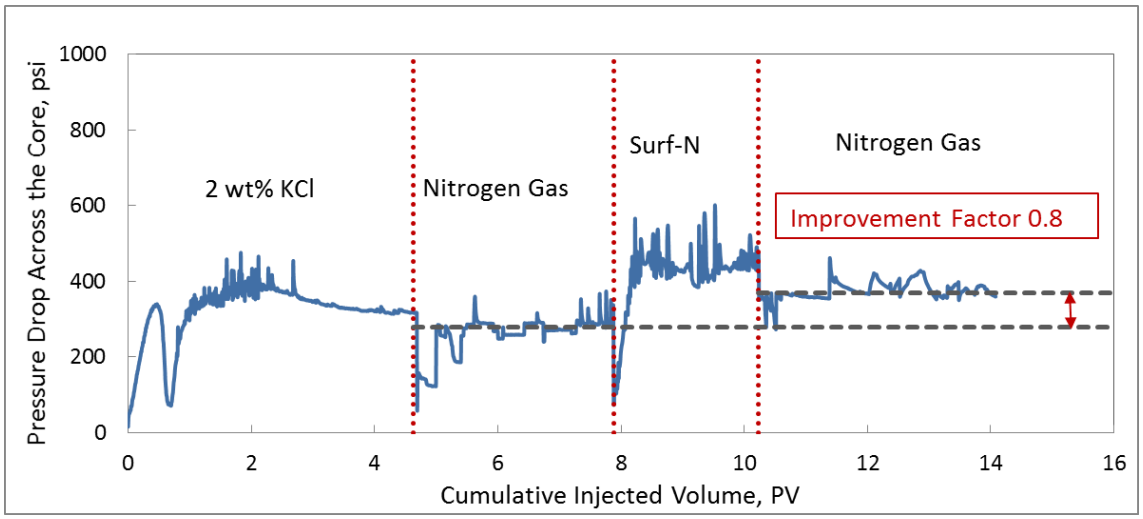

Fig. 40—Pressure drops across the core vs. cumulative injected volume for chemical treatment with non-ionic surfactant Surf-N at concentration of 0.2 wt% Surf-N in 2 wt% KCl at 165°F.

The surfactant solutions couldn't enhance the gas permeability as effective as the microemulsion treatment fluid. Penny et al. (2005) explains the reason for better efficiency of microemulsions as, "when oil-in-water microemulsions are used in a cleanup or remediation operation, the modes of action for both a microemulsion-forming surfactant and an organic solvent are combined to increase the penetration and cleaning capability that outperforms pure organic solvents or pure surfactant systems when used independently." A comparison of relative gas permeability values and improvement factors for the microemulsion ME-V, the anionic surfactant, and the non-ionic surfactant is summarized in Table 11. When compared to the anionic and non-ionic surfactants, a high permeability improvement of 2.37 was achieved by injection of 0.2 wt% ME-V into the Bandera sandstone core. **Figs. 41** to **43** show the gas relative permeability curves for brine and chemical treatments. It can be seen from the curves that unlike surfactant solutions, after microemulsion chemical treatment, the irreducible water saturation decreased and gas relative permeability increased.

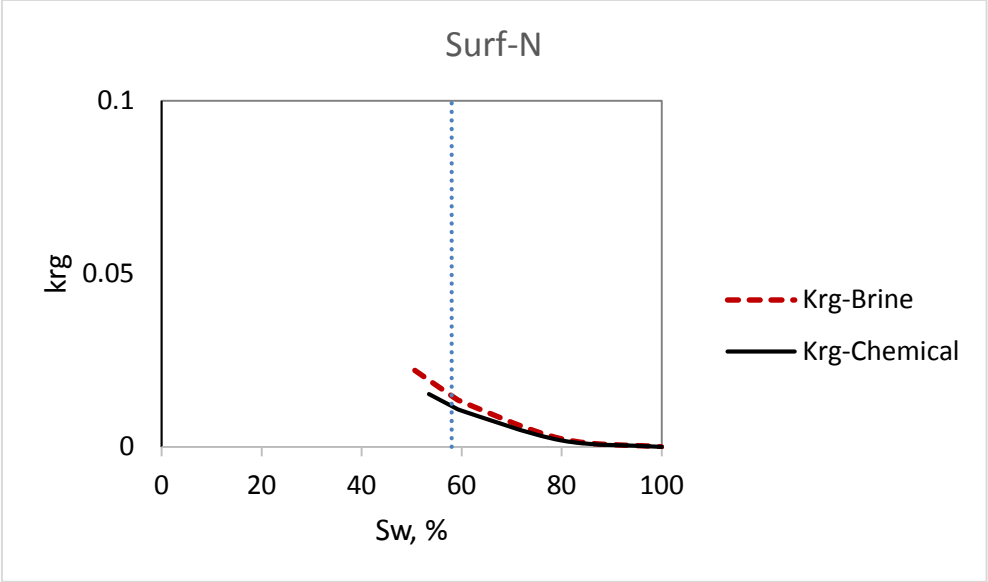

Fig. 41—Gas relative permeability curves for brine and Surf-N showed reduced gas permeability after chemical treatment.

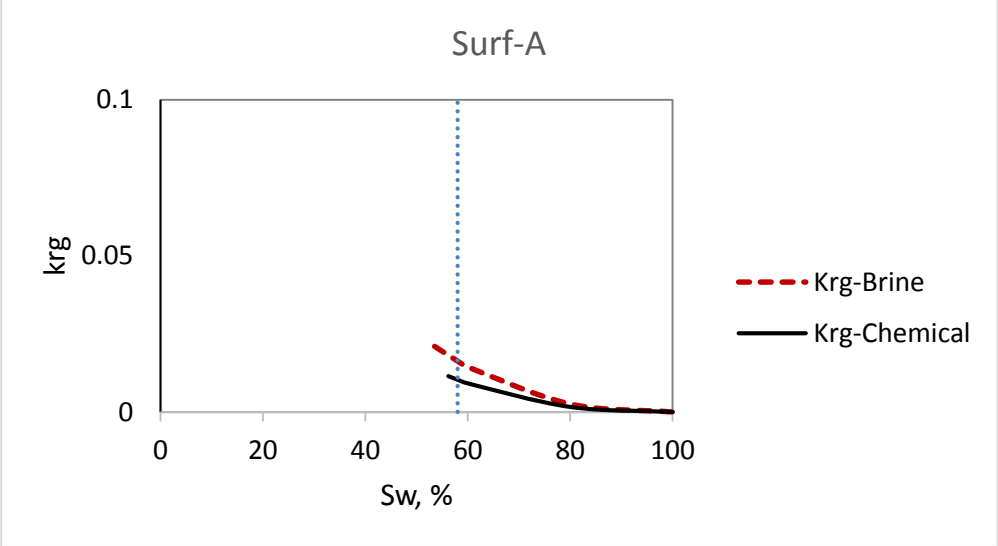

Fig. 42—Gas relative permeability curves for brine and Surf-A showed reduced gas permeability after chemical treatment.

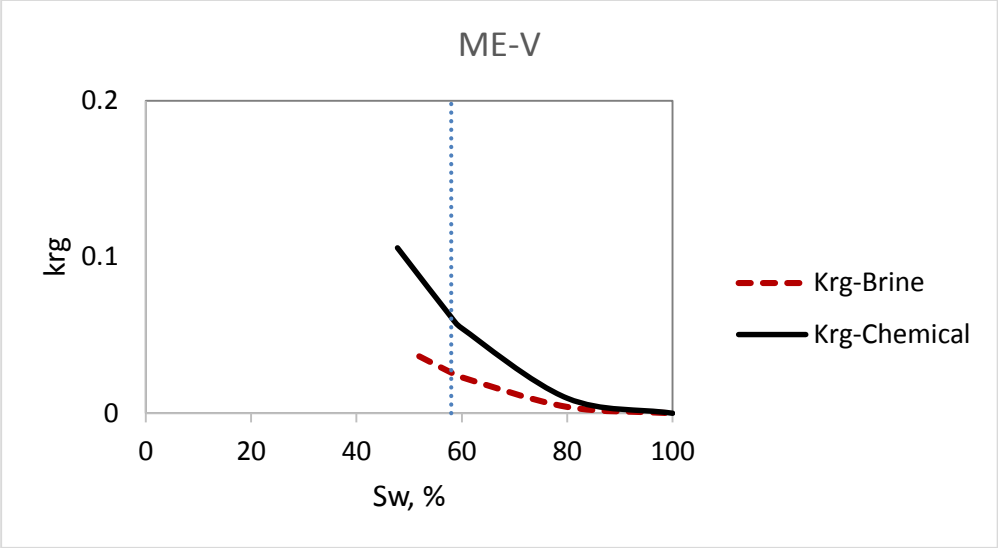

Fig. 43—Gas relative permeability curves for brine and ME-V showed increased gas permeability after chemical treatment.

METHODOLOGY

Effect of Salinity

Efficiency of microemulsions in reducing surface tension in the presence of different brine solutions were tested at 25°C. Experiments were done by preparing 0.5 wt% of microemulsion in different brine solutions including NaCl, KCl, $CaCl_2$, and $MgCl_2$ at concentrations of 2, 5, and 10 wt%. The compatibility tests resulted in phase separation and incompatibity for some of the solutions.

Compatibility tests showed that microemulsion-N was not compatible with any type of brine solutions at low and high salt concentrations. There was separation of emulsions from the solution after mixing microemulsion-N with different concentrations of NaCl, KCl, $CaCl_2$, and $MgCl_2$ at 25°C. No precipitation, phase separation, or color changes were observed for the ME-V and ME-E. **Fig. 44** shows the picture of the microemulsions in 2 wt% KCl at 25°C. Surface tensions of microemulsion fluids ME-V and ME-E were measured at 25°C to investigate the effect of salinity on the surface tension values of microemulsions. **Figs. 45** and **46** show the results for ME-E and ME-V, respectively. For both microemulsions, increasing the concentration of the salts in the solutions did not change the surface tension values significantly. These two microemulsions had low surface tensions at low and high salinity fluids.

ME-E	ME-N
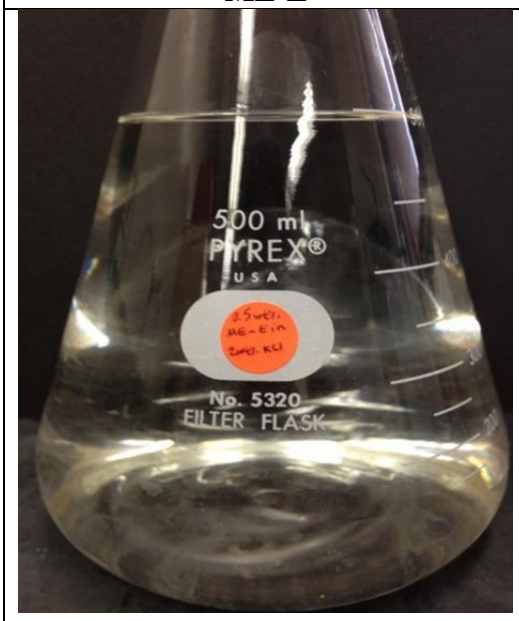	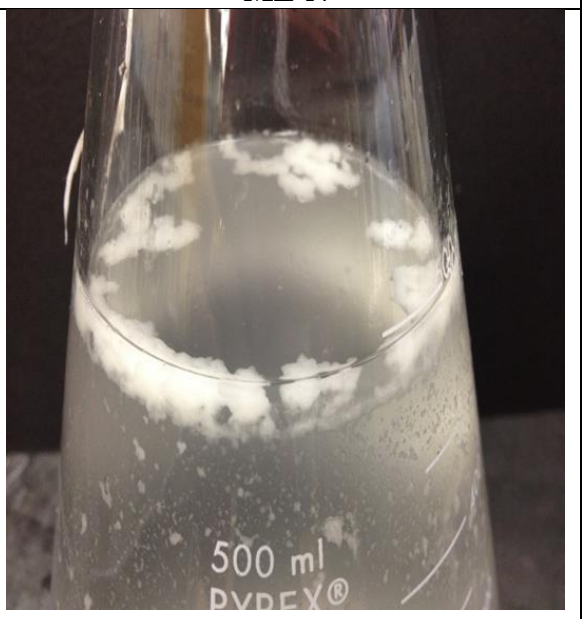
Compatible	**Not Compatible**

Fig. 44—Compatibility tests for 0.5 wt% of microemulsions in brine solutions showing the incompatibility of ME-N with all different concentrations of NaCl, KCl, CaCl2, and MgCl2 at 25°C.

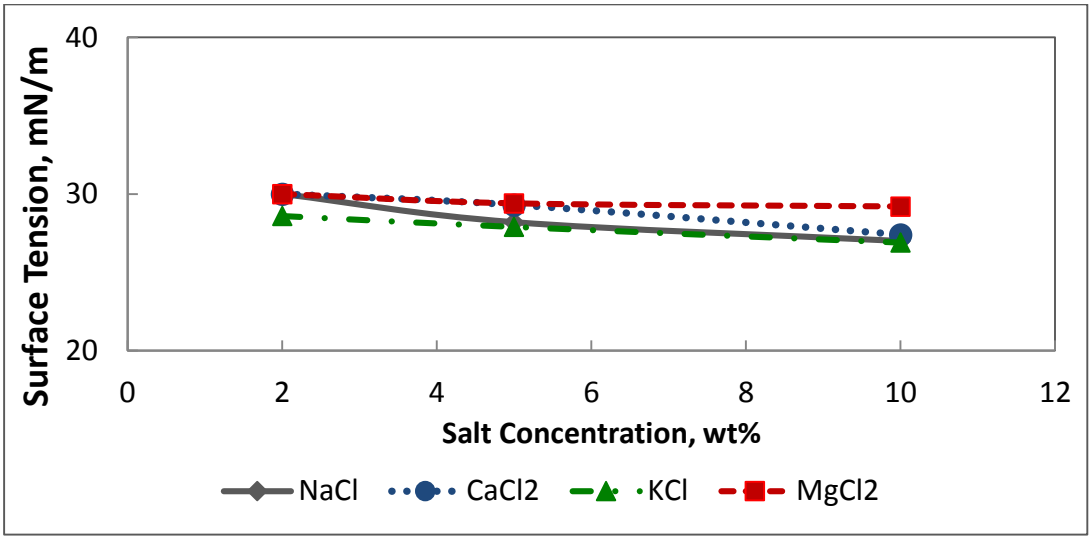

Fig. 45—Surface tension of microemulsion-E at low and high salinity solutions.

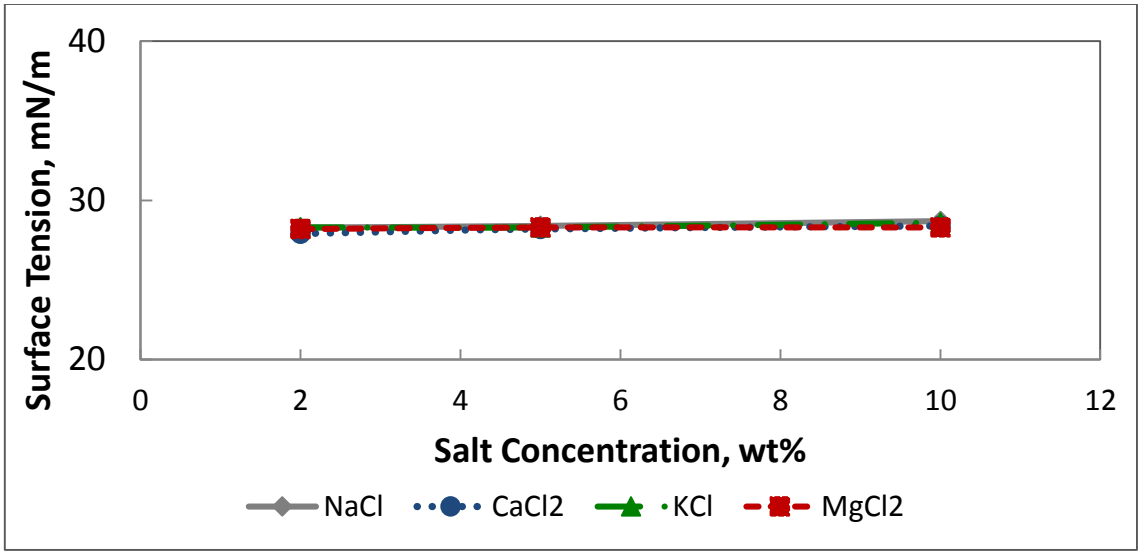

Fig. 46—Surface tension of microemulsion-V at low and high salinity solutions.

By changing the concentration of the microemulsions from 0.5 to 2 wt% in 2 wt% of brine solutions, no significant change in surface tension measurements was observed as shown in **Figs. 47** and **48**. Brine solutions included KCl, NaCl, $CaCl_2$, and $MgCl_2$. This result is important when designing a chemical treatment to optimize the performance of the treatment and consider the economical aspect of the project.

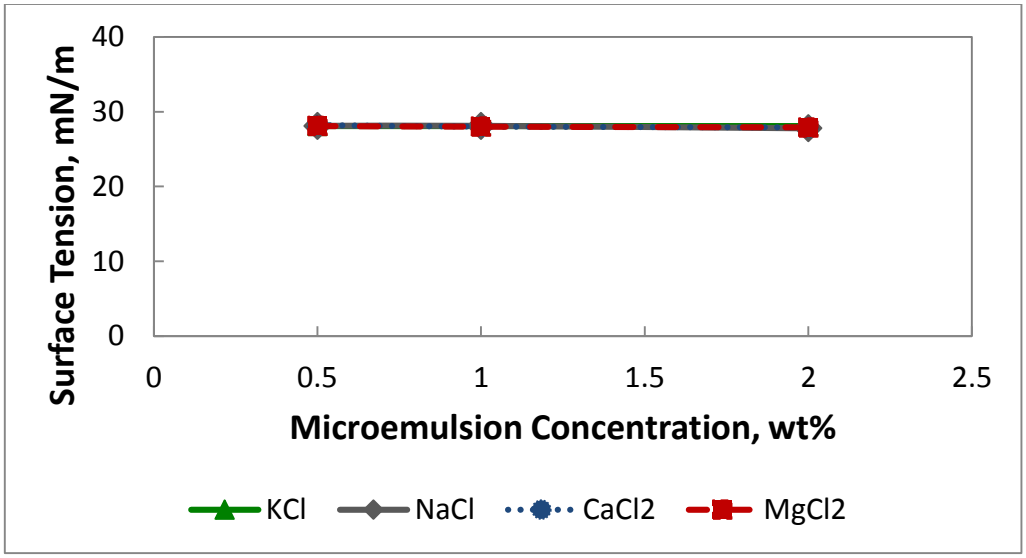

Fig. 47—Surface tension of microemulsion-V at different concentrations in 2 wt% of brine solutions.

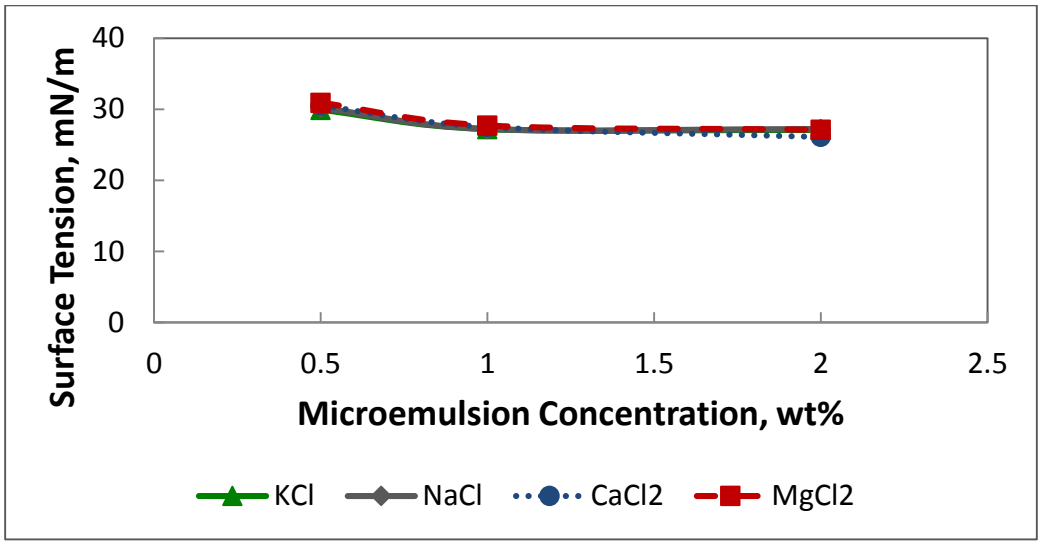

Fig. 48—Surface tension of microemulsion-E at different concentrations in 2 wt% of brine solutions.

Aging Effect

Four different shale rocks including the outcrop of Barnett shale, Mancos shale, Marcellus shale, and the reservoir rock of the New Albany shale were sieved and the rock particles of 140 mesh size corresponding to average particle size of 105 µm was used to study the aging effect on fluid-rock interactions.

All samples were prepared by mixing 1 wt% of rock samples in 0.5 wt% of different solutions including two microemulsions, ME-V and ME-E, deionized water and 2 wt% KCl. The samples were left for different time intervals and the concentration of some elements in the sample after being aged at different time intervals was measured. ICP test were running of the sample to measure the concentration of the Ca, Mg, Si, and Al elements in different solutions. Results for different shale rocks is summarized as follows:

Barnett Shale

Figs. 49 to **52** show the results of ICP for the Barnett shale rock after different contact time. As can be seen from the figures, the concentration of the elements in the solution is increasing after the rock is in contact with the solution as the contact time increased.

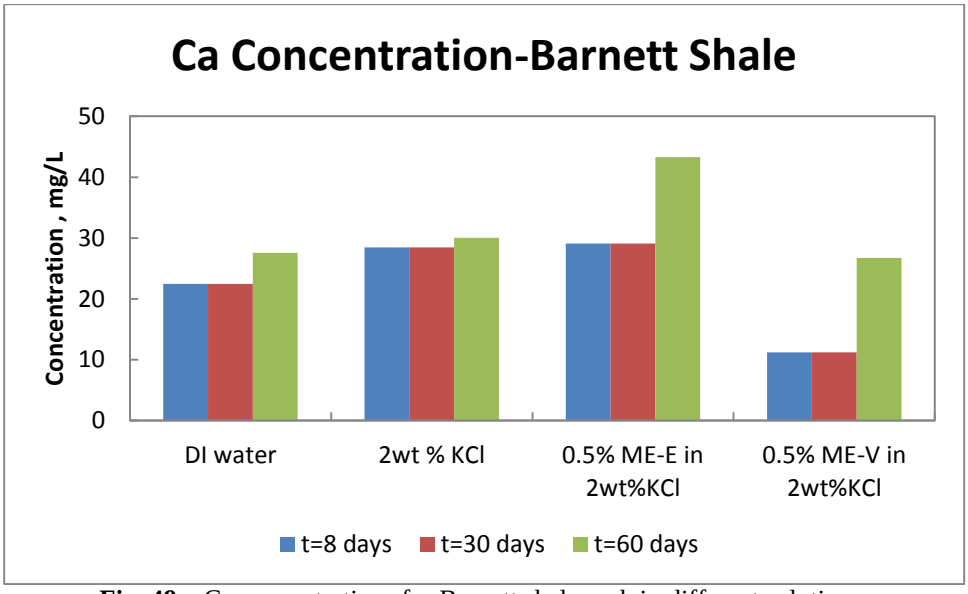

Fig. 49—Ca concentrations for Barnett shale rock in different solutions.

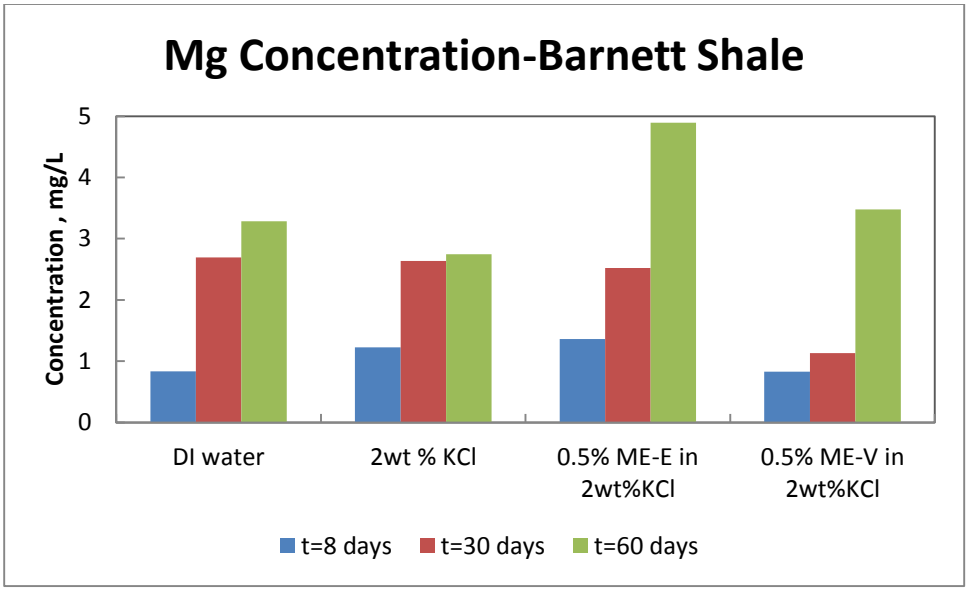

Fig. 50—Mg concentrations for Barnett shale rock in different solutions.

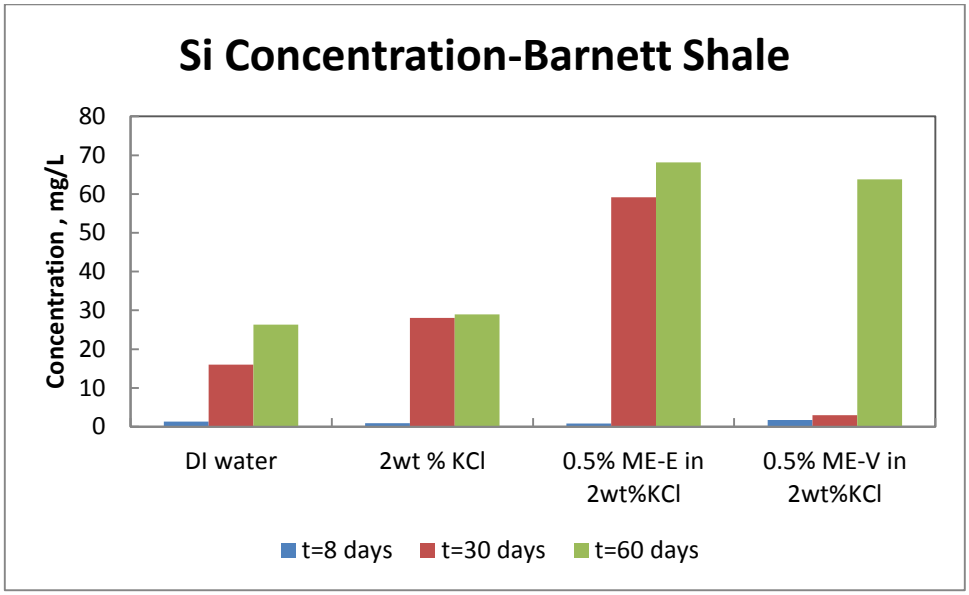

Fig. 51—Si concentrations for Barnett shale rock in different solutions.

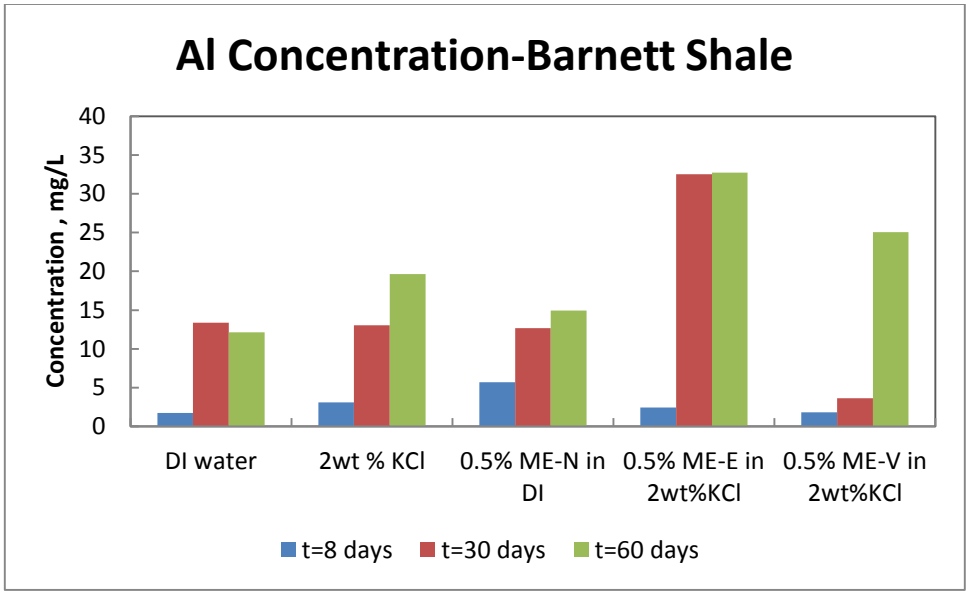

Fig. 52—Al concentrations for Barnett shale rock in different solutions.

Mancos Shale

Figs. 53 to **56** show the results of ICP for the Mancos shale rock after different contact time. As can be seen from the figures, the concentration of the elements in the solution is increasing after the rock is in contact with the solution as the contact time increased.

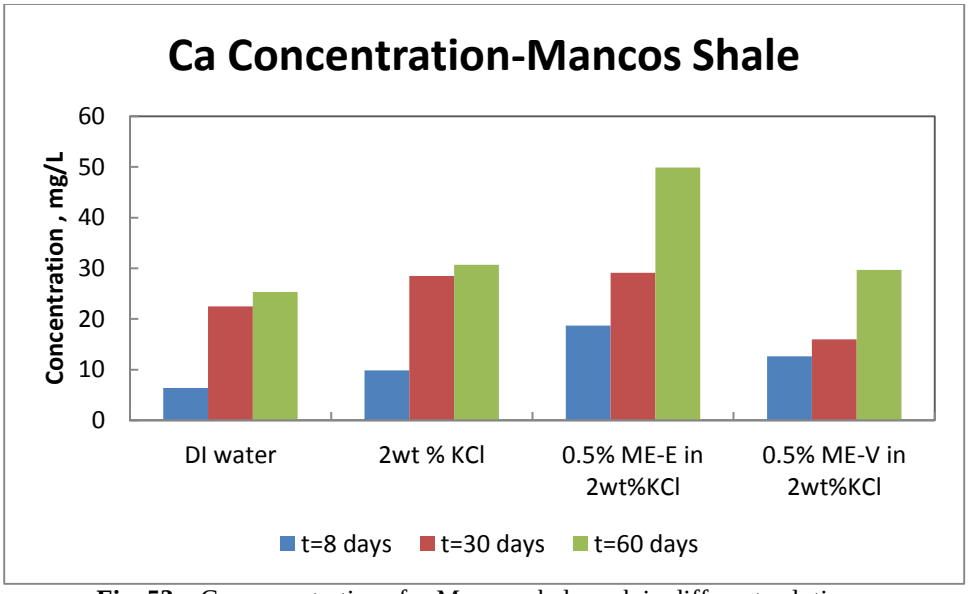

Fig. 53—Ca concentrations for Mancos shale rock in different solutions.

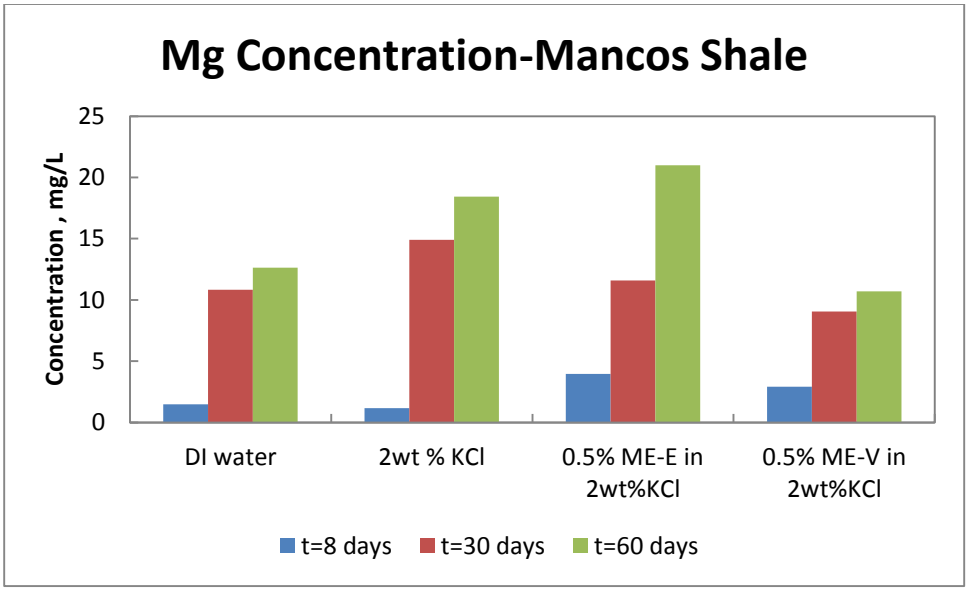

Fig. 54—Mg concentrations for Mancos shale rock in different solutions.

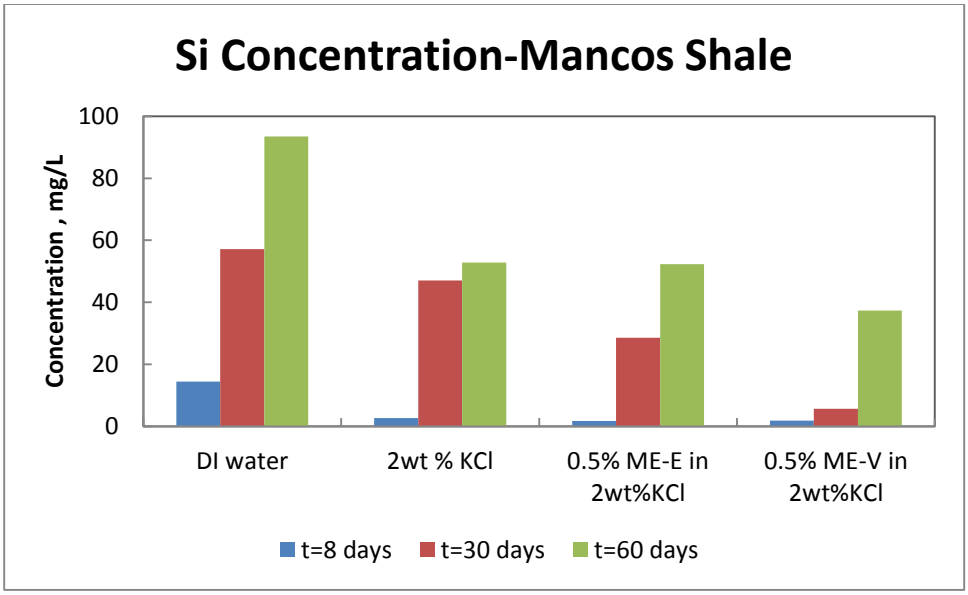

Fig. 55—Si concentrations for Mancos shale rock in different solutions.

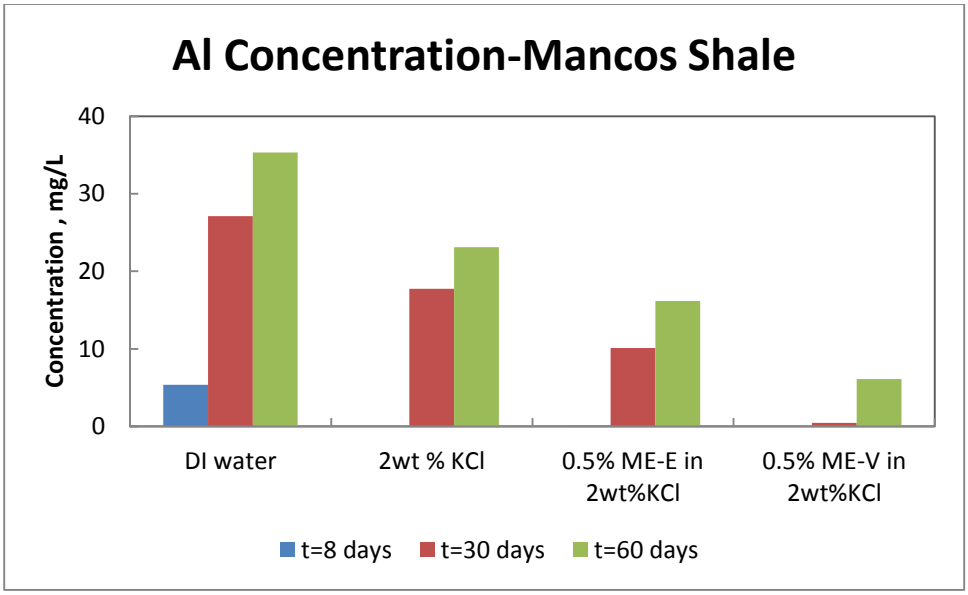

Fig. 56—Al concentrations for Mancos shale rock in different solutions.

Marcellus Shale

Figs. 57 to **60** show the results of ICP for the Marcellus shale rock after different contact time. As can be seen from the figures, the concentration of the elements in the

solution is increasing after the rock is in contact with the solution as the contact time increased.

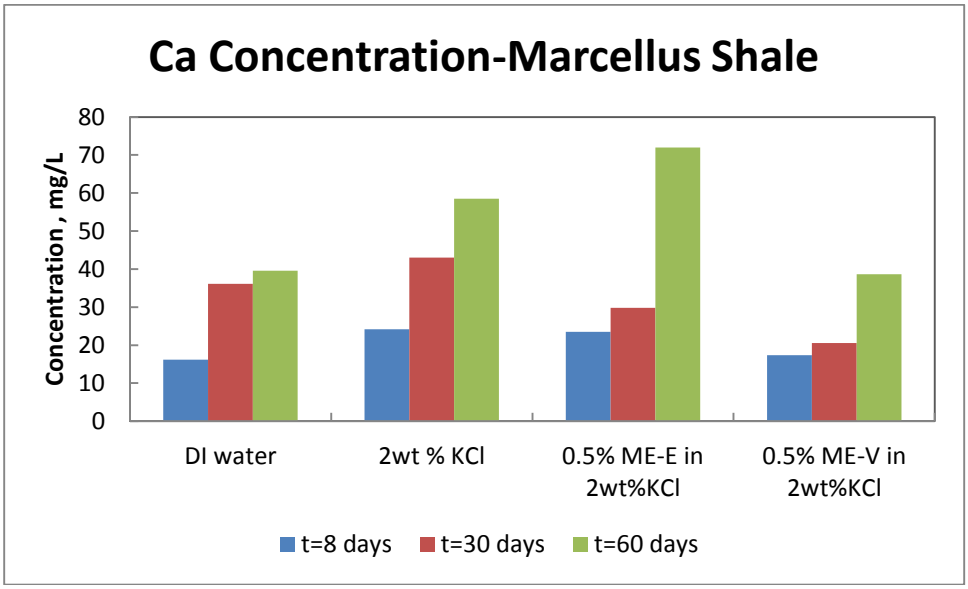

Fig. 57—Ca concentrations for Marcellus shale rock in different solutions.

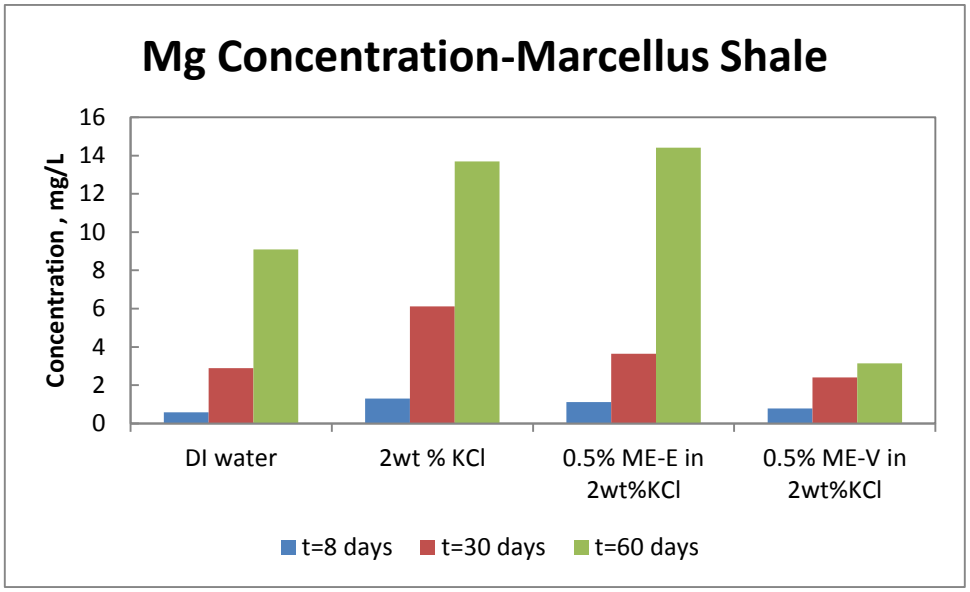

Fig. 58—Mg concentrations for Marcellus shale rock in different solutions.

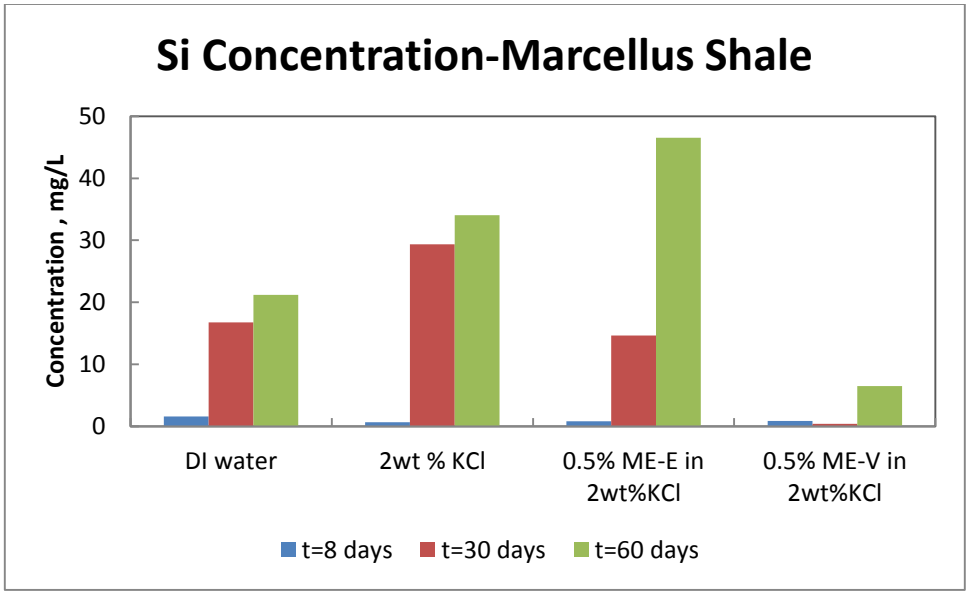

Fig. 59—Si concentrations for Marcellus shale rock in different solutions.

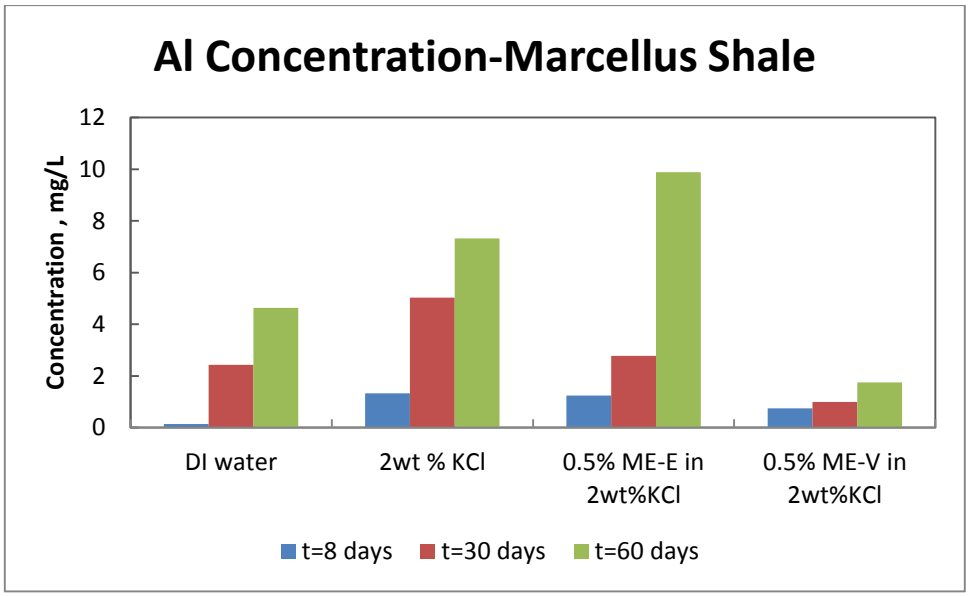

Fig. 60—Al concentrations for Marcellus shale rock in different solutions.

New Albany Shale

Figs. 61 to **64** show the results of ICP for the New Albany shale rock after different contact times. As can be seen from the figures, the concentration of the elements in the

solution is increasing after the rock is in contact with the solution as the contact time increased.

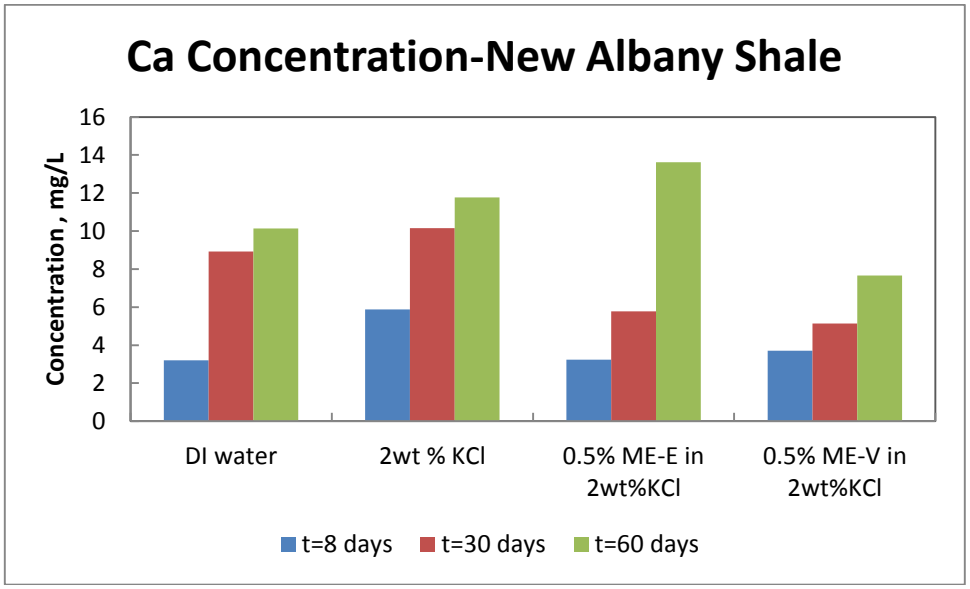

Fig. 61—Ca concentrations for New Albany shale rock in different solutions.

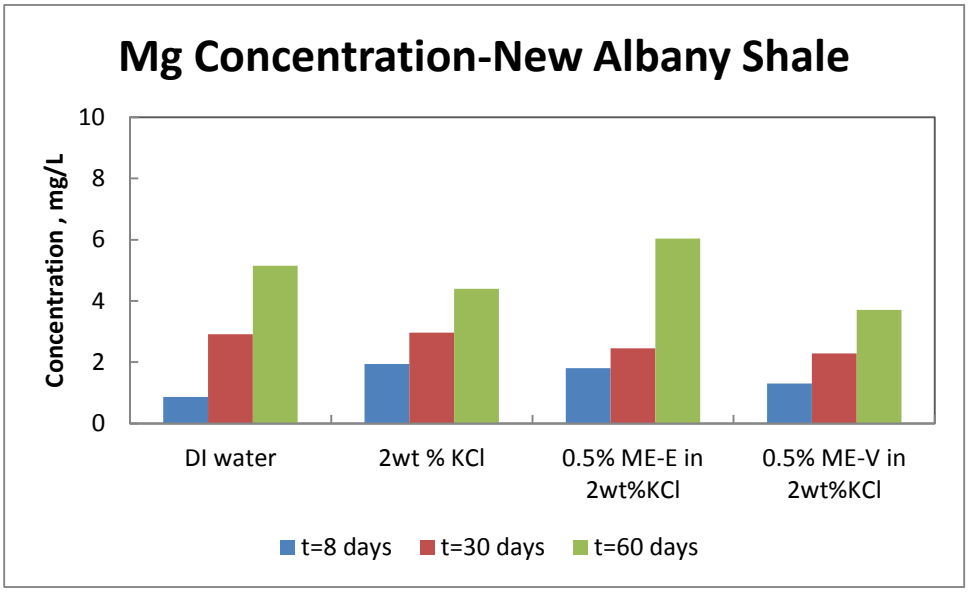

Fig. 62—Mg concentrations for New Albany shale rock in different solutions.

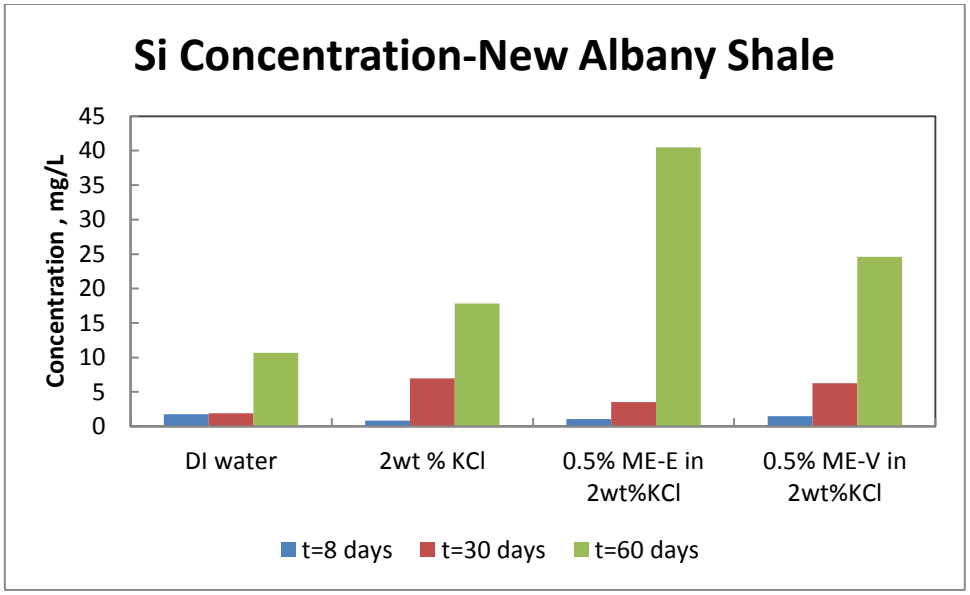

Fig. 63—Si concentrations for New Albany shale rock in different solutions.

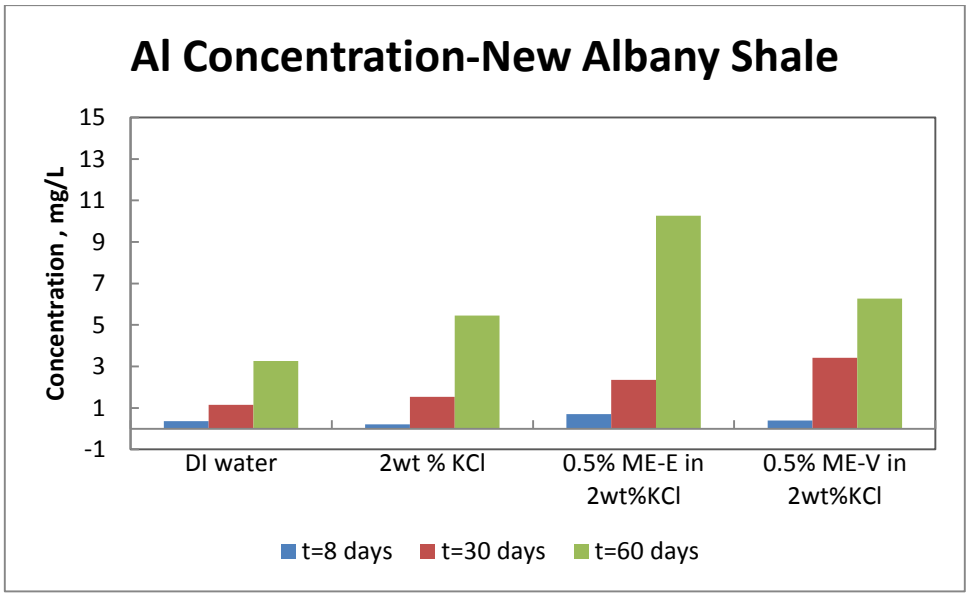

Fig. 64—Al concentrations for New Albany shale rock in different solutions.

CONCLUSIONS AND RECOMMENDATIONS*

Conclusions

Three microemulsions were tested and compared with the cationic, anionic, and non-ionic surfactants to investigate their effectiveness in reducing surface tension and change in rock wettability characteristics and also in enhancing the gas permeabilities. Mutual solvent and fluorocarbon polymer were used for comparison purposes in enhancing the gas relative permeability and were tested on Bandera sandstone cores with permeabilities greater than 10 md. Based on the results obtained, the following conclusions were made:

Droplet Size Distribution of Microemulsion System

The average size of microemulsion (as received) detected by Transmission electron micrographs (TEM) was in the range of 30-60 nm. This is an important factor to be considered in low permeability reservoirs where small pore-throat will be plugged by injected fluid. Smaller value of microemulsion droplet size compared to the surfactant droplets results in a good infectivity and penetration without filtration to the formation.

---

*Part of this chapter is reprinted with permission from *Improving Gas Relative Permeability in Tight Gas Formations by Using Microemulsions* by A. Rostami, D.T. Nguyen, H.A. Nasr El Din, 2014, Paper IPTC 17675, Copyright [2014] by International Petroleum Technology Conference. And *Microemulsion vs. Surfactant Assisted Gas Recovery in Low Permeability Formations with Water Blockage* by A. Rostami and H.A. Nasr El Din, 2014, Paper SPE 169582, Copyright [2014] by Society of Petroleum Engineers.

Surface Tension Measurements

Surface tension was less for microemulsions compared to the cationic, anionic, and non-ionic surfactants at concentrations ranging from 0.05 to 2 wt%. Longer interfacial contact and higher surfactant solubility capacity of microemulsion compared to the surfactants could be an explanation of the results. Lower surface tension will result in a lower capillary pressure in pores of the rock and will lead to higher production. This result is especially important in low permeability reservoirs where capillary forces are high and fluid invasion is one of the main sources of fluid trapping inside the formation.

Thermal Stability Study

Insignificant change in surface tension values of microemulsions after being aged for 24 hours at 150, 250, and 400ºF showed high thermal stability of the microemulsions. No precipitation, phase separation, and color changing was observed after being at high temperatures up to 400°F for 24 hours.

Compatibility Tests

Two microemulsions, ME-V and ME-E, showed compatibility with the brine solution (2 wt% KCl) and condensate. ME-N was incompatible with both the brine solution and the condensate.

Rock Characterization

The results of the XRD on three shale rocks showed that Barnett and New Albany shale had the most amount of clays including kaolinite and Illite, and some smectite. Marcellus had the most amount of carbonate, and New Albany shale had the most amount

of minerals which main part was quartz, in addition to feldspar, pyrite, barite and other minerals. Mineralogy and clay content of the rock plays an important role in fluid-rock interactions.

Zeta Potential Test

The results of the zeta potential tests for microemulsions showed that the ME-V has the lowest negative value of zeta potential, which resulted in lower water wettability characteristics compared to the other microemulsions. The values of zeta potential for Barnett and New Albany shale were the highest compared to the other rock types due to high clay content in these rocks as determined by XRD.

Contact Angle Measurements

Contact angle values showed that microemulsion ME-V was the least water-wet compared to the other tested fluids and the 2 wt% KCl solution was characterized as the most wetting chemical on Barnett shale rock at 165°F and atmospheric pressure.

Coreflood Study

When compared to mutual solvent and fluoropolymer surfactant, which caused damage to the cores, both microemulsions improved the effective gas permeability. The highest permeability improvement was achieved by an injection of 0.2 wt% ME-V into the 20 in. Bandera sandstone core, while mutual solvent and fluoropolymer surfactant solutions, caused damage to the core. The microemulsion, ME-V, showed long term sustainability against wash-off, which makes this chemical a candidate for fracturing applications.

In second set of experiments, microemulsion ME-V (0.2 wt% ME in 2 wt% KCl) was compared with anionic and non-ionic surfactant solutions at the same concentrations and experimental conditions and showed the best results in improving relative permeability to gas and fluid recovery compared to anionic and non-ionic surfactant solutions.

Salinity Effect

Salinity effect results showed that ME-V and ME-E were compatible with the KCl, NaCl, $CaCl_2$, and $MgCl_2$ brine solutions at 2, 5, 10 wt% concentrations. ME-N was incompatible with all brine solutions tested and caused phase separation. Microemulsions had different components in their structures, and reacted differently to the presence of salts.

For ME-V and ME-E, increasing the concentration of the salts did not change the surface tension values significantly. These two microemulsions had low surface tensions at 2, 5, and 10 wt% KCl, NaCl, CaCl2, and MgCl2 brine solutions.

Aging Effect

Aging the rock particles in contact with different treatment fluids showed an increase in the concentration of tested elements including Ca, Mg, Al, and Si in the solutions that can be an explanation of high total dissolved solid (TDS) in the flow back fluid after completion.

Recommendations

Effect of aging on the fluid-rock interactions at high temperatures and high pressures is recommended to simulate the reservoir conditions and for time intervals more than 60 days.

Effect of rock mineralogy on the relative gas permeability and water blockage is recommended to be conducted using microemulsions as the chemical treatment.

REFERENCES

Ahmadi, M., Sharma, M.M., Pope, G.A. et al. 2011. Chemical Treatment to Mitigate Condensate and Water Blocking in Gas Wells in Carbonate Reservoirs. *SPE Prod & Oper* **26** (1): 67-74. SPE-133591-PA. http://dx.doi.org/10.2118/133591-PA.

Ahmed, T. and McKinney, P.D. 2005. *Advanced Reservoir Engineering*. Gulf Professional Publishing/Elsevier. Chap. 1, 1/9.

AMETECH. http://www.ametech.it/ma_microemulsions.htm (accessed 2 July 2012).

Ali, S.A., Couillet, I., England, K.W. et al. 2011. Microemulsion to Improve Shale Gas Production by Controlling Water Imbibition. US Patent No.2011/0021386 A1.

Al-Anazi, H.A., Okasha, T.M., Haas, M.D. et al. 2005. Impact of Completion Fluids on Productivity in Gas/Condensate Reservoirs. Paper SPE 94256 presented at the SPE Production Operations Symposium, Oklahoma City, Oklahoma, 16-19 April. http://dx.doi.org/10.2118/94256-MS.

Alotaibi, M.B., Nasralla, R.A., and Nasr-El-Din, M.A. 2011. Wettability Studies Using Low-Salinity Water in Sandstone Reservoirs. *SPE Res Eval & Eng* **6** (14): 713-725. SPE-149942-PA. http://dx.doi.org/10.2118/149942-PA.

Babadagli, T. 2005. Mature Field Development-A Review. Paper SPE 93884 presented at the SPE Europe/EAGE Annual Conference held in Madrid, Spain, 13-16 June. http://dx.doi.org/10.2118/93884-MS.

Bang, V.S.S., Pope G.A., Sharma, M.M. et al. 2010. A New Solution to Restore Productivity of Gas Wells with Condensate and Water Blocks. *SPE Res Eval & Eng* **13** (2): 323-331. SPE 116711-PA. http://dx.doi.org/10.2118/116711-PA.

Bennion D.B., Bietz, R.F., Thomas, F.B. et al. 1994. Reductions in the Productivity of Oil and Low Permeability Gas Reservoirs Due to Aqueous Phase Trapping. *JCPT* **33** (9). PETSOC-94-09-05. http://dx.doi.org/10.2118/94-09-05.

Bennion, D.B., Thomas, F.B., and Bietz, R.F.1996. Low Permeability Gas Reservoirs: Problems, Opportunities and Solutions for Drilling, Completion, Stimulation and Production. Paper SPE 35577 presented at the SPE Gas Technology Symposium, Calgary, Alberta, Canada. 28 April-1 May. http://dx.doi.org/10.2118/35577-MS.

Bennion, D.B., Thomas, F.B., and Ma, T. 2000a. Recent Advances in Laboratory Test Protocols to Evaluate Optimum Drilling, Completion and Stimulation Practices for Low Permeability Gas Reservoirs. Paper SPE 60324 presented at the SPE Rocky

Mountain Regional/ Low-Permeability Reservoirs Symposium and Exhibition, Denver, Colorado, 12-15 March. http://dx.doi.org/10.2118/60324-MS.

Bennion, D.B., Thomas, F.B., and Ma, T. 2000b. Formation Damage Processes Reducing Productivity of Low Permeability Gas Reservoirs. Paper SPE 60325 presented at the SPE Rocky Mountain Regional/Low-Permeability Reservoirs Symposium and Exhibition. Denver, Colorado, 12-15 March. http://dx.doi.org/10.2118/60325-MS.

Bennion, D.B., Thomas, F.B., Imer, D. et al. 2000c. Low Permeability Gas Reservoirs and Formation Damage -Tricks and Traps. Paper SPE 59753 presented at the SPE/CERI Gas Technology Symposium, Calgary, Alberta, Canada, 3-5 April. http://dx.doi.org/10.2118/59753-MS.

Bennion, D.B., Thomas, F.B., Schulmeister, B. et al. 2006. Water and Oil Base Fluid Retention in Low Permeability Porous Media- an Update. Paper PETSOC-2006-136 presented at the Petroleum Society's 7th Canadian International Petroleum Conference (57th Annual Technical Meeting) held in Calgary, Alberta, Canada, 13-15 June. http://dx.doi.org/10.2118/2006-136.

Branagan, P., Cotner, G., and Gettman, G. 1981. Evidence of Permeability Enhancement ThroughCyclic Dry Gas Injection. Paper SPE 9854 presented at SPE/DOE Low Permeability Gas Reservoirs Symposium. Denver, Colorado. 27-29 May. http://dx.doi.org/10.2118/9854-MS.

Castro Dantas, T. N.; Dantas Neto, A. A., and Moura, E. F. 2001a. Microemulsion Systems Applied to Breakdown Petroleum Emulsions. *J Petrol Sci Eng* **32** (2-4): 145-149. 10.1016/S0920-4105(01)00156-5.

Castro Dantas, T. N., Silva, A. C., and Dantas Neto, A. A. 2001b. New Microemulsion Systems Using Diesel and Vegetable Oils. *Fuel* **80** (1): 75-81 10.1016/S0016-2361(00)00068-5.

Castro Dantas, T. N., Santanna, V. C., and Dantas Neto, A.A. et al. 2003. Application of Surfactants for Obtaining Hydraulic Fracturing Gel. *J Petrol Sci Technol* **21** (7-8): 1145-1157. 10.1081/LFT-120017880.

Dantas Neto, A. A., Fernandes, M. R., Barros Neto, E. L. et al. 2011. Alternative Fuels Composed by Blends of Nonionic Surfactant with Diesel and Water: Engine Performance and Emissions. *Braz J Chem Eng* **28** (3): 521-531. http://dx.doi.org/10.1590/S0104-66322011000300017.

Davis, B.B.J. and Wood, W.D. 2004. Maximizing Economic Return by Minimizing or Preventing Aqueous Phase Trapping During Completion and Stimulation

Operations. Paper SPE 90170 presented at the SPE Annual Technical Conference and Exhibition. Houston, Texas, 26-29 September. http://dx.doi.org/10.2118/90170-MS.

Delshad, M., MacAllister, D.J., Pope, G.A. et al. 1985. Multiphase Dispersion and Relative Permeability Experiments. *SPE J.* **25** (4):524-534. SPE-10201-PA. http://dx.doi.org/10.2118/10201-PA.

Dubey, S.T. and Doe, P.H. 1993. Base Number and Wetting Properties of Crude Oils. *SPE Res Eval & Eng* **8** (3):195-200. SPE-2298-PA. http://dx.doi.org/10.2118/22598-PA.

Fanun, M. 2008. *Microemulsions: Properties and Applications*. Surface Science Series. Chap. 15: 429-430.

Florence, F.A., Rushing, J.A., Newsham, K.E. et al. 2007. Improved Permeability Prediction Relations for Low Permeability Sands. Paper SPE 107954 presented at the SPE Rocky Mountain Oil and Gas Technology Symposium held in Denver, Colorado, USA, 16-18 April. http://dx.doi.org/10.2118/107954-MS.

Friberg, S.E. and Bothorel, P. 1987. *Microemulsions: Structure and Dynamics*. CRC Press, ISBN 0849365988. Boca Raton. Chap. 2: 27-31.

Gupta, D.D.S. and Leshchyshyn, T.T. 2005. CO2-Energized Hydrocarbon Fracturing Fluid History and Field Application in Tight Gas Wells. Paper SPE 96061 presented at the SPE Latin American and Caribbean Petroleum Engineering Conference. Rio de Janeiro, Brazil. 20-23 June. http://dx.doi.org/10.2118/95061-MS.

Gurgel, A., Moura, M.C.P.A., Dantas, T.N.C. et al. 2008. A Review on Chemical Flooding Methods Applied in Enhanced Oil Recovery. *Braz J Petrol Gas* **2** (2): 83-95. ISSN 1982-0593.

Hamberlin, C.W., Thomas, D.C., and Trbovich, M.G. 1990. Combination of Selected Solvents and Mutual Solvents Successful in Removing Hydrocarbon Based Formation Damage. Paper PETSOC-90-58 presented at the Annual Technical Meeting. Calgary, Alberta, 10-13 June. http://dx.doi.org/10.2118/90-58.

Hirasaki, G.J. 1991. Wettability: Fundamentals and Surface Forces. *SPE Form Eval* **6** (2): 217-226. SPE-17367-PA. http://dx.doi.org/10.2118/17367-PA.

Hussain, S.A., Demiric, S., and Ozbayoglu, G. 1996. Zeta Potential Measurements on Three Clays from Turkey and Effects of Clays on Coal Flotation. *J. Colloid Interface Sci*. **184** (2):535-541. http://dx.doi.org/10.1006/jcis.1996.0649.

Jamaluddin, A.K.M., Hamelin, M., Harke, K. et al. 1996. Field Testing of the Formation Heat Treatment Process. Paper PETSOC-96-88 presented at the Annual Technical Meeting, Calgary, Canada, 10-12 June. http://dx.doi.org/10.2118/96-88.

Lake, L.W. 1989. *Enhanced Oil Recovery*. Prentice Hall. New Jersey. Chap. 5: 1-19.

Li, K. and Firoozabadi, A. 2000. Experimental Study of Wettability Alteration to Preferential Gas-Wetting in Porous Media and Its Effects. *SPE Res Eval & Eng* **3** (2): 139-149. SPE-62515-PA. http://dx.doi.org/10.2118/62515-PA.

Lif, A., Stark, M., Nydén, M. et al.2010. Fuel Emulsions and Microemulsions Based on Fischer–Tropsch Diesel. *Colloid Surface A* **354**(1-3): 91-98. DOI: 10.1016/j.colsurfa.2009.08.020.

Lingen, P.P., Bruining, J., and van Kruijsdijk, C.P.J.W. 1996. Capillary Entrapment Caused by Small-Scale Wettability Heterogeneities. SPE Res & Eng **11** (2): 93-100. SPE -30782-PA. http://dx.doi.org/10.2118/30782-PA.

Liu, D., Fan, M., Yao, L., et al. 2010. New Fracturing Fluid with Combination of Single Phase Microemulsion and Gelable Polymer System. *Pet. Sci. & Eng*. 73: 267-271. ISSN 0920-4105.

Luo, K., Li, S., Zheng, X. et al. 2001. Experimental Investigation into Revaporization of Retrograde Condensate by Lean Gas Injection. Paper SPE 68683 presented at the SPE Asia Pacific Oil and Gas Conference and Exhibition, Jakarta, Indonesia, 17-19 April. http://dx.doi.org/10.2118/68683-MS.

Mohan, K.K., Vaidya, R.N., Reed, M.G. et al. 1993. Water Sensitivity of Sandstones Containing Swelling and Non-Swelling Clays. *Colloid Surface A* **73** (1993): 273-254. DOI: 10.1016/0927-7757(93)80019-B.

Moura, E.F., Wanderley Neto, A.O., Castro Dantas, T.N. et al. 2009. Applications of Micelle and Microemulsion Systems Containing Aminated Surfactants Synthesized from Ricinoleic Acid as Carbon-Steel Corrosion Inhibitors. *Colloid Surface A* **340** (1-3): 199-207. DOI: 10.1016/j.colsurfa.2009.03.031.

Nasr-El-Din, H.A., Lynn, J.D., and Al-Dossary, K.A. 2002. Formation Damage Caused by a Water Blockage Chemical: Prevention Through Operator Supported Test Programs. Paper SPE 73790 presented at the International Symposium and Exhibition on Formation Damage Control, 20-21 February, Lafayette, Louisiana. http://dx.doi.org/10.2118/73790-MS.

National Institute of Standards and Technology (NIST). 2012, http://webbook.nist.gov/chemistry/fluid.html (accessed 21 September 2012).

Neasham, J.W. 1977. The Morphology of Dispersed Clay in Sandstone Reservoirs and Its Effect on Sandstone Shaliness, Pore Space and Fluid Flow Properties. Paper SPE 6858 presented at the SPE Annual Fall Technical Conference and Exhibition. Denver, Colorado, 9-12 October. http://dx.doi.org/10.2118/6858-MS.

Nguyen, D.T. 2013. Microemulsion Flowback Aid Composition and Method of Using Same. US Patent No. 20130261033 A1.

Noh, M.H. and Firoozabadi, A. 2008. Wettability Alteration in Gas-Condensate Reservoirs to Mitigate Well Deliverability Loss by Water Blocking. *SPE Res Eng* **11** (4): 676-685. SPE-98375-PA. http://dx.doi.org/10.2118/98375-PA.

Ochoterena, R., Lif, A., Nydén, M. et al. 2010. Optical Studies of Spray Development and Combustion of Water-in-Diesel Emulsion and Microemulsion Fuels. *Fuel* **89** (1): 122-132. DOI: 10.1016/j.fuel.2009.06.039.

Oskouei, S.J.P., Moore, G.R., Maini, B.B. et al. 2010. Feasibility of In-Situ Combustion in the Mature SAGD Chamber. Paper SPE 137832 presented at the Canadian Unconventional Resources and International Petroleum Conference. Calgary, Alberta, Canada, 19-21 October. http://dx.doi.org/10.2118/137832-MS.

Paktinat, J., Pinkhouse, J.A., Stoner, W.P. et al. 2005. Case Histories: Post-Frac Fluid Recovery Improvements of Appalachian Basin Gas Reservoirs. Paper SPE 97365 presented at the SPE Eastern Regional Meeting, Morgantown, West Virginia, 14-16 September. http://dx.doi.org/10.2118/97365-MS.

Passey, Q.R., Bohacs, K., Esch, W.L. et al. 2010. From Oil-Prone Source Rock to Gas-Producing Shale Reservoir- Geologic and Petrophysical Characterization of Unconventional Shale Gas Reservoirs. Paper SPE 131350 presented at the International Oil and Gas Conference and Exhibition held in China. Beijing, China. 8-10 June. http://dx.doi.org/10.2118/131350-MS.

Penny, G.S., Conway, M.W., and Briscoe, J.E. 1983. Enhanced Load Water-Recovery Technique Improves Stimulation Results. Paper SPE 12149 presented at the SPE Annual Technical Conference and Exhibition. San Francisco, California, 5-8 October. http://dx.doi.org/10.2118/12149-MS.

Penny, G., Pursley, J.T., and Holcomb, D. 2005. The Application of Microemulsion Additives in Drilling and Stimulation Results in Enhanced Gas Production. Paper SPE 94274 presented at the SPE Production and Operation Symposium. Oklahoma City, Oklahoma, 17-19 April. http://dx.doi.org/ 10.2118/94274-MS.

Pursley, J.T., Penny, G., and Holcomb, D. 2004. Microemulsion Additives Enable Optimized Formation Damage Repair and Prevention. Paper SPE 86556 presented at SPE International Symposium and Exhibition on Formation Damage Control. Lafayette. Louisiana, 16-20 February. http://dx.doi.org/10.2118/86556-MS.

Ramez, A.N., Bataweel, M.A., and Nasr-El-Din, H.A. 2013. Investigation of Wettability Alteration and Oil-Recovery Improvement by Low-Salinity Water in Sandstone Rock. *JCPT* **52** (2): 144-154. SPE-146322-PA. http://dx.doi.org/10.2118/146322-PA.

Reyes, Y., Rodriguez, F. J., del Rio, J. M. et al. 2005. Characterization of an Anticorrosive Phosphated Surfactant and Its Use in Water-Borne Coatings. *Prog Org Coat* **52** (4): 366-371. DOI: 10.1016/j.porgcoat.2004.09.008.

Samuel, M.M., Card, R.J., Nelson, E.B. et al. 1999. Polymer-Free Fluid for Fracturing Applications. *SPE Drill & Compl* **14** (4): 240-246. SPE-59478-PA. http://dx.doi.org/10.2118/59478-PA.

Santanna, V.C., Curbelo, F.D.S., Castro Dantas, T.N. et al. 2009. Microemulsion Flooding for Enhanced Oil Recovery. *J Petrl Sci Eng* **66**(3-4): 117-120. DOI: 10.1016/j.petrol.2009.01.009.

Santanna, V.C., Dantas, T.N.C., and Neto, A.A.D. 2012. *Microemulsions - An Introduction to Properties and Applications*. Federal University of Rio Grande do Norte Brazil. ISBN 978-953-51-0247-2. Chap. 8: 161-174.

Sayed, M.A.I. and Nasr-El-Din, H.A. 2013. Acid Treatments in High Temperature Dolomitic Carbonate Reservoirs Using Emulsified Acids: A Coreflood Study. SPE Paper 164487 presented at SPE Production and Operations Symposium, Oklahoma City, Oklahoma, USA. 23-26 March. http://dx.doi.org/10.2118/164487-MS.

Vijapurapu, C.S. and Rao, D.N. 2003. Effect of Brine Dilution and Surfactant Concentration on Spreading and Wettability. Paper SPE 80273 presented at the International Symposium on Oilfield Chemistry, Houston, Texas, 5-7 February. http://dx.doi.org/10.2118/80273-MS.

Wang, W. and Gupta, A. 1995. Investigation of the Effect of Temperature and Pressure on Wettability Using Modified Pendent Drop Method. Paper SPE 30544 presented at the SPE Annual Technical Conference and Exhibition, Dallas, 22-25 October. http://dx.doi.org/10.2118/30544-MS.

Willhite, G.P., Green, D.W., Okoye, D.M. et al. 1980. A Study of Oil Displacement by Microemulsion Systems Mechanisms and Phase Behavior. *SPE J.* **20** (6):459-472. SPE-7580-PA. http://dx.doi.org/10.2118/7580-PA.

Yang, Y., Dismuke, K.I., Penny, G.S. et al. 2009. Lab and Field Study of New Microemulsion-Based Crude Oil Demulsifiers for Well Completions. Paper SPE 121762 presented at SPE International Symposium on Oilfield Chemistry. The Woodlands. Texas, 20-22 April. http://dx.doi.org/10.2118/121762-MS.

Zelenev, A.S., Champagne, L.M., and Hamilton, M. 2011. Investigation of Interactions of Diluted Microemulsions with Shale Rock and Sand by Adsorption and Wettability Measuremenst. *J. Colloid Surf A: Physicochem. Eng. Asps* **391**: 201-207. doi:10.1016/j.colsurfa.2011.07.007.

Zhang, N.S., Somerville, J.M., and Todd, A.C. 1993. An Experimental Investigation of the Formation Damage Caused by Produced Oily Water Injection. Paper SPE 26702 presented at the Offshore Europe Conference, Aberdeen, United Kingdom, 7-10 September. http://dx.doi.org/10.2118/26702-MS.

Ziarani, A.S., Aguilera, R. 2012. Knudsen's Permeability Corrections for Tight Porous Media. *Transp Porous Med* **91** (1): 239-260. DOI 10.1007/s11242-011-9842-6.